Engineering Failure Analysis 159 (2024) 108065

Contents lists available at ScienceDirect

Engineering Failure Analysis

journal homepage: www.elsevier.com/locate/engfailanal

Review

Effects of different microstructural parameters on the corrosion and cracking resistance of pipeline steels: A review

Meekness Nnoka *, Tonye Alaso Jack, Jerzy Szpunar

Department of Mechanical Engineering, University of Saskatchewan, 57 Campus Drive, Saskatoon S7N 5A9, Saskatchewan, Canada

ARTICLE INFO

Keywords:
Pipeline steel
Microstructure
Corrosion
Cracking
Hydrogen

ABSTRACT

Several environmental challenges such as corrosion, low temperature, hydrogen-induced cracking (HIC), stress corrosion cracking (SCC), sulfide stress corrosion cracking (SSCC), and various other failure mechanisms contribute to the deterioration of the mechanical properties of pipeline steels, ultimately resulting in failure. In this review, diverse hydrogen attack sources, their possible failure mechanisms, and various strategies for their mitigation in different environments are explored. Optimizing the microstructure of pipeline steels can greatly improve their resistance to corrosion and cracking. This involves tailoring several microstructural parameters like the phase composition, dislocation density, crystallographic texture, grain size, grain boundary, and inclusions/precipitates, amongst others to the needs of the steel's service environment. The evolving research landscape concerning the role of these microstructural parameters in corrosion, HIC, SCC, and other failure mechanisms was discussed in this study. It was established that crystallographic texture and grain boundary characteristics have roles to play in improving the SCC resistance of pipeline steels. However, the degree to which crystallographic texture, amidst other microstructural parameters, affects cracking is not yet established. For instance, the direct influence of crystallographic texture in the arrest of propagating cracks is still unclear and debated, while low-angle grain boundaries and CSL boundaries have been seen to arrest cracks in steels. It was also established that dislocation density, amongst other microstructural parameters, has a more profound effect on the HIC resistance of pipeline steels. Furthermore, this review examines the effect of hydrogen in pipeline welds. It investigates strategies to adapt existing pipelines' microstructure to meet the demands of operations in arctic environments. It was established that grain size, amongst other microstructural parameters, has a more profound effect on the mechanical properties of pipelines designated for cold applications. Finally, this review explores recent advancements in the transportation of gaseous hydrogen using existing pipeline steels (natural gas infrastructure). Ultimately, this study reinforces the importance of microstructure optimization in pipelines designated for different service environments, detailing the contribution of individual microstructural parameters to their overall performance and failure susceptibility in these environments.

1. Introduction

High-strength pipeline steels encounter harsh operational conditions such as corrosive, low temperature, and hydrogen

* Corresponding author.
E-mail address: ysr538@usask.ca (M. Nnoka).

https://doi.org/10.1016/j.engfailanal.2024.108065
Received 24 November 2023; Received in revised form 23 January 2024; Accepted 31 January 2024
Available online 5 February 2024

environments, which accelerate structural failures and compromise their integrity. The hydrogen environment, whether aqueous or gaseous, is of grave concern, and the manifestation of cracks in pipelines can be attributed to the uptake of hydrogen into the steel structure. Over the years, research has shown that these vulnerabilities can be mitigated through meticulous control of the micro-alloying elements and processing parameters during thermomechanical processing (TMCP) while providing a good balance of strength and toughness for the steel [1]. However, it's important to note that elevating pipeline strength can increase its likelihood of failure, which is attributed to significant changes in the microstructural characteristics of the steel [2]. This empirical strength and failure relationship highlights the necessity of attaining a delicate compromise between properties, such as strength, weldability, toughness, corrosion, and cracking susceptibility. Achieving the proper balance requires careful analysis of the specific environmental conditions and intended applications of the pipelines, as well as the relevance of microstructure in determining the susceptibility of pipelines to failure [3–8]. Microstructure plays a pivotal role in the distribution of hydrogen within the crystal lattice, thereby dictating the vulnerability to hydrogen-induced degradation of pipelines. It encompasses a range of parameters such as phase composition, grain size, grain boundary characteristics, dislocation density, and crystallographic texture, all of which have been reported to exert a substantial impact on the corrosion and hydrogen-induced cracking resistance of pipelines [9]. For instance, it has been reported that boundaries between grains having {1 1 0} and {1 1 1} planes oriented parallel to the pipeline steel surface are more resistant to hydrogen-related degradation [10]. It has been also reported that a large amount of coincident site lattice (CSL) boundaries and low-angle grain boundaries (LAGBs) can improve SCC resistance in pipeline steels [11]. In this review, the role of these microstructural parameters in corrosion, HIC, SCC, and other failure mechanisms has been made known. These microstructural parameters can be optimized to improve pipeline steel performance in different service environments. The microstructural characteristics obtained after thermomechanical processing and microalloying hold the potential to significantly reduce the degradation of steel in different service environments. However, despite extensive work on the subject, HIC and SCC remain the most important failure mechanisms that must be mitigated. Understanding the deteriorating effect of hydrogen and developing pipeline steels having optimum resistance to hydrogen embrittlement (HE) is pivotal and remains the driving force behind this review. Due to the catastrophic failures that often occur because of HE, our focus is mainly on pipeline steel. However, other types of steel are occasionally mentioned. While extensive research has been conducted on the role of microstructure in hydrogen diffusion, the detrimental consequences of hydrogen in pipeline steels, the various hydrogen degradation mechanisms, and contemporary techniques for characterizing microstructures, controversies, and debates persist within the field [12–14]. Apart from microstructural phases, and control, sulfur, and hydrogen sulfide (H_2S) are significant impurities in pipeline steels because of their potential to cause corrosion and embrittlement, which can compromise the integrity of the pipeline. Elevated amounts of sulfur can foster the formation of manganese sulfide (MnS) inclusions, which have been reported to cause HIC in pipeline steels [15–18]. While the shape of MnS matters, it has been reported that elongated inclusions have a lesser effect on pipeline steels [19]. There are several ways of controlling the morphology of inclusions. For instance, the use of fine oxide inclusions as heterogeneous nucleation sites by adding titanium, magnesium, and zirconium. Also, the use of calcium or rare earth treatment has been reported. However, there are shortcomings of this method because controlling the calcium sulfide (CaS) content in steel is difficult as it requires a very sensitive range of oxygen content for Calcium treatment. H_2S on the other hand fosters the ingress of hydrogen atoms into the pipeline structure, by acting as a recombination poison [20]. This review also discusses past and recent techniques used for controlling the morphology of inclusions. Another focus of this study is on the application of TMCP as a means of tailoring the microstructural parameters of pipeline steels to impact crack resistance, while pointing out the use of inhibitors to prevent pipeline failure due to corrosion. Apart from cracking being induced environmentally, the mismatch in deformation between the ferrite and cementite during cold forming can facilitate cracking which seriously deteriorates the fatigue life of spheroidized ferrite-cementite steel (SFC) steels. Wang et al. were able to utilize experiments and multiscale simulations to investigate the damage mechanisms and the dependence of microstructure features under uniaxial tension in SFC steel [21]. The authors found three damage mechanisms in SFC steel under uniaxial tension: cementite cracking, ferrite/cementite interface debonding, and ferrite cracking, after the in situ tensile test, and the matrix cracking was attributed to dislocation pile up or the crossing of multiple slip bands.

Furthermore, heightened operational demands for high-strength pipeline steel have driven increased research focus toward understanding the inherent failures observed in high-grade pipeline steel welded joints. These failures have significant implications for the microstructure, structural safety, and overall integrity of the welded joints [22,23]. For instance, Chen et al. revealed the effect of welding residual stress (WRS) on the fatigue life of rib-to-deck double-sided welded joints in orthotropic steel decks. The authors observed that WRS has a significant effect on fatigue life, and the fatigue life of the weld toe without considering WRS is about twice that of considering WRS [24]. Moving forward, it is also known that to improve the microstructure and properties of duplex stainless steel welded joints, it is very important that an appropriate N2 content was added in shielding gas during the DSS CMT-P welding process. Zhang et al. experimentally recommended Ar + 4 % N2 as the shielding gas to join DSS by using the CMT-P welding technique [25]. It is also imperative to understand the effect of hydrogen in pipeline welds, amidst other possible causes of cracking. As such, this review discusses the effect of hydrogen on the cracking resistance of pipeline welds. Our focus is on pipeline steels; however, other steels were also mentioned in this study. In the end, it outlines recent advances for transporting gaseous hydrogen using pipeline steels not originally designed for such purposes, while shedding light on the recent adaptation of current pipelines to operate effectively in demanding arctic environments. Overall, this study reinforces the importance of microstructure optimization in pipelines designated for different service environments, detailing the contribution of individual microstructural parameters to their overall performance and failure susceptibility in these environments.

2. Pipeline corrosion – Overview

Pipeline corrosion is the backbone of the most environmentally induced failure mechanisms encountered in pipeline steels. It

remains a broad topic to discuss and can more easily be understood by discussing it in parts. Corrosion involves material deterioration due to environmental factors. It is an electrochemical process that involves electron ejection due to metal dissolution at the anodic site, and electron transfer to the cathodic site, resulting in the formation of ions and/or hydrogen evolution [26]. Understanding the reduction–oxidation (redox) reactions that make corrosion possible is most fundamental, and they are given as follows:

Anodic Reaction

$Fe \rightarrow Fe^{+2} + 2e^{-}$ (Iron Dissolution)(1)

Cathodic Reactions.

$2H_20_{(L)} \rightarrow O_2(g) + 4H^{+}_{(aq)} + 4e^{-}$(2)

$2H^{+} + 2e^{-} \rightarrow H_2$ (Hydrogen reduction)(3)

$O_2 + 2H_2O + 4e^{-} \rightarrow 4OH^{-}$ (Oxygen reduction in neutral or alkalis media)(4)

$O_2 + 4H + 4e^{-} \rightarrow 2H_2O$ (Oxygen reduction in acidic media)(5)

$Fe + 2H^{+} \rightarrow Fe^{+2} + H^2$ (Overall corrosion reaction)(6)

The above corrosion reactions occur in the anodic and cathodic regions of the pipeline. These anode and cathode sites are usually on the surfaces of the pipelines, and in combination with electrolytes, they make corrosion possible.

The role of the electrolyte is to complete the corrosion circuit, facilitating the flow of ions. In pipeline steels, corrosion usually occurs in the presence of carbon dioxide (CO_2) or hydrogen sulfide (H_2S). All the above corrosion agents are mostly present in oil and gas, and sometimes, with the combination of other corrosive agents like water, sand, microbes, and other organic compounds.

2.1. CO_2 corrosion (Sweet Corrosion)

This type of corrosion is also called sweet corrosion because it happens in the presence of CO_2. Sweet corrosion happens by an acidic reaction where water (H_2O) reacts with CO_2. It is called sweet because it is usually less aggressive than sour corrosion (corrosion in the presence of a high amount of H_2S). In this process, the corrosion agent is H^{+} from H_2CO_3. CO_2 can be present in pipeline steels due to certain processes like steel recovery. As iron (Fe) reacts with CO_2, sweet corrosion begins. The reaction is seen below:

$Fe + CO_2 \rightarrow FeCO_2$(7)

H_2O reacts with the absorbed surface complex, forming Fe^{2+} (aq) and H_2CO_3, producing the cathodic reactant H^{+} during dissociation. To date, the cathodic reaction mechanism for sweet corrosion is a complex reaction. However, it can be approximated as:

$2H^{+}$ (aq) $+ 2e^{-} \rightarrow H_2$(8)

$2H_2CO_3 + 2e^{-} \rightarrow H_2 + 2HCO_3^{-}$(9)

$H_2CO_3 + e^{-} \rightarrow H^{+} + HCO_3^{-}$ (Dissociation of H_2CO_3 in solution).(10)

Several interpretations have been made of the sweet corrosion process however, the cathodic reaction mechanism of sweet corrosion is not understood [27].

It was inferred that when the pH value is lower than 4, hydrogen reduction becomes the dominant mode for corrosion, while when the pH value varies between 4 and 7, the adsorbed H_2CO_3 reduction becomes the dominant mode for corrosion [28]. For many oil and gas pipelines, sweet corrosion is not a threat, this is because of the presence of hydrogen sulfide (H_2S). Sweet corrosion occurs in the absence of hydrogen sulfide (H_2S).

2.2. Sour corrosion (H_2S)

Unlike sweet corrosion, sour corrosion occurs in the presence of hydrogen sulfide (H_2S). This is a major concern in the oil and gas industries, as H_2S is present in the transported substances. In sour corrosion, H_2S is decomposed into H + and HS^{-} ions. HS^{-} ion acts as a hydrogen recombination poison, limiting the formation of hydrogen molecules. The following reactions occur during sour corrosion:

$H_2S \rightarrow HS^{-} + H^{+}$(11)

$HS^{-} \rightarrow S^{-2} + H^{+}$ (12)

Hydrogen atoms in the form of protons attract electrons from iron (Fe) and form hydrogen atoms:

$H^{+} + e^{-} \rightarrow H_{ads}$(13)

$H_{ads} + H_{ads} \rightarrow H_2$(14)

The hydrogen atoms which do not recombine to form a hydrogen molecule, because of the recombination poison (HS^{-}) are absorbed

Table 1
Different microstructures of the X80 pipeline carbon steel [56].

Heat Treatment	Microstructure
For the as-received specimen	Ferrite and pearlite bands, having dispersed precipitates.
Quenched and tempered specimen	Incomplete recrystallized grains with incipient acicular ferrite and isolated pearlite grains.
Watered-sprayed specimen	Partial transformation of perlite grains with few precipitates.
Water-quenched specimen	Martensite with high segregation at martensitic lath boundaries and dispersion of precipitates.

into the pipeline's lattice.

Upon entering the steel, a lot of regions act as accumulation zones as the hydrogen atoms diffuse through the lattice [29]. They might be trapped at grain boundaries, dislocations, precipitates, inclusions, etc. The hydrogen atoms tend to recombine around defects or strong trapping sites to cause the degradation of mechanical properties, and eventually failure [30]. Also, the sulfide corrosion products passivate the steel at low temperatures, as far as chloride ions and oxygen are absent. When those substances are present, they may form a galvanic couple with the pipeline steel to aggravate the localized corrosion problems [31].

2.3. Under-deposit corrosion (UDC)

UDC due to the presence of deposits has become a major threat to the integrity of pipelines in oil and gas fields. UDC refers to the localized corrosion that occurs beneath or around deposits present on a metal surface. These deposits include silica sand, calcite, clays, alumina, corrosion products, organics, etc. [32]. UDC tends to cause the perforation of pipelines and they occur unexpectedly, resulting in unacceptable failures [33]. One of the ways of mitigating UDC in pipelines is by scale controlling, which involves preventing depositing (scale inhibition) and removing the deposits/scales that have already existed on pipeline surfaces [34]. Mitigating UDC by adding specially developed corrosion inhibitors is still promising, however, some inhibitors promote UDC in pipeline steels, therefore specialized inhibitors are recommended.

2.4. Microbiologically influenced corrosion (MIC)

MIC involves the pollution of pipeline steel surfaces by microorganisms and the subsequent creation of corrosive oxygen concentration cells [9]. It has been reported that MIC accounts for more than 20 % of pipeline infrastructure failures [35]. Many studies have been made regarding the corrosive actions of sulfate-reducing bacteria (SRB) and nitrate-reducing bacteria (NRB) on metal surfaces, in fostering MIC. SRBs, as anaerobic bacteria, reduce sulfur/sulfur ($S0_4^{-2}$ $S0_3^{-2}$ $S_20_3^{-2}$, and sulfur) compounds to sulfide (H_2S) from available carbon sources [36]. When they adhere to pipeline steel surfaces, they mature into a multitude of SRBs due to means of extracellular polymeric substances (EPS) secreted by their biofilms [37]. This fosters the production of H_2S, leading to electrochemical reactions that lead to localized corrosion modes [36].

3. Improving the corrosion resistance of pipeline steel

The use of cathodic protection (CP) has been a technique that favors the corrosion resistance of pipeline steels [38]. CP is a system that uses direct electrical current to mitigate the normal external corrosion that occurs on a metal pipeline due to soil and moisture conditions. CP is used where all or part of a pipeline is buried underground or submerged in water. Another method is the use of pipeline coatings and linings, as they protect the bare steel from coming in direct contact with corrosive conditions [39]. Corrosion inhibitors are also used to improve the corrosion resistance of pipeline steels. They can be added to the pipeline substance running through the pipeline to decrease the rate of attack of internal corrosion on the steel. As CP cannot protect against internal corrosion, inhibitors are of particular use in "wet" gas pipelines. Inhibitors like Pectin/nano CeO_2 (mixture-based corrosion inhibitor) and Hydroxyquinoline-KI (mixture-based corrosion inhibitor) have been proven to reduce corrosion in pipeline steels, respectively [40,41]. The production of corrosion inhibitors poses high cost and time constraints. However, in a contemporary context, He et al. utilized machine learning, revealing the controlled synthesis of carbon dots-based corrosion inhibitors [42]. The optimization process increases time management while reducing cost and contributing to the sustainability and cleaner production of inhibitors.

3.1. Stress corrosion cracking (SCC)

Stress corrosion cracks are formed from the combined effect of sustained tensile stress and corrosion. The surface corrosion type can be either sweet or sour, while the tensile stress can be residual or externally applied. Pipelines are prone to SCC because of their corrosive environment and tensile stress which facilitates cracking. As such, SCC is often called environmentally assisted cracking (EAC) and has always been of major interest to gas pipeline manufacturers [20,43–45]. The SCC resistance of pipelines depends on their microstructure [46–50]. Different microstructural parameters influence the stress corrosion cracking susceptibility of pipeline steels [9]. Abubakar et al. reviewed several factors affecting SCC initiation and propagation in carbon steels [51]. Several types of microstructural phase constituents are observed in pipeline steels such as austenite, pearlite, ferrite, bainite, and martensite. The cooling rate applied during processing and the nucleate contents determine the different forms of ferrite grains that will be nucleated such as acicular ferrite, polygonal ferrite, allotriomorphic ferrite, globular ferrite, and idiomorphic ferrite [52]. Among these

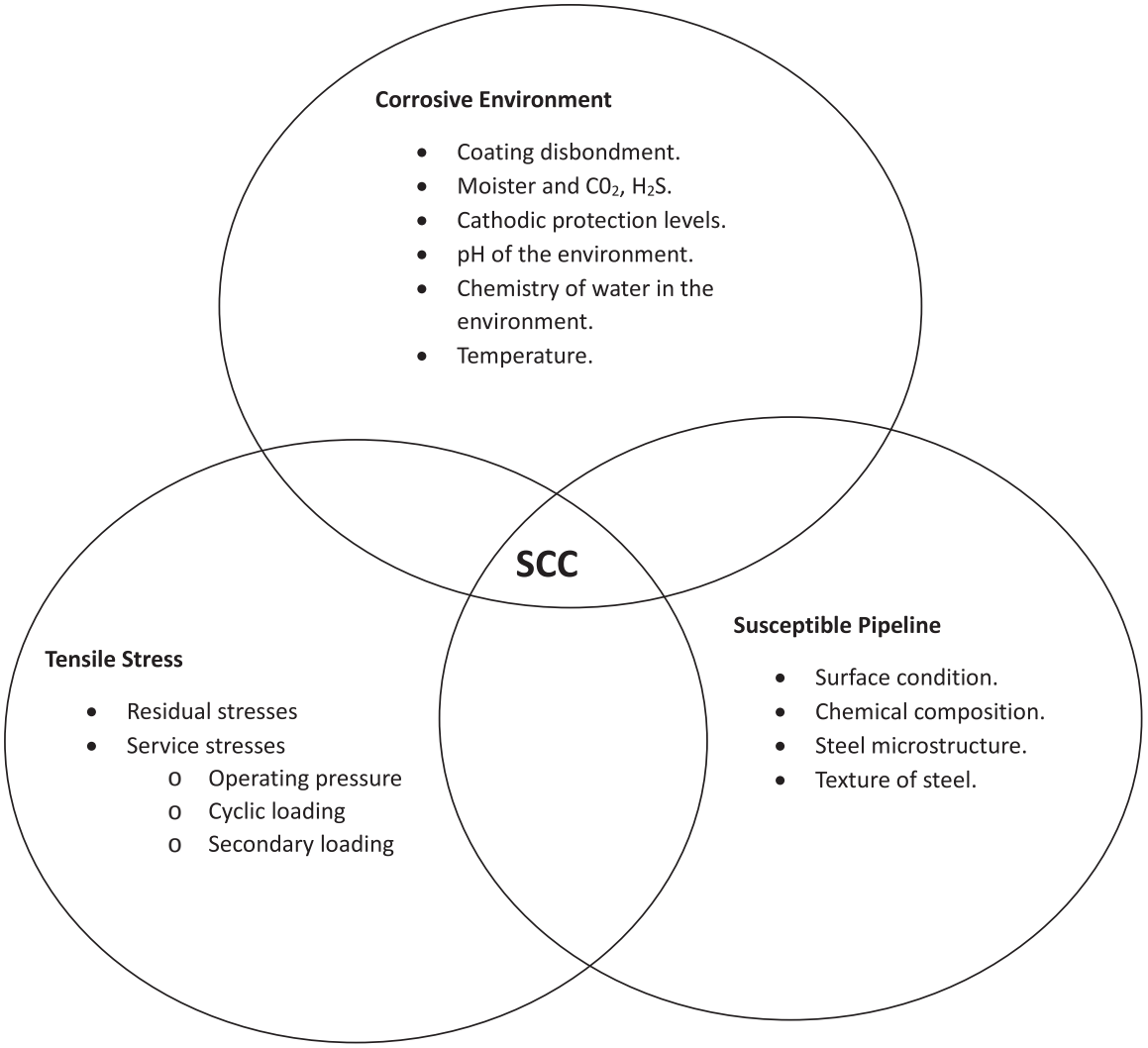

Fig. 1. Factors affecting SCC crack initiation and propagation in pipeline steel [27].

microstructures, acicular ferrite, which is a thin needle-like form of ferrite grain, possessing high dislocation density due to its fine-grained nature, has been understood to possess better SCC resistance [53,54]. On the other hand, pipeline steels with under-tempered martensitic or bainitic microstructures or those without post-weld heat treatment in the heat-affected zones (HAZ) are understood to have less SCC resistance [55].

Liu et al. investigated the SCC behavior of API 5L X70 pipeline steel with different applied heat treatments and microstructures as shown in Table 1 [56]. They conducted the test using the SSRT method with a strain rate of 5×10^{-7} in/s in an acidic soil extract (pH of 4.41) collected from 1.5 m underground. Cathodic potentials of − 650 mV saturated caramel electrode (SCE), −850 mV (SCE), and − 1200 mV (SCE) below the corrosion potential were used in these tests. Interestingly, the results showed a dual-mode SCC mechanism, having a combined effect of anodic dissolution and hydrogen embrittlement. The water-quenched specimen having bainite grains had a higher susceptibility to SCC in the acidic soil extracts, while the as-received sample with ferrite matrix grains had a lower susceptibility to SCC. It can be deduced that the primary SCC mechanism changed with varying applied potentials. For instance, when a lower negative applied potential, the SCC mechanism was highly due to anodic dissolution. But when the applied potential was highly negative, hydrogen became the major SCC mechanism causing the cracking process, and *trans*-granular cracks were observed. With more negative potentials, the SCC mechanism became completely based on a hydrogen-induced mechanism, with a riverbed-shaped brittle character of the fractured surface.

This was also in line with Fu et al. study on the SCC behavior of X70 carbon steel at different cathodic potentials below E_{corr} [57]. They observed that at an applied potential of − 450 mV (SCE), the mechanism of SCC was anodic dissolution, while at a reduced potential of − 850 mV (SCE), the anodic dissolution of the X70 steel was inhibited. Now, when a more negative potential of − 1200 mV (SCE) was applied, the specimens showed a higher SCC susceptibility, and the major SCC mechanism was completely hydrogen embrittlement.

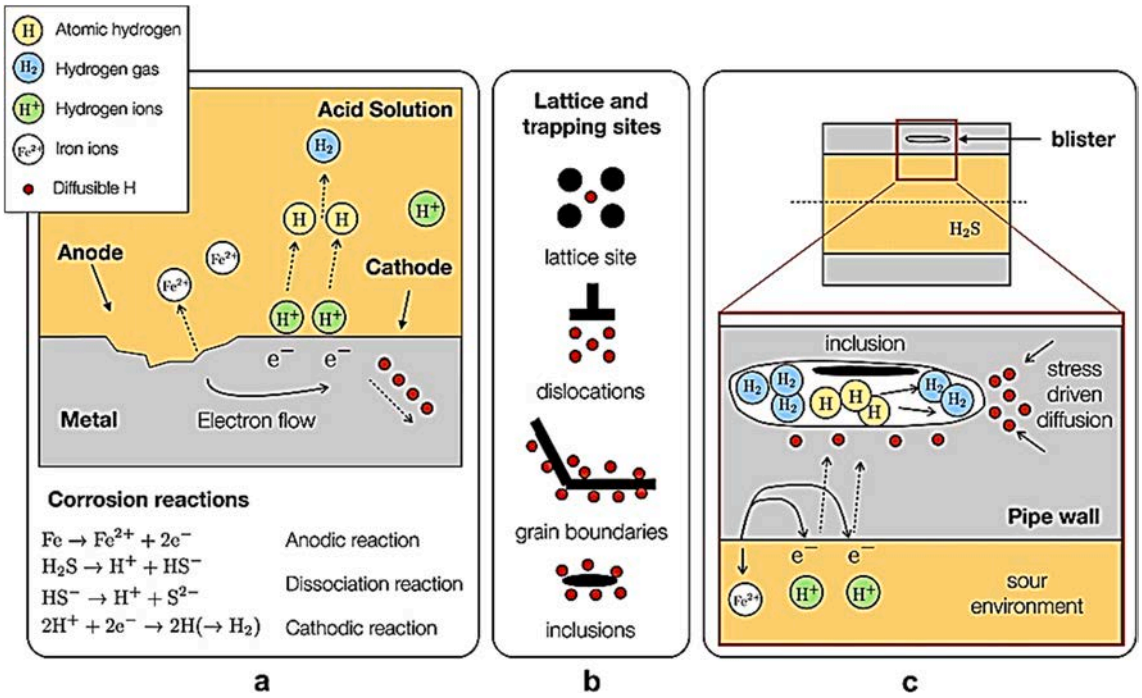

Fig. 2. (a) Mechanisms of hydrogen absorption in a steel plate exposed to H_2S environment; (b) interstitial lattice sites and trapping sites in steel; (c) hydrogen pressure build-up inside a defect located inside the wall of a steel pipe [66].

In addition to microstructure, chemical composition, residual stress, crystallographic texture, water chemistry in the field, applied stress, pH of the environment, and AC density also affect the SCC crack initiation and propagation [27,58,59]. For example, Zhang et al. investigated the SCC susceptibility of API 5L X70 carbon steel in various CO_2 concentrations, using the SSRT technique at a strain rate of 1×10^{-6} in/s. Increasing CO_2 concentrations of 0 %, 5 %, 10 %, 15 %, 20 %, and 100 % balanced with nitrogen gas in soil extracts solution were used for the tests. The test results indicated a rapid fall in area reduction of specimens with increasing CO_2 concentration. The susceptibility of the specimens to SCC increased with increasing CO_2 partial pressure until a steady state value was reached at about 20 % CO_2 concentration.

There is also a chance that SCC may occur in the absence of hydrogen in pipelines. However, in such a scenario, passive film dissolution is usually responsible for crack propagation [9]. Fig. 1 shows the various factors affecting the SCC crack propagation in pipeline steels.

4. Improving the SCC resistance of pipeline steels

The role of microstructure plays a major role in SSC mitigation. For instance, engineering grain boundary and crystallographic texture have been proven to improve the SCC resistance of pipeline steels. Arafin and Szpunar investigated the role of texture on X65 pipeline steel and concluded that tailoring the texture and grain boundary character will help to produce new pipeline steels with improved intergranular SCC resistance. It has been reported that boundaries between grains having {1 1 0} and {1 1 1} planes oriented parallel to the pipeline steel surface are more resistant to SCC. It has also been reported that large amounts of CSL boundaries and LAGBs can improve SCC resistance in pipeline steels [11]. Pipeline steels having a lesser number of inclusions or with a uniform distribution of inclusions will also possess better SCC resistance. This is because, the oxide and silicon-enriched inclusions are considered as SCC micro-crack initiation sites, as concluded by [60] Wang et al. In terms of microstructural phase constituents, Bulger et al. studied the effect of microstructure in pipeline steels on SCC resistance in near-neutral pH. The authors found out that fine-grained bainite and ferrite microstructure showed better SCC resistance unlike the pipeline steels having ferrite and pearlite microstructure [61].

4.1. Hydrogen-related failures in pipeline steel

Hydrogen has been linked to several failures of pipeline steels [62]. Apart from understanding the harmful effects of hydrogen in pipelines carrying petroleum resources, it is also important to understand how pipelines respond to transporting hydrogen gas in the future. Usually, pipelines fail due to atomic hydrogen accumulation in the interstitial sites. Fig. 2 shows the mechanisms of hydrogen absorption in pipeline steel exposed to an acidic H_2S environment. In Fig. 2a, the evolution of hydrogen occurs due to the corrosive interaction of the acidic solution and the pipe's surface. Fig. 2b shows the various trapping sites that hold hydrogen after its ingress into

the pipe's structure. While Fig. 2c shows typical hydrogen damage resulting in blisters, and cracks, caused mainly by stress-driven diffusion. This means more hydrogen would migrate to local stress concentrators to initiate pipeline steel failure.

Atomic hydrogen is introduced into the pipeline's structure through different processes:

1. Molecular hydrogen dissociation and atomic hydrogen absorption from the pipeline's surroundings into the steel.
2. Production and fabrication processes (e.g., welding).
3. The presence of agents with a strong affinity for producing hydrogen, electrochemical processes like corrosion, and/or hydride precipitation in hydride-producing components.

The risk of a pipeline crack in sour environments is high, because of the hydrogen recombination poison effect of H_2S [63]. After pipeline cracks, there is leakage or rupture, and eventually, an economic loss. It is therefore imperative for pipelines to be capable of resisting severe environmental conditions, especially under sour environments. The effects of hydrogen often result without cracking. This reveals that cracking precedes hydrogen degradation mechanisms and acts in synergy with other factors like stress or corrosion [64]. In addition, the decohesion of structure can also occur, reducing the strength of the metallic bonds and facilitating failure below yield strength without the presence of a crack. Nevertheless, the internal defects formed during and after steel processing determine the extent of hydrogen-related degradation [65].

Hydrogen-related failures are better understood by different types of processes.

4.1.1. Types of hydrogen-related failures

Hydrogen-related failures in pipeline steels are of significant concern in the oil and gas industry, as they can lead to potentially catastrophic incidents. These failures primarily result from the ingress of hydrogen into the steel structure, causing various forms of embrittlement and cracking. Some common hydrogen-related failures in pipeline steels include:

4.1.2. Hydrogen-induced cracking (HIC)

From recent literature, a lot of attention has been given to hydrogen-induced cracking [20,43,63,64,67,68] because of the deleterious effect of hydrogen on the ductility and strength of pipelines. In offshore environments, hydrogen can also be introduced into the pipeline steel structure through moisture from cathodic protection (CP) [69]. Cathodic protection (CP), which involves the use of electric current to prevent pipeline corrosion, might become disastrous when uncontrolled [69]. This happens as the cathodic protection wears off, exposing the pipeline to the twofold effect of the cathodic environment and subsequently HIC. Cracking becomes inevitable, because of the synergistic effect of hydrogen concentration and stress level on pipelines. Also, the effect of interstitial atoms (H, C, N, etc.) migration on the physicochemical and mechanical properties of pipelines has been understood as time-dependent [63]. This reveals the dependence of the atom's migration in the lattice on exposure time, ambient temperature, and atom size. Within the α-Fe lattice, H is usually less soluble than N atoms, though its small atom has an affinity for movement [70]. The decrease in hardness and ductility because of aging is a known effect in steels, involving C and N. However, the presence of H could simultaneously soften as well as harden metals, altering the results of their yield and tensile strengths, and creating a long-lasting controversy [71,72]. These controversies make it difficult to properly understand the effects of H on mechanical properties, making this subject very ambiguous even in recent times.

As said earlier, many studies on the effect of hydrogen exist, however, a lot of controversies abound. These controversies stem from different experimental designs and used methodologies, sample sizes, microstructural differences, and probing. Overall, pipeline embrittlement is attributed to the effect of hydrogen-induced failure, because of its deleterious effect on ductility. The degrading strength of steel depends on the mobility and effectiveness of hydrogen trapping sites. The mobility and trapping sites of hydrogen have been discussed in some studies [73,74]. These studies have shown the relationship between the HIC resistance of pipelines and their microstructural phase composition (bainite, martensite, ferrite, pearlite, etc.) as well as other microstructural features (grain boundary, dislocations, crystallographic texture, microalloying, inclusions, etc.). These HIC relationships with microstructure will be discussed later in detail.

Interestingly, a pipeline can have cracking initiated by the dual effects of both HIC and SSC. Some researchers define such an effect as hydrogen-assisted stress corrosion cracking. For instance, it was reported that anodic dissolution is dominant to stress corrosion cracking in a near-neutral pH environment, while a mix of hydrogen-based mechanisms becomes prominent at high pH [75]. According to the literature, the pH of the environment also affects the crack propagation, after crack initiation. For instance, the crack propagation mode is often *trans*-granular in near-neutral pH conditions but tends to be intergranular in high pH [75,76]. On the other hand, pipeline steels that are protected cathodically with highly negative applied potential, and with proper control of the protection processes, have better chances of withstanding hydrogen degradation [69]. When pipelines are not catholically protected, or when these cathodic protections are not controlled, pipeline coating is not immune to hydrogen blistering. The blistering process in coatings is referred to as cathodic disbondment, and it is exacerbated by interactions between pipeline coating and OH^- ions produced during water reduction [77]. Pipeline coatings experience accelerated water permeation at the edges at high cathodic potentials, which proceeds into pockets of hydrogen blisters and sites for localized hydrogen attack on the steel [77]. Inferences were also made that the high resistivity of coatings has a knock-on effect on the cathodic shielding, by preventing the permeation of cathodic current towards pipeline steel, thereby increasing the chances of SCC [78]. To confirm this inference, the cathodic-shielding behavior of high-density polyethylene and fusion-bonded epoxy coatings on pipelines were compared. Reports showed that high-density polyethylene (HDPE) coatings shielded cathodic protection current from reaching the pipeline's surface [79]. It can be assumed that pipelines coated with HDPE will experience hydrogen degradation under-coating. However, it was observed that the fusion-bonded epoxy-coated pipeline allowed permeation of CP current, creating more room for cathodic protection.

4.1.3. Improving the HIC resistance of pipeline steels

It is widely reported that higher-strength pipeline steels are more susceptible to HE compared to lower grades. However, recent studies have reported the embrittlement in iron of much lower strength [80]. There are lots of debates when it comes to the effect of microstructure on the cracking susceptibility of pipeline steels. Some authors recommend acicular ferrite and bainitic ferrite for better resistance to HIC than ferritic pearlite or martensitic microstructure, but evidence in the literature has remained either inconsistent or less proven [81–86]. These inconsistencies might be a result of the different forms of hydrogen damage besetting pipeline steels. However, is it imperative to mention that tailoring the crystallographic texture, dislocation density, and grain boundary properties can positively influence susceptibility to HIC in pipeline steel [87–91]. Several studies have shown that dominant {1 1 1}, {1 1 0}, and {3 3 2}, planes oriented parallel to the pipeline surface can better resist crack propagation, unlike {0 0 1} planes of the same orientation. However, cracks have been observed across {1 1 0} ||ND textured grains, which necessitates further research on the influence of crystallographic texture on the HIC resistance in pipelines.

4.2. Sulfide stress corrosion cracking (SSCC)

Like SCC, SSCC is a pipeline failure mechanism that also involves the combined effect of stress and corrosion. It is a more devastating failure mechanism that leads to HE in wet H_2S media containing steel oil and gas lines [20]. The key parameters of SSCC are susceptible microstructure, corrosive environment, and tensile stresses. The kind of microstructural composition of the pipeline either increases or reduces SSCC susceptibility. As microstructure tends to control the mobility of hydrogen within the steel, it has been greatly investigated [1,92,93]. The hydrogen atoms generated at the surface of the steel substrates during cathodic reactions diffuse within the steel material. The diffused hydrogen atoms reside in reversible (e.g., grain boundaries, dislocations.) or irreversible (e.g., inclusions, precipitates) traps, though escape from the latter is possible at ambient conditions [73]. Liu et al. reported the impacts of grain boundaries and dislocations on the SSCC susceptibility in casing steel [94]. Their results show that dislocations influenced SSCC behavior much more than grain boundaries. This could be due to the localized plastic deformation associated with hydrogen-mobilized dislocations. However, looking at the effect of dislocation and grain boundary separately will throw more light on their influence on SSCC. SSCC is usually classified by relating the two types: *type 1 and type 2* [95]. For *type 1,* the formation of a hydrogen-induced blister crack may take place along the direction of the applied tensile stress, stress-oriented hydrogen-induced cracking (SOHIC). The failure mechanism of *type 1* may be in two stages depending on the direction of crack propagation (parallel or perpendicularly) concerning the applied stress. *For type 2*, the crack is propagated from the typical location of hydrogen embrittlement. There is a distinct difference between HIC (no external loading required for failure) and hydrogen-induced blister crack (HIBC) (stress is required for failure), however, these processes have similarities too - They are both explained by the internal pressure theory [96], which proposes that the accumulation of hydrogen in voids or cracks creates high pressures of hydrogen gas within the metal thereby initiating cracks [97] and after crack nucleation, they both propagate along the rolling direction of the steel. There remains insufficient literature revealing the understanding between HIC and SSCC resistance in the SOHIC mode [98]. From the literature, Cayard et al. showed that most HIC-resistant steels may also be more prone to SOHIC than some conventional ones; this further adds more difficulty to the selection criteria for SOHIC-resistant steel grade [99]. Kim et al. [95] have also tried to show a correlation between HIC and Type I SSCC failure mechanism in high-strength pipeline steel. They compared the SSCC resistance of pipelines under applied tensile stress with the one charged with hydrogen. They concluded that HIC occurs as an initial crack of type I SSCC.

Generally, hydrogen embrittlement is pronounced after crack initiation in a susceptible material from a combination of defined amounts of hydrogen and critical stress levels. While this situation is accepted to some extent, the exact hydrogen embrittlement mechanism is still a subject of intense controversy [100]. Formerly, it was inferred that hydrogen embrittlement is a result of restricted or promoted movement of dislocation under the influence of hydrogen within interstitial spaces in steel. To support this reasoning, it was reported that hydrogen influenced the decrease in cohesion between cleavage planes and/or grain boundaries [101]. Interestingly, Campari et al. utilized the machine learning approach to predict the hydrogen embrittlement susceptibility of metallic materials [102]. In their study, experimental data of tensile tests carried out in a hydrogen environment was performed and analyzed through an advanced machine learning approach. According to the authors, the embrittlement index was estimated and used as the determinant parameter for predicting the likelihood of component failures, which has an accuracy rate of 88.6 %.

Many theories and models have been introduced to shed more light on hydrogen embrittlement in pipeline steels. The first theory is the hydrogen-enhanced decohesion (HEDE) model which infers that bonding strength is reduced by interstitial atomic hydrogen [103–107]. It was revealed that in the HEDE theory, the hydrogen-induced weakening of metal–metal bonds leads to decohesion instead of slip. The HEDE mechanism is characterized by smooth brittle fracture surfaces with limited plasticity. Katzarov et al. were able to report the HEDE mechanism in sub-grain boundaries and *trans*-granular fracture of micro-alloyed steel. The authors also investigated HEDE within bcc a-Fe (1 1 1) crystal planes [108]. The second model proposes that the occurrence of localized plastic deformation is due to hydrogen-induced dislocation processes. This happens as hydrogen atoms cause the movement of dislocations, causing localized stress in the steel lattice. In case of defects, such stresses can easily initiate a crack. This is the Hydrogen-Affected Localized Plasticity (HALP) model, pioneered by Beachem [109]. In recent times, this model has been modified into two: hydrogen-enhanced localized plasticity (HELP) [110,111] and Adsorption induced dislocation emission (AIDE) [101,112]. When the applied hydrogen-induced stress is in a magnitude greater than the cohesive strength along interfaces, the presence of impurities reduces the gross cohesive strength resulting in decohesion, and finally, the initiation/propagation of interfacial cracks [108]. Birnbaum also reported potential regions with greater affinity for hydrogen-related decohesion: (a) at crack tips as adsorbed species, (b) at particle–matrix pivots ahead of cracks, especially where dislocation shielding effects lead to the highest tensile stress, and (c) at locations of utmost hydrostatic stress [113]. The hydrogen-enhanced localized plasticity (HELP) model has also grown in popularity. The

Table 2
Pipeline steel grades and their strength requirements.

API 5L Grade[a]	Min YS (Mpa/ Ksi)	Max YS (Mpa/Ksi)	Min TS (Mpa/Ksi)	Max TS (Mpa/Ksi)	Min elongation (%) for 0.2 sq in sample
A25	172/20	——	310/45	——	——
A	207/30	——	331/48	——	——
B	241/35	448/65	413/60	758/110	22.5
X42	289/42	496/72	413/60	758/110	22.5
X46	317/46	524/76	434/63	758/110	21.5
X52	358/52	531/77	455/66	758/110	21.0
X56	386/56	544/79	489/71	758/110	19.5
X60	413/60	565/82	517/75	758/110	18.5
X65	448/65	600/87	530/77	758/110	18.0
X70	482/70	621/90	565/82	758/110	17.0
X80	551/80	690/100	620/90	827/120	15.5
X90	625/90	775/112	695/100	915/132	–
X100	690/100	840/121	760/110	990/143	–

[a] American Petroleum Institute (grading system where identification number for each steel corresponds to minimum yield strength measured in Ksi); YS – yield strength; TS – tensile strength.

Table 3
Classification of the new generation of high-strength pipeline steels based on microstructural control.

API- 5XL Steel grades	Steel manufacturing process	Microstructure	Microstructural features
X70	TMCP + QT	Bainite-Martensite multiphase steel: B + M + F	Slender bainitic sheaves along with martensite laths [124].
X80	TMCP + AcC	Bainite dual-phase steel: B + F	Smaller prior austenite grain (PAG) and fine ferrite grains [125]. Martensite laths [124].
	TMCP + AcC + HOP	Bainite-Martensite multiphase steel: B + M + A	High volume fraction of filmy Austenite [126,127].
X100	TMCP + AcC + HOP	Bainite dual-phase steel: B-F	Polygonal and granular ferrite acts as the second phase in the bainite matrix [128].
X120	TMCP + AcC	Martensite dual-phase steel: M + F Tempered Lath Martensite: TLM	Fine ferrite acts as the second phase in the martensite matrix [129]. Martensite laths [130].

HELP model considers crack propagation through the coalescence of defects. Depending on specific temperatures and strain rates, the HELP model proposes that atomic hydrogen inside the steel lattice causes dislocation motion, leading to increasing deformation at localized regions [110]. When these hydrogen-engaged dislocations are close to defects(cracks), the resulting damage is no longer embrittlement but a localized plastic-type fracture [114]. Since both theories are not related to each other, it is best to understand that HEDE proposes that decohesion precedes cracking, while HELP proposes that enormous plasticity, which is induced by the enhanced velocity of dislocations precedes cracking. For HELP, when the elastic energy of steel is reduced due to hydrogen, there will be minimized obstructions and enhanced velocity of dislocation. As dislocations continue to interact, they pile up at microstructural defects, and this results in material failure [115].

Ultimately, a comprehensive understanding of these models indicates that the microstructural characteristics provide valuable insights into their intricate functions concerning the resistance of pipeline steels against cracking and corrosion.

4.3. Improving SSCC resistance in pipeline steels

From a few studies, the elimination of residual stress can greatly improve the SSCC resistance of pipeline steels [116,117]. Zhao et al. proposed the use of nano-sized carbonitrides as a way of improving the SSCC resistance of acicular ferrite pipeline steel [118]. The reductions of inclusions in pipeline steel or attaining inclusions will also improve SSCC resistance. For welded joints, lowering the heat input can greatly improve SSCC resistance, especially in the heat-affected zone (HAZ) [118,119]. In addition, tailoring dislocation density, and crystallographic texture will favor SSCC resistance [117].

5. Microstructure overview

The role of microstructure in influencing the susceptibility of pipeline steels to hydrogen-related degradation mechanisms is crucial. However, a holistic comprehension of these functions hinges upon our grasp of the thorough range of microstructural analysis. The new generation of API-5XL steels is classified into four categories based on microstructural control, as shown in Table 4

In essence, microstructure constitutes an amalgamation of different features that exert a profound influence on the mechanical

Table 4
Shows how hydrogen at different pressures affect the mechanical properties of pipeline steels.

Pressure (psig)	Pressure (atm)	UTS (ksi)	Elongation (gage: 30 mm) %	Reduction of Area (%)
Ambient (Air)	1 (Air)	70.8	32	64
147 (H_2)	10 (H_2)		34.5	52
294 (H_2)	20 (H_2)		33	47
735 (H_2)	50 (H_2)		30	50
1470 (H_2)	100 (H_2)		30	36.5
2205 (H_2)	150 (H_2)		26	28
1470 (Argon)	100 (Argon)		36	62

properties of a material. It transcends mere phase composition, encompassing factors such as grain size, grain boundary attributes, dislocation density, crystallographic texture, and so on [9]. These diverse characteristics contribute to the understanding of the mechanical properties of pipelines (see Table 3). Table 2 shows pipeline steel grades and their strength requirements. To illustrate, consider the case of three API 5L X65 pipeline samples sharing identical microstructural phase compositions, characterized by pearlite and ferrite. These samples exhibited varying mechanical properties following quenching in different quenchants at different cooling rates. These differences in cooling rates introduced dissimilarities in crystallographic texture and altered the microstructure without necessarily affecting the phase composition [120]. Apart from microstructure, the choice of pipeline also depends on operational parameters like pressure, temperature, fluid velocity, and flow pattern [121]. A pipeline of higher tensile strength should be used to carry high-pressure substances to be able to withstand stress without deformation or failure. Additionally, pressure fluctuations, especially in systems with frequent changes, require pipelines capable of handling cyclic loading without fatigue. Elevated temperatures often cause a reduction in steel's strength and increased susceptibility to corrosion or embrittlement [122]. Pipeline steel with high-temperature resistance or insulation should be used for such conditions. On the other hand, pipeline steels with high fracture toughness and low ductile–brittle transition temperature (DBTT) should be used in arctic regions [123]. Lastly, high fluid velocities can cause corrosion within pipelines, especially at bends or areas of turbulence. The flow pattern, whether laminar or turbulent, also affects the forces exerted on the pipeline walls.

Our following sections will delve into an exploration of these diverse microstructural parameters and their respective contributions to the HIC and corrosion resistance of pipeline steels.

5.1. Microstructural phase composition

The microstructural phase composition of steel is normally used to define the microstructure of steel. However, we have explained how broad microstructure can be. Phase composition reveals the microconstituents of steel after processing. There are several microconstituents found in steels depending on their processing route, ferritic pearlite, polygonal ferrite, quasi-polygonal ferrites, Widmanstatten ferrite, acicular ferrite, bainitic ferrite, bainite, martensitic microstructural phases, etc. All these microstructural phase compositions can be formed by controlling critical TMCP parameters such as the cooling rate applied after hot rolling [1,93]. From various studies, different phase compositions have known advantages on the mechanical properties of steel, as regards the formation and propagation of cracks.

According to published reports, in ferrite grains, a decrease in slip length and a decrease in the deformation around the crack tip during crack propagation is observed [128]. In comparison, smaller prior austenite grains foster a decrease in dislocation pileups or increase the barriers against crack propagation [128]. Film-like austenite grains facilitate crack-tip blunting through the transformation of the retained austenite to the martensite. It is also known that a decrease in the propagation rate of the main crack due to the compressive residual stress formation and propagation of the secondary crack is associated with the transformation-induced plasticity effect (TRIP) [131]. In comparison, Martensite laths induce the uniform distribution of dislocations and the rearrangement of stress concentration along the high-angle grain boundaries and act as a blockage of cleavage crack propagation along martensite lath boundaries [126].

Polygonal ferrite, as a second phase in the bainite matrix, can significantly increase the yield strength and low-temperature toughness and optimize the fatigue limit of pipeline steels [131]. The bainitic phase with a smaller width of the bainite laths has a higher stress intensity factor than the threshold value (kth) for crack blunting [125,126]. In terms of toughness, acicular ferrite is known for its high toughness. From historical studies, the API 5L X70 plates have a ferrite-pearlite microstructure for the most part, and acicular ferrite (AF) microstructure was induced as the best microstructure in terms of toughness [132]. Also, the formation of quasi-polygonal ferrite (QPF), fine polygonal ferrite (FPF), globular ferrite (GF), and AF microstructural phases with fine grains and more dislocations, increases ductility, as well as contributes to a reduction in pearlite bands according to the conclusions of Amirjani et al. [132].

While tempered martensite is inferred to have better ductility, the bainite and martensite regions having low ductility have high SSCC susceptibility. This further reflects the difficulty in balancing the strength and toughness properties of pipeline steels, regarding HIC [133,134]. After quenching and tempering, the martensitic phases are more refined and uniformly distributed. Quenching/tempering is mostly used to produce SSCC-resistant martensitic steels.

Interestingly, accelerating the cooling rates of steel processing can result in desired micro constituents like acicular ferrite and polygonal ferrite, thus bringing a better balance in pipeline steel's strength and toughness [135]. Amirjani et al. reported that increasing the accelerated cooling rate and reducing the finishing rolling temperature was responsible for the ductile fracture of API 5L

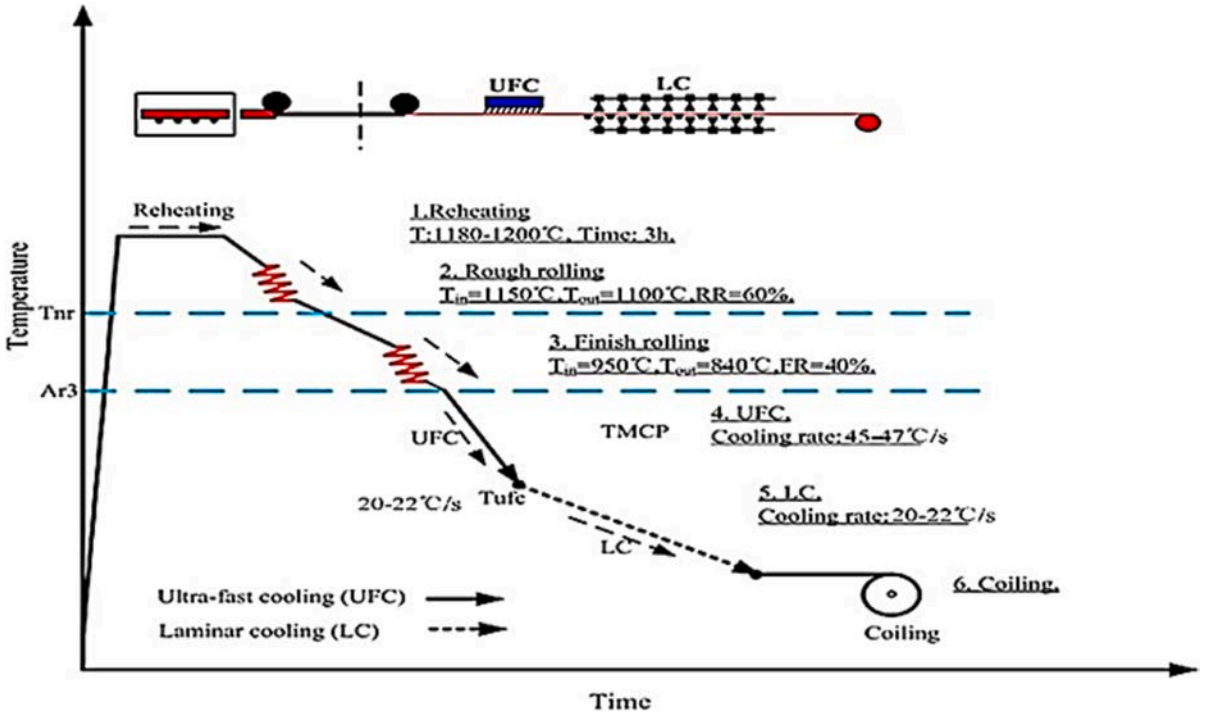

Fig. 3. Schematic diagram of thermomechanical-controlled processing (TMCP) showing dual cooling as an ultrafast cooling technique [136].

X70 after the drop-weight tear test (DWDT), and subsequently, the brittle fracture decreased due to the formation of QPF, FPF, GF, and AF microstructures that had fine grains and more dislocations [132]. Wang et al. proposed ultrafast cooling as a technique for balancing strength and ductility in pipelines, using dual colling. The first cooling rate was faster cooling (45–47 °C/s) while the second was a slower cooling rate (20–22 °C/s) [136]. Fig. 3 shows a Schematic diagram of thermomechanical-controlled processing (TMCP) showing dual cooling as an ultrafast cooling technique for balancing toughness and strength in pipeline steels. Meanwhile, employing cooling rates above 25-30c/s for steel plates might be challenging in industrial settings, as such rapid cooling requires specialized equipment and precise control over the cooling process, which might attract huge costs and technicality. However, with advancements in technology, boundaries can be pushed in this subject. This has led to new developments in hot-rolling technology, as new-generation TMCP technology combined with ultrafast cooling (UFC) has been applied to the hot-rolling line [136].

While this might seem difficult to comprehend and implement as an experimental approach, there are modern thermodynamic software like JMAT PRO and MUCG83 that aid the simulation of solid-state phase transformations in steel [67]. MUCG83 is a thermodynamic model developed by Bhadeshia [137]. Time-temperature-transformation (TTT) curves can be easily obtained from the MUCG83 model by feeding it the chemical composition of the steel. Now, JMAT PRO can be used in providing critical continuous cooling transformation (CTT) curves and other critical steel parameters [138]. With these models, we can try to understand how several parameters like cooling rate and finishing rolling temperature affect the mechanical properties of steels. Several researchers have used thermo-calc to predict the microstructural, mechanical properties, and continuous cooling transformations of pipeline steels [139–141].

5.2. *Microstructural trapping sites for hydrogen*

Understanding the effects of hydrogen trapping sites on the cracking and corrosion susceptibility of pipelines is essential. For pipeline steels, the type of trapping site within the steel is crucial, as it determines the susceptibility to hydrogen damage. Hydrogen-induced attacks are highly dependent on the trapping behavior of the steel lattice structure [44,73]. Trapping sites are divided into two parts: reversible and irreversible. Reversible hydrogen-trapping sites include grain boundaries and dislocations, and irreversible hydrogen-trapping sites include inclusions, precipitates, and some other elements of microstructure. Reversible traps tend to trap hydrogen for a short period, while irreversible traps can trap and house hydrogen for a longer period. In previous studies, reversible traps have been reported to be more critical to performance than irreversible traps [142–144]. While this remains a debatable subject, mobile or diffusible hydrogen is a hazard for pipeline steel operations.

Moving on, the introduction of hydrogen atoms into the steel structure and consequent attraction towards trapping sites and structure imperfections constitute the basis of hydrogen-related degradation. Hydrogen and its isotopes are among the smallest elements that have piqued the interest of researchers [96]. The high potential energy barrier of irreversible trapping sites must be overcome to allow the escape of hydrogen atoms. Fig. 4 shows a schematic representation of known trapping sites for hydrogen.

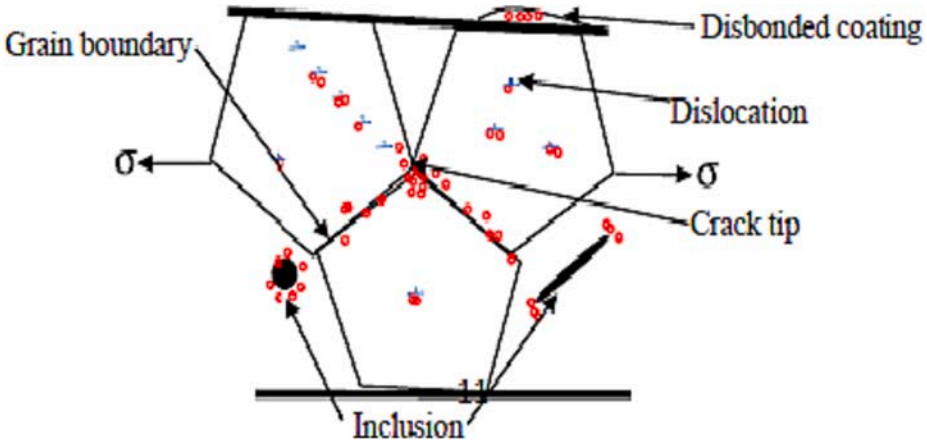

Fig. 4. Schematic representation of various trapping sites for hydrogen in pipeline steel [145].

Irreversible traps like martensitic interface and mixed dislocations were reported to possess binding energy in the range of 61.3–62.2 kJ/mol [146]. To prove the strong trapping proficiency of irreversible traps, the authors also recorded a higher hydrogen trap binding energy of up to 89.1–89.9 kJ/mol at grain boundaries with high misorientation and undissolved carbides. Their results spawned the conclusion that hydrogen atoms trapped irreversibly are excluded from those diffusing through the steel. On the other hand, the trapping sites where atomic hydrogen is weakly trapped are called reversible traps. These trapping sites require low potential energy barriers to permit atomic hydrogen escape. The strong presence of reversible traps has been noticed in cold rolled pipeline steels [143,147–150]. When enough plastic strain is in the pipeline steel because of cold rolling, a multiplication of dislocations and grain boundaries increases the number of reversible traps [147]. Till now, the detection of hydrogen atoms during their interaction with the steel structure remains complicated. To better understand the relationship between hydrogen embrittlement and trapping sites, information about the placement of hydrogen atoms concerning microstructural features at the nano/micro scale is required. However, because of the low atomic number of hydrogen, analyzing it at the nano/micro-scale has proven difficult by most available characterization techniques. For instance, lighter atoms like hydrogen pose scattering difficulties when X-rays and electrons are incident on them, unlike heavier atoms, making it difficult to analyze them through electron microscopy [151]. Even with thermal desorption spectroscopy (TDS) which provides macroscale information about hydrogen desorption, it remains difficult to evaluate hydrogen in traps, since this hydrogen originates from every possible trapping site, making it difficult to distinguish the different quota of contributions from the different types of hydrogen-containing defects [152]. However, neutron diffraction has achieved a significant milestone in the study of hydrogen interactions with metallic compounds [153–156]. While neutron diffraction might have shed light on hydrogen interaction with steel structure, its usage poses some challenges like cost and accessibility to users. Also, Mass spectroscopy techniques have been used to identify the location of hydrogen through the ratio of mass to charge state [151]. It was reported that the high spatial and mass resolution of atom probe tomography (APT) caused the easy mapping of hydrogen in nanoscale features in three dimensions [157–160]. Most times, APT is used to account for both precipitate analyses and the identification of microstructural defects such as grain boundaries and dislocations through associated elemental segregation [161–163]. According to reports, grain boundaries are the most efficient interface for trapping hydrogen in steels [164]. Yi-Sheng Chen et al. were able to observe the hydrogen-trapping behavior of grain boundaries, precipitates, and dislocations. They showed that the trapping affinity of many dislocations could override the trapping effects of grain boundaries in martensitic steel. However, on the annealed ferritic steel which had low dislocation density, more hydrogen-trapping affinity for the grain boundaries and carbide precipitates was observed [144]. Meanwhile, the types of hydrogen trapping sites and their role in hydrogen damage remain debatable within the scientific community. There are inferences that the high presence of irreversible hydrogen traps will increase the amount of hydrogen present within steel and will also reduce diffusible hydrogen within the lattice [165–168]. These inferences are because the irreversible traps starve the steel lattice of the much-needed hydrogen for crack initiation and propagation. Therefore, the strongly trapped hydrogen atoms are regarded as less likely to cause degradation. In other words, the combination of atomic hydrogen within irreversible traps is believed to produce hydrogen molecules and impede their diffusion through interstitial spacing towards crack-susceptible regions. It was also reported that widely distributed irreversible trap sites could potentially diminish hydrogen from reversible traps; hence lowering the chances of hydrogen embrittlement [169]. Jack et al. reported that more irreversible traps were responsible for the less severe cracks observed in the API 5L X65 pipeline after hydrogen charging when compared to the steel with more reversible traps. They also reported that hydrogen mobility through the steels was most prominent along the grain boundaries, indicating the significance of grain boundary character on HIC [142]. This was also in line with Diniz et al., as they mathematically simulated the effect of reversible hydrogen trapping effect on crack propagation in the API 5CT P110 steel. They concluded that crack initiation and propagation are both slower in pipelines with irreversible traps than in pipelines with reversible traps [170].

Peng et al. investigated the effect of MnS inclusions (irreversible trapping site) on the hydrogen trapping and HIC susceptibility of X70 pipeline steels. They found that most submicron scale inclusions in their steel were MnS, serving as irreversible traps for hydrogen. They also claimed that the amount of the trapped hydrogen can be significantly reduced by controlling the size of MnS inclusions below

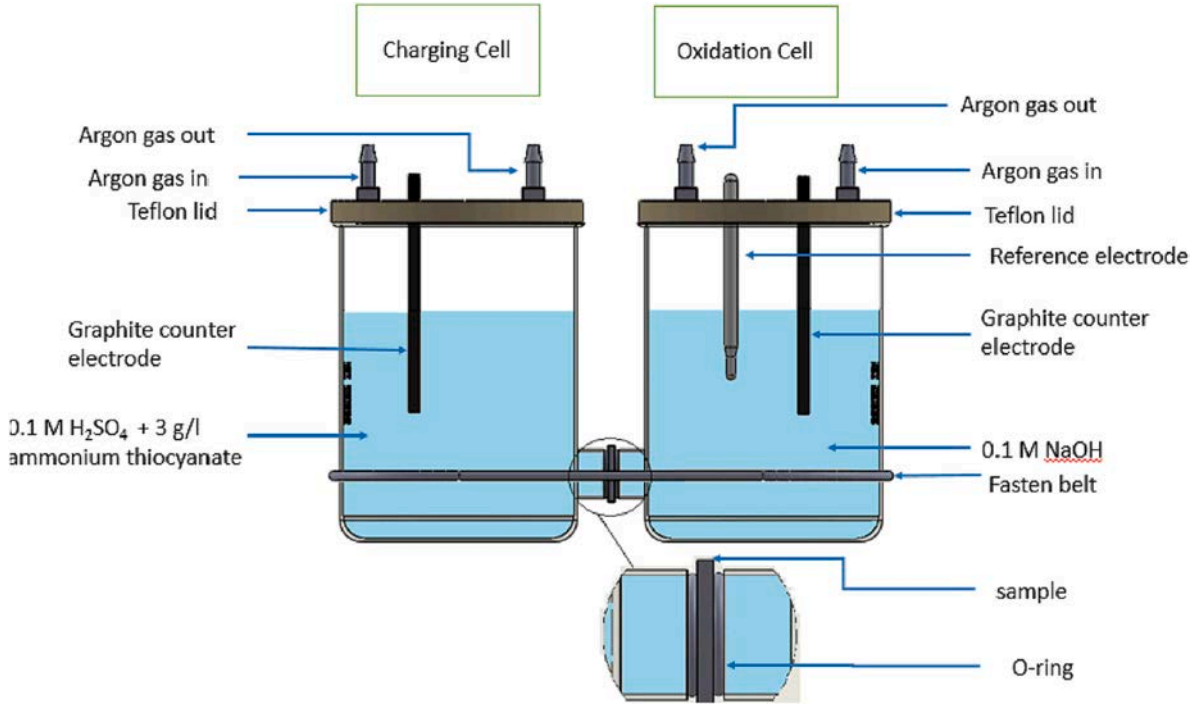

Fig. 5. Devanathan and Stachurski's setup for the hydrogen permeation experiment [173].

the submicron scale and distributing the inclusions uniformly in the steel, thereby reducing HIC susceptibility. This was also in line with Luu W et al. investigations on the effect of MnS on hydrogen transport in steels, where they concluded that MnS has more trapping affinity for hydrogen [15]. However, there are scanty studies regarding the multiplication of irreversible traps as a technique for minimizing reversible hydrogen trapping. This has to do with changes in other microstructural features, which play different roles in the HIC susceptibility of pipeline steels. Finally, the idea behind irreversible traps is that they mitigate the mobility of hydrogen in the steel matrix. It is believed that hydrogen in motion is a moving hazard to pipeline steels. However, Dadfarnia et al. concluded that although irreversible traps limit the amount of mobile hydrogen, we cannot infer that irreversible traps can be used to mitigate hydrogen embrittlement [171].

On the other hand, reversible traps, having low binding energy allow higher mobility of hydrogen, thereby increasing crack susceptibility [170,172]. With these parameters, the overall density of different trapping sites can be estimated. Fig. 5 shows the image of hydrogen permeation equipment used to determine the diffusivity of hydrogen, and for estimating the density of trapping sites in pipeline steels.

Interestingly, the impact of having a greater number of a particular trapping type in steel lattice has not been fully understood. Dadfarnia et al. used numerical simulation to predict that the greater density of one type of trap (whether weak or strong) can lower effective diffusion, but it does not necessarily affect the amount of hydrogen diffusing through normal interstitial lattice sites and any other type of trap [171]. However, this becomes a debate since it is somehow believed that the accumulation of hydrogen in traps could result in internal pressure, leading to crack initiation at high-stress concentration zones. Nevertheless, it was reported that increasing the density of irreversible traps can slow down the kinetics of hydrogen embrittlement [174,175].

5.3. Dislocation density

The dislocation density within the steel structure affects its mechanical properties, and therefore it should be considered when discussing microstructure. Generally, increasing dislocation density is a strengthening mechanism in materials. However, strengthening has a knock-on effect on the cracking susceptibility of pipelines. It has been reported severally that higher dislocation density reduces the HIC resistance of pipeline steels. Momotani et al. investigated the effect of dislocation density on martensitic steel [176]. In their research, it was concluded that high dislocation density facilitated hydrogen accumulation around prior austenite grain boundaries during deformation within the visible elastic strain regime. In the end, higher dislocation density led to the cracking of the steel. This can also be related to the HELP mechanism, where dislocations can move, interact, and pile up, thus causing bigger damage. Connoley also investigated the effect of dislocation on the HIC susceptibility of pipelines. From his interesting study, the steel sample with higher dislocation density had more cracks when compared with the sample with lower dislocation density [177]. When it comes to hydrogen trapping, dislocation density plays a bigger role in HIC susceptibility. Perng and Altstetter reported that the increased dislocation density allowed the trapping of more hydrogen, and it increased the effective hydrogen concentration[178]. The effect of

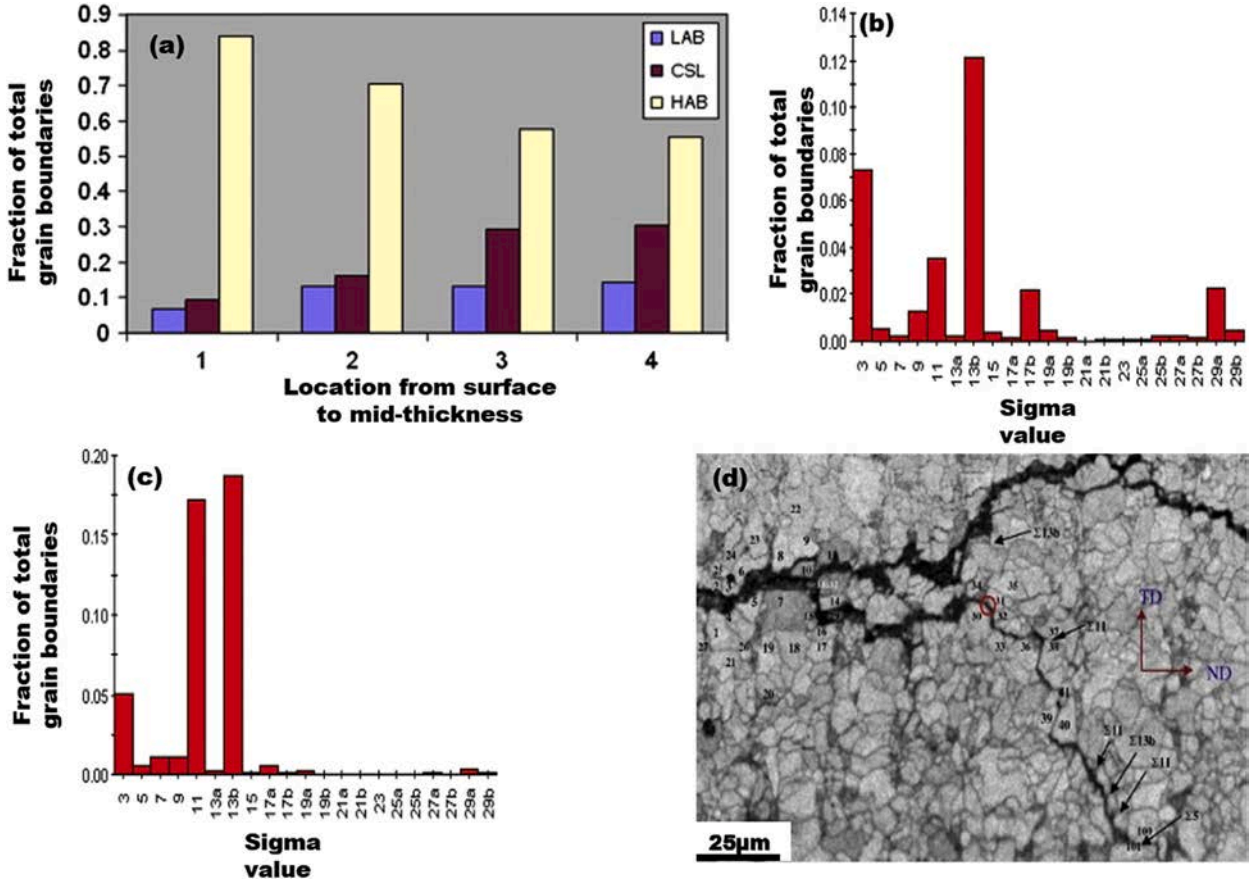

Fig. 6. (a) Distribution of grain boundaries from pipeline outer surface (location 1) through to mid-thickness (location 4), (b-c) shows the distribution of special CSL grain boundaries around crack-tips in X65 pipeline steel, and (d) EBSD IQ map showing crack propagation pattern along grain boundaries on ND-TD plane [11].

grain boundary and dislocation on the HIC resistance of pipelines has also been investigated. Grain boundaries are known to attract more hydrogen atoms than other trapping sites [164]. However, the conclusion of Yi-sheng et al. showed that dislocation density has a more pronounced effect on HIC than grain boundaries [144]. As such, dislocation density remains a vital parameter of note when optimizing pipelines for higher HIC resistance. On the contrary, few researchers have given different views about the effect of dislocation density on HIC resistance. Dislocations, to these researchers, are not trapping sites. Louthan and Derrick concluded that trapping sites were absent in austenitic steel that had dislocations induced through cold rolling [179]. However, dislocation density remains an important microstructural feature. Thomas and Szpunar showed that higher dislocation density due to cold working reduced the permeability and the effective diffusion coefficient of X70 steel relating to an increase in reversible trapping sites of hydrogen [150]. Generally, evaluating the effect of grain size without considering dislocation density is difficult. In such a scenario, pipelines are annealed to minimize the effect of dislocation on hydrogen transport within the steel lattice. Nevertheless, separating the mechanisms governing the transportation of hydrogen within the pipeline's structure, particularly in areas of pronounced transport propensity such as grain boundaries, and evaluating the significance of these regions, continue to be subjects of interest.

5.4. Grain boundary engineering

The character and distribution of grain boundaries are important, especially to pipelines under sour environments. Because hydrogen atoms accumulate in grain boundaries, it is imperative to understand the effect of grain boundaries on the HIC susceptibility of pipelines and to properly engineer them to improve their performance in sour/acidic environments [164]. Grain boundaries possessing low energies are more resistant to HIC, and thus TMCP processes are used in engineering low-angle grain boundaries (LAGB) and special CSL boundaries in steels [180]. Generally, three different grain boundary distributions have been discussed in the literature, they include high-angle grain boundaries (HAGB), LAGB, and special CSL. It was reported that large amounts of HAGB were seen at the surface (RD) of X65 steel, while LAGB and CSL were dominant in the mid-thickness region [11]. Arafin and Szpunar investigated the role of grain boundary on pipelines' intergranular stress corrosion cracking resistance. They found out that cracks were arrested more often at LAGB and CSL (Σ11, Σ13b, and, probably, Σ5). Also, cracking happened more often at grain boundaries having HAGB

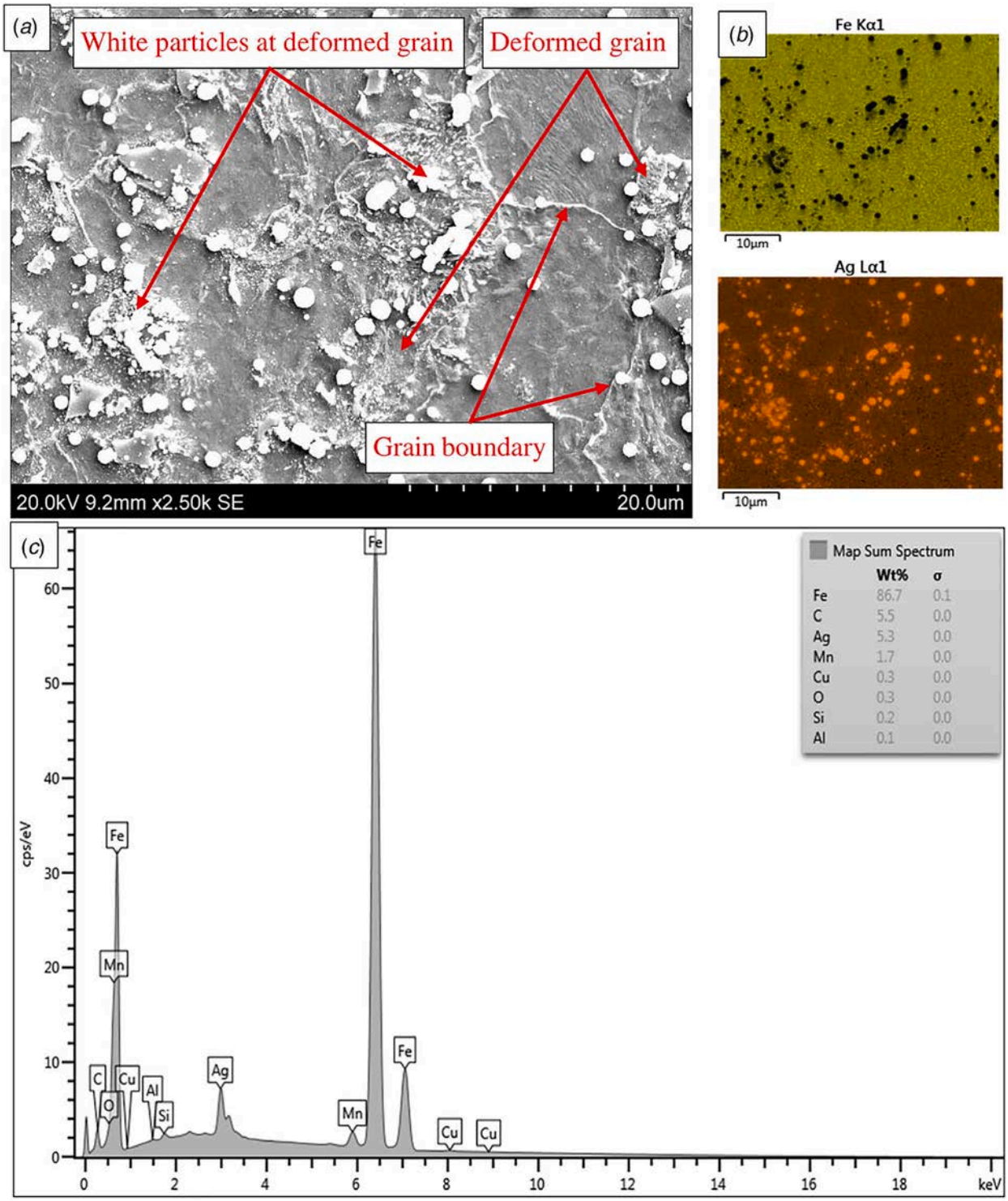

Fig. 7. Hydrogen diffusion in sample after HMT experiment (a) SEM image of deformed grains, (b) EDS maps of deformed grains, and (c) The EDS spectrum of deformed grains [150].

structure with an angle of misorientation greater than 15^0. With the four different grain boundary types and the probability of cracking in a sour/acidic environment, it can be deduced that HAGB favors intergranular cracking. Interestingly, this was also confirmed as the cracking path followed the HAGB direction until it encountered a triple junction of HAGB, LAGB, and CSL sites as shown in Fig. 6(a – d). Thomas and Szpunar also investigated the effect of cold rolling on hydrogen diffusion in the X70 pipeline. They showed that grain

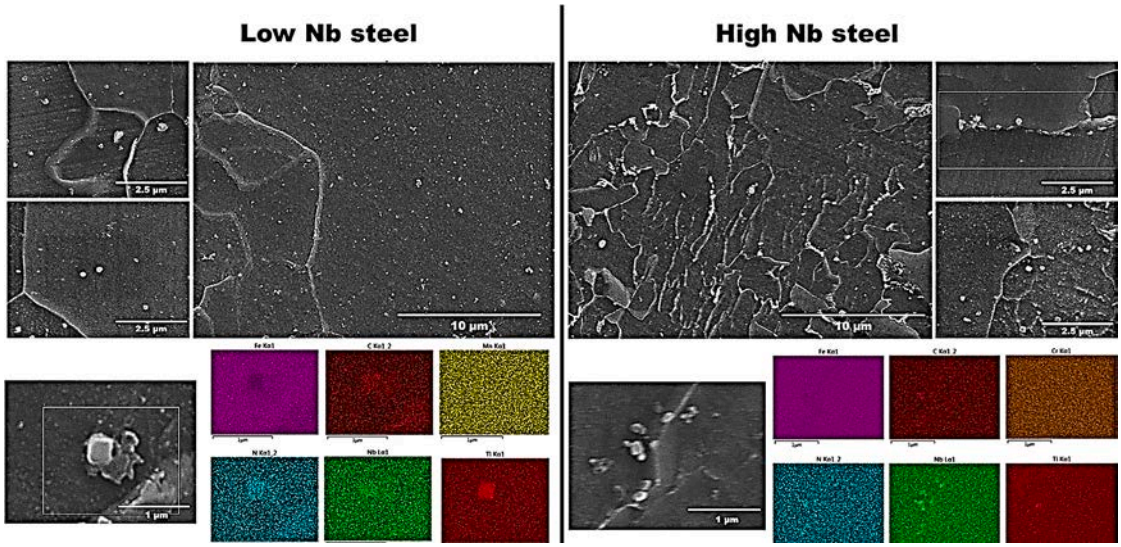

Fig. 8. Electron micrographs and energy dispersive X-ray spectroscopy of carbides observed on the top RD – TD planes of the low(left) and high (right) Nb steels [186].

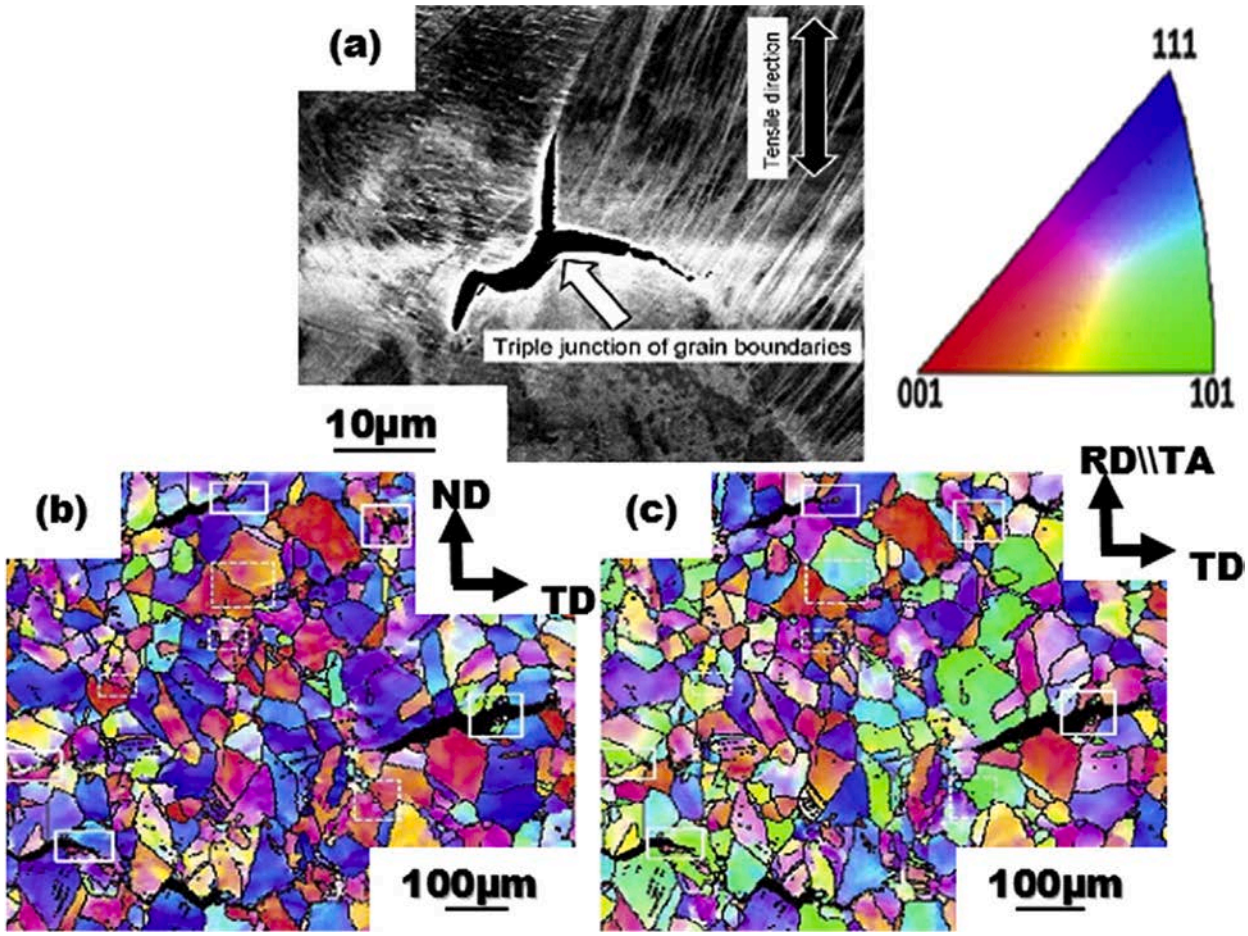

Fig. 9. HIC stricken TWIP steel (a) intergranular crack initiating at a triple junction (b) IPF map for ND-TD plane of the fractured tensile specimen (c) IPF map for RD-TD plane of the fractured tensile specimen(ND: normal direction, TD: transverse direction RD: rolling direction TA: tensile axis) [188].

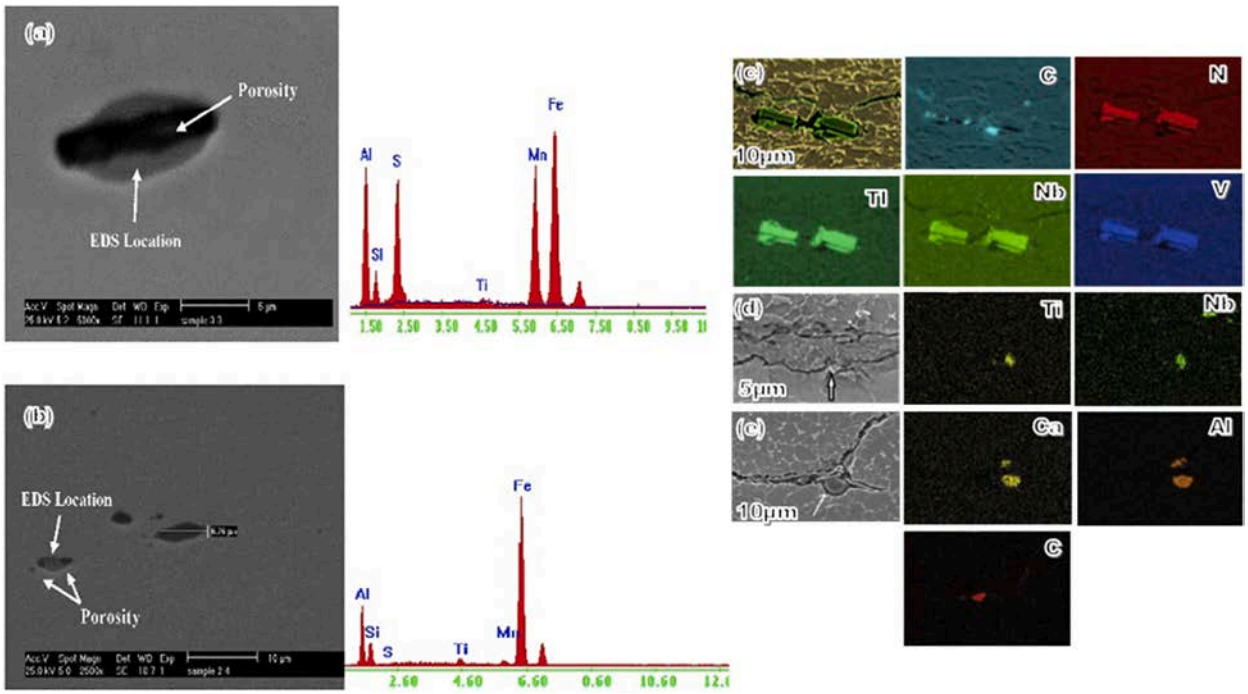

Fig. 10. EDS point analysis on inclusions in pipeline steel (a, b) [200], inclusion maps of HIC nucleating at Ti-Nb-V enriched carbonitrides (c) [88] and Al-Ca-C enriched oxide inclusions in X70 pipeline steel (d, e) [182].

boundaries are reversible trapping sites through HMT experiments, visible in Fig. 7(a-d). The multiplication of grain boundaries due to 50 % cold rolling reduced the permeability and effective diffusion coefficient during the permeation test. This shows the overall effect of grain boundaries on hydrogen transportation within the steel lattice. However, when compared with the hydrogen diffusion rate on deformed grains, the grain boundary hydrogen-diffusion rate seems to be lower.

There is limited literature on proven methods for engineering pipeline steels towards having CSL and LAGB character, however, it has been reported that low stacking faults give rise to CSL boundaries. Also, twinning can give rise to these special grain boundaries. However, twinning is difficult to see in pipeline steels [181]. According to some researchers, warm (ferritic) rolling can induce a higher fraction of LAGB and CSL sites in pipeline steels [89]. Many publications have addressed the importance of low-energy grain boundaries in the reduction of HIC in pipelines [89,90,182,183]. It has been revealed that another characteristic of CSL boundaries and LAGB is that they act as reversible trapping sites, as they do not hold hydrogen for long. This is contrary to other inferences on grain boundaries. However, the theory behind it is that the low-energy grain boundaries do not allow hydrogen to build up to the critical levels of initiating cracks. Instead, they allow uniform distribution of atomic hydrogen within the steel lattice and subsequently allow desorption processes without tendencies of crack initiation [182]. Another interesting study showed that Σ11 type CSL boundaries are usually present around grains having orientations of ⟨1 1 0⟩, reducing their susceptibility to HIC[184]. Another area to consider is the relationship between grain boundary migration and pipeline steel. The pinning mechanism, known as the Zener drag/pinning effect is known to control grain boundary migration [185]. While there is no consensus on how halting grain boundary migration affects the corrosion resistance of pipeline steels, a study by Jack and Szpunar had an interesting insight. In their study, the addition of more niobium (Nb) resulted in the improved corrosion resistance of the steel due to certain favorable microstructural features, as against Nb deficient steel. Amidst many reasons for the improved corrosion resistance by the authors, the grain boundary pinning due to precipitates around them resulted in more refined grains, which was more beneficial for the steel in the selected acidic solution, hence improving its corrosion resistance [186] as shown in Fig. 8.

Also, in terms of corrosion resistance, Wright and Field proposed that the combined effect of grain boundary and crystallographic texture can effectively influence the corrosion resistance of polycrystalline materials [187]. Interestingly, with characterization techniques like transmission electron microscopy (TEM), electron backscatter diffraction (EBSD), and electron channeling contrast imaging (ECCI), the inner workings relating hydrogen interaction with dislocation pileups in grain boundaries have been probed. Koyama et al. made an interesting milestone in probing the effect of hydrogen-assisted degradation mechanism in twinning-induced plasticity (TWIP) steel. They concluded that initiated HIC is easily propagated at grain boundaries [188] as Fig. 9a shows crack initiating at a triple junction before.

propagating along grain boundaries. Fig. 9 (b-c) shows that most micro-cracks that were found along HAGB as indicated in the EBSD inverse pole figure (IPF) maps obtained for both ND-TD (Fig. 7b) and RD-TD (Fig. 7b) planes respectively.

With hydrogen trapping sites like grain boundaries gaining attention based on their affinity to hold hydrogen, it is imperative to understand other trapping zones and their role in the HIC sensitivity of pipeline steels.

5.5. Inclusions and precipitates

Unlike other microstructural features, there are few techniques available for investigating the role of inclusions and precipitations on HIC nucleation at the microscopic level. Nonetheless, many studies have been made on the effects of inclusions/precipitates on the HIC resistance of pipeline steels [189]. It is believed that inclusions and precipitates foster hydrogen attacks on pipeline steel, as they provide accumulation sites for hydrogen, which has a deleterious effect on the mechanical properties of pipeline steel [27,190,191]. It has also been implied that inclusions/precipitates are irreversible trapping sites, having higher binding energies to hold hydrogen for longer periods. Inclusions, which are usually harder than the steel matrix, are seen as crack initiation/propagation regions, as they can create an incoherent interface with the pipeline steel matrix, thus increasing hydrogen trapping and causing failure by cracking [191]. However, not all inclusions are incoherent sites. The coherent sites have less affinity for cracking initiation.

Inclusions that are either coherent or semi-coherent with the steel matrix have lower binding energy for hydrogen compared to those that are incoherent [146,192]. Wei et al. investigated the role of incoherent TiC precipitates in hydrogen trapping [193]. Incoherent TiC was revealed as a hydrogen trapping site based on temperature and volume of particles instead of the interfacial area with the steel matrix. According to the authors, the high affinity for hydrogen trapping within incoherent TiC particles was related to the high concentration of octahedral carbon vacancies in the semi-coherent particles with fewer carbon vacancies. In the trapping sites, an increase in the activation energy required for cracking with a reduction in coherency was noticed. Since in the service environment pipelines experience fluctuating temperatures, it is imperative to understand how the temperature affects the trapping nature of reversible traps or irreversible traps. From Fig. 10, the hydrogen accumulation mechanism around different inclusion types can be understood. An interesting region to note is voids. These voids become hydrogen-trapping sites and consequently become problematic. When hydrogen migrates into the interfacial voids, consequently, we might observe an increase in internal pressure and high-strain conditions to form cracks [194]. Usually, inclusions are either spherical or elongated, with both having their hydrogen-trapping uniqueness. Elongated inclusions are known to have hydrogen atoms accumulating more at the edges where there is a high-stress concentration. It has been observed that there are often colonies of several metallic inclusions along the HIC propagation path in pipeline steel [195]. Jack and Szpunar were also able to show how precipitates/particles that pinned grain boundaries induced some corrosion resistance on high niobium pipeline steel [186]. Given that cubic and rectangular-shaped particles were mostly found in the high Nb steel, a stronger and more effective pinning of grain boundary movement was reported. Ringer et al. also reported that cubic-shaped particles are far more effective than spherical and ellipsoidal particles in pining grain boundaries, with a Zener pining pressure almost two times that of the globular (spherical) particles [196]. The effect of the shape or morphology of inclusions and precipitates on the HIC resistance in pipeline steels has been controversial. There is a general belief that spherical-shaped inclusions don't affect the HIC resistance of pipeline steel, as much as other morphologies. Bonab et al. reported that spherical inclusions of oxides formed by aluminum (Al), calcium (Ca), manganese (Mn), and magnesium (Mg), which constituted 70 % of the total amount of inclusions did not cause HIC damage to X70 pipeline steel. Instead, the inclusions fostered a significant decrease in fracture toughness. While the authors believe that the significant reduction of HIC damage was a result of the spherical-shaped inclusions, which also supports the general belief, there still exists a controversy. Jin et al. reported that oxide inclusions of Al and Si induced HIC amidst other oxides of Ca-S-Al-O type and MnS found in X100 pipeline steel [194]. Fig. 10 a and b mainly show MnS and aluminum oxide types of inclusions surrounded by porous voids at the pipeline steel matrix/inclusion interface. It can be concluded from these results that cracks nucleated at the cavities formed because of poor adhesion of pipeline steel matrix and inclusion. In addition, Fig. 10e indicates HIC nucleating from oxide inclusions of Al and Ca, as well as carbonitride precipitates of Ti, Nb, and V (Fig. 10c and d). More findings also supported the findings that oxide inclusions of Ca and Al induce HIC in X70 pipeline steel [65,182]. Techniques for controlling the morphology of MnS inclusions have gained significant attention. For instance, the use of fine oxide inclusions as heterogeneous nucleation sites by adding titanium, magnesium, and zirconium [17,197]. Another method is modifying the morphology of the MnS inclusions by calcium or rare earth treatment [198,199]. Wang et al. proposed the addition of tellurium as a way of controlling the morphology of MnS inclusions [19].

While precipitates and inclusions are usually irreversible traps, several studies have shown that the precipitates are less harmful. Martensitic steels having carbide precipitates have higher strength, which often results in cracking and easy crack propagation. Qifeng et al. reported that carbide precipitates resulted in higher local normal stresses and lower plastic deformation, which increased the overall strength. The carbide precipitates impeded dislocation motion, resulting in high local stresses around the carbide precipitates, which led to large crack opening stresses on cleavage planes of {1 0 0}[201]. Inclusions, which are already inherent in the steel during the production phase, remain a bigger threat to the steel's HIC resistance. Peng et al. investigated the effect of non-metallic inclusions on the critical size for HIC initiation and their role in hydrogen trapping. Their study covered some MnS inclusions and some oxide inclusions. It was reported that MnS inclusions brought about a larger critical size tolerance of HIC nucleation (approximately 2.5 μm), but for some typical oxide inclusions, it ranged between 0.1 and 0.4 μm. From their study, it can be deduced that finely dispersed non-metallic inclusions can trap more diffusible hydrogen and improve the HIC resistance of steel [202].

Overall, several inclusions have been identified in pipeline steels, which are enriched with silicon, aluminum oxide, magnesium, calcium oxide, carbide, iron, and manganese as shown in Figs. 11 and 12. The effect of inclusions on the HIC resistance of pipelines is dependent on their type, amount, size, and distribution. For instance, Kim et al. reported that the hydrogen-induced cracks primarily nucleated at inclusions enriched with Al and Ca oxides. Also, inclusions with a size over 20 μm in length induced HIC damage in steels that contained a bainitic ferrite structure [203].

The number of inclusions also contributes to HIC in pipeline steels. Huang et al. investigated the effects of inclusions on the HIC susceptibility of X120 pipeline steel and concluded that the larger number of inclusions contributes to the HIC of the steel [204]. While it might be difficult to control the number of inclusions, the geometry of inclusion can be largely controlled. It was demonstrated that

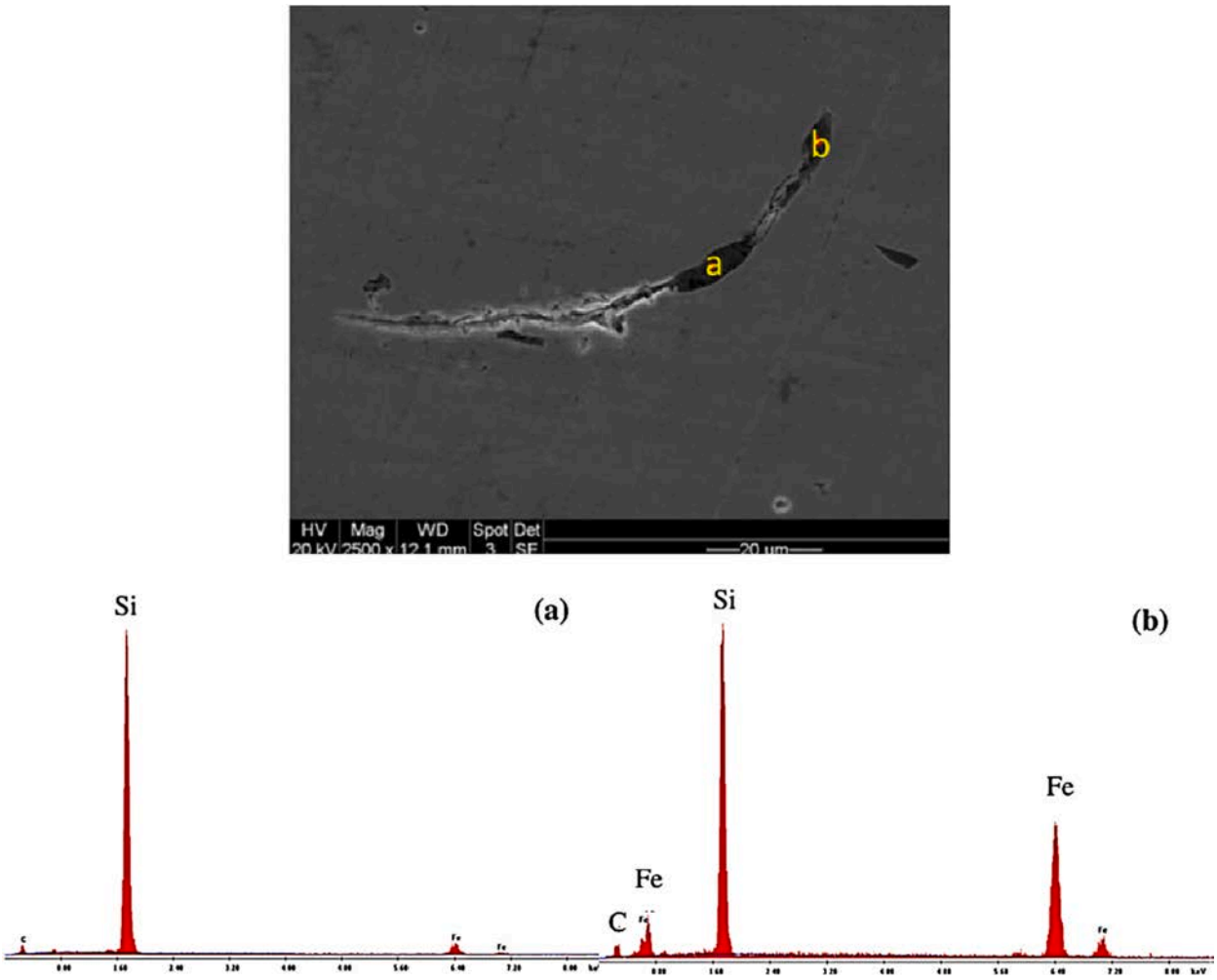

Fig. 11. SEM image of a crack initiating from a Si-enriched inclusion [204].

the resistance of steels to HIC can be improved by controlling the nature and geometric characteristics of the non-metallic inclusions [18]. Interestingly, Jiang et al. simulated the modification of inclusions by rare earth metals Ce and checked the SCC resistance, experimentally. The authors concluded that the risk of cracking was eliminated or alleviated, and the SCC resistance of the steel was improved [205]. Also, they reported that the composition of inclusions containing Ce will change during solidification, combining with S in molten steel to reduce its activity and further help to avoid the formation of CaS + Ca–Al–O duplex inclusions.

Interestingly, recent research indicates that the orientation of grains in pipeline steels also exerts an impact on their resistance to hydrogen-induced cracking (HIC). This preferred grain orientation is called crystallographic texture, and it has been a subject of interest to material scientists.

5.6. Crystallographic texture

Another important microstructural feature of pipeline steel is crystallographic texture. Texture represents the preferred orientation of grains and has been discussed concerning pipeline corrosion and HIC resistance. This is because TMCP induces deformation on the pipeline steel, causing grains to be oriented. The texture is often inhomogeneous through the thickness of the steel and these inhomogeneities have been reported to influence crack initiation and propagation in pipeline steel [206]. With these unavoidable texture inhomogeneities after hot rolling, it has been reported that boundaries between grains having {1 1 0} and {1 1 1} planes oriented parallel to the pipeline steel surface are more resistant to hydrogen-related degradation [142,207–209]. To ascertain the effect of crystallographic texture on the HIC resistance of pipeline steel, Lavigne et al. utilized three-dimensional crack images obtained from cracked X65 pipeline steel through X-ray microtomography. From Fig. 13, the cracks are observed to begin perpendicular to the pipe's outer surface but deviate out of its path on approaching the mid-thickness region.

To get a better understanding regarding the reason for the deviation, the authors applied neutron diffraction texture measurements, where they observed that the point at which the crack path deviated corresponds to the region where the crack encountered a strong

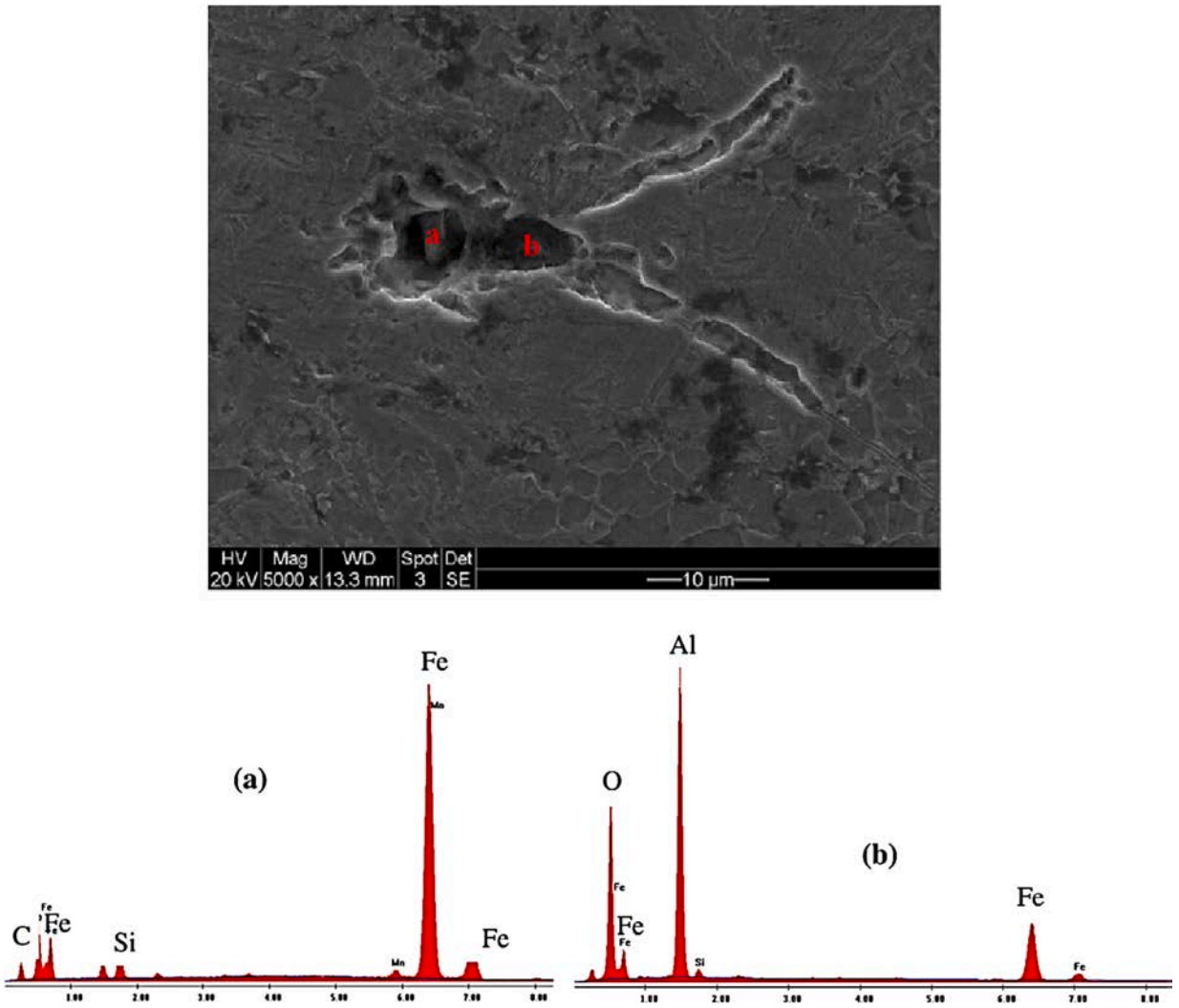

Fig. 12. SEM image of a crack initiating from an inclusion enriched in Si and ferric carbide [204].

presence of shear texture such as ⟨1 1 0⟩||TD with {1 1 2}⟨111⟩orientation as maxima. However, the region where the crack propagated perpendicular to the outer surface before deviating was dominated by ⟨1 1 1⟩||ND (-fibre) and ⟨1 1 0⟩||Ralpha fiber-oriented grains, with {1 0 0}⟨110⟩, {11}⟨110⟩ and {1 1 1}⟨112⟩ as maxima.

Interestingly, Jack and Szpunar had an observation regarding the role of texture on the corrosion resistance of high and low niobium steels. They found that the high Nb steel had conventional shear texture components, indicated by {0 1 1} <1 0 0> and {0 1 1} <2 1 1> along the ζ-fiber in Euler space as shown in Fig. 14. This was also marked by stable <1 1 0>||ND-oriented grains observed in the IPF and more {1 1 0} (green-colored) grains on the steel surface, as seen in the EBSD maps. The ODF of the low niobium indicated a strong presence of the rotated cube texture component, {0 0 1} <1 1 0>, with more {1 0 0} (red-colored) grains observed in the EBSD maps. Also, from the IPF for the low Nb steel, the grains seem to be oriented more towards <1 0 0>||ND than any of the other low-index directions. While these crystallographic texture dissimilarities were linked to internal strain differences between the two steel samples, it is worth noting that the high niobium steel showed better corrosion resistance than the low niobium steel because of their difference in texture [186].

Also, Arafin and Szpunar were able to establish that several patterns of intergranular crack propagation of the X65 pipeline were dependent on texture [11]. In their study, some cracks were mitigated at points having LAGB. This study confirms the general belief that HAGB promotes crack propagation, and it is imperative to understand that the cracking resistance of any pipeline steel is not always linked to one microstructural parameter, and most of the time several parameters are responsible for the cracking of pipelines, and this is why microstructure is greatly considered when studying hydrogen pipeline embrittlement. After the texture analysis of different cracks was obtained and the corresponding crack tip regions, it was established that texture was responsible for this result. From texture analysis, the cracks propagated dominantly through grains with {1 0 0} ||RP (rolling plane). However, the crack tip region was dominated by grains with {1 1 0} ||RP oriented grains and spawned the conclusion that intergranular cracks were arrested

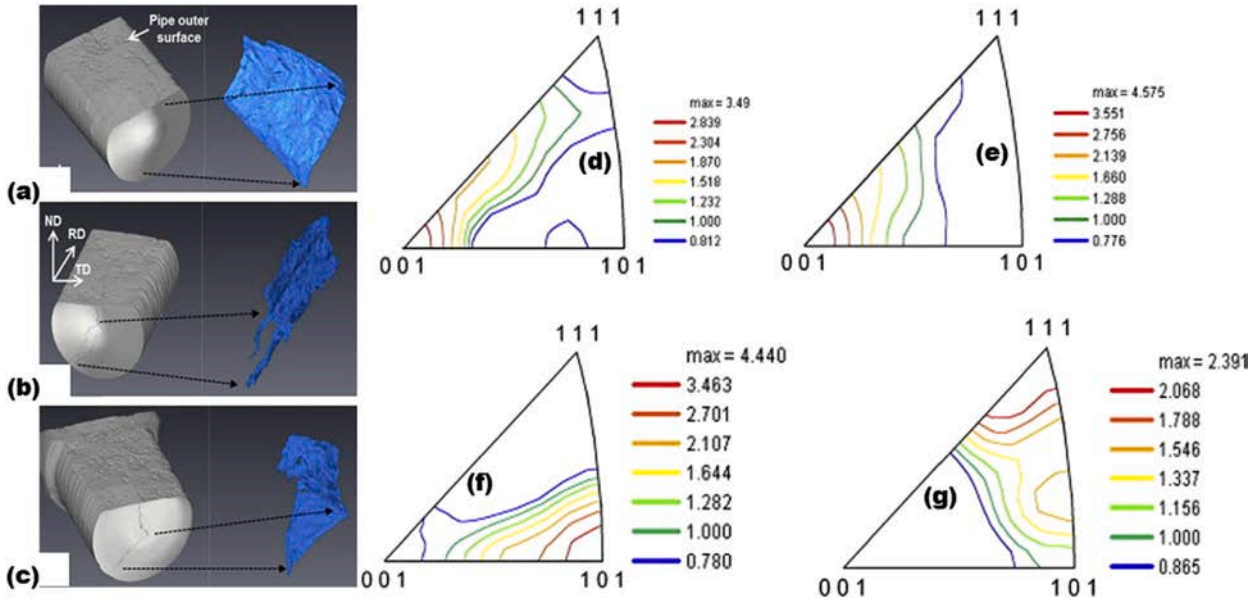

Fig. 13. Reconstructed three-dimensional X-ray microtomography images showing deflected cracks and volumetric segments of cracked area in (a-c) [10], IPF obtained from cracked regions (d, e), and IPF obtained ahead of crack tips (f, g) [11].

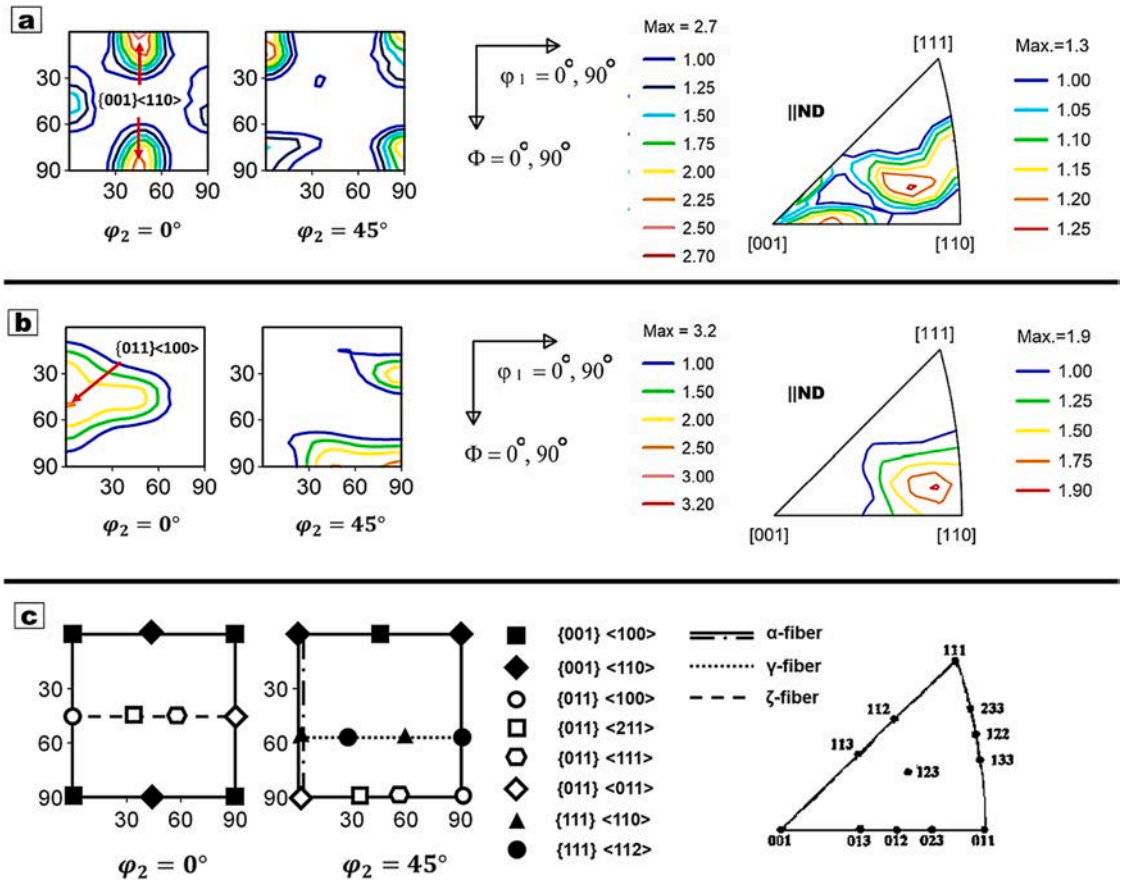

Fig. 14. XRD results showing the ODF and IPF of the top RD – TD planes of the (a) low and (b) high Nb steels, and (c) Some ideal texture components and fibers [186].

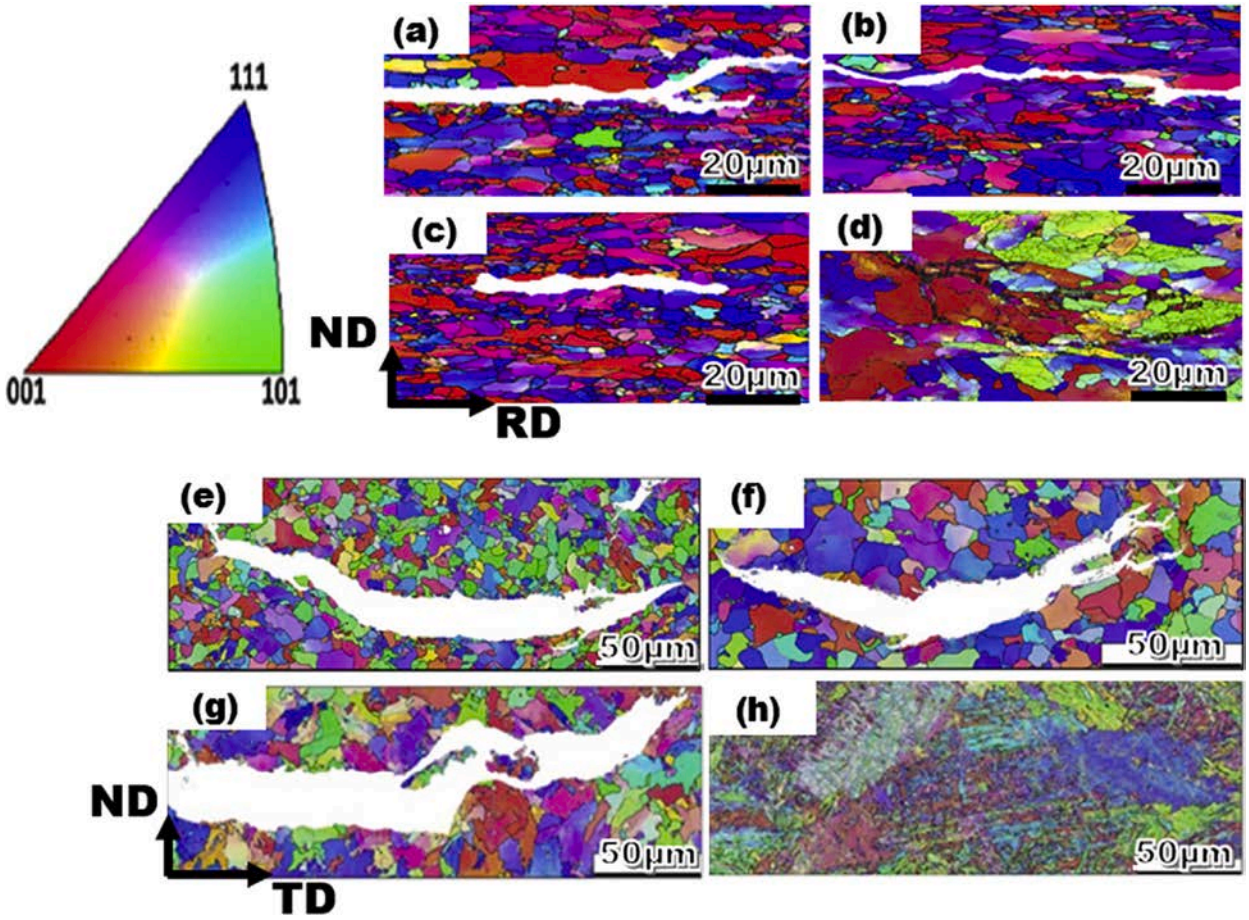

Fig. 15. EBSD orientation maps for HIC in X70 pipeline steel with different microstructures and texture (a to c) shows cracking at different spots containing small grains [10] (d) crack initiation and propagation through the boundary of {1 0 0} grain [87], (e)banded ferritic-pearlite (f) ferritic-granular bainite (g) equiaxed ferritic-pearlite (h) bainitc-ferrite[182](ND: normal direction, RD: rolling direction and TD: transverse direction of pipeline steel plate).

at grains with {1 1 0}||RP texture. While the authors studied intergranular cracks, it will be also good to look at other cracking types and their correlation with crystallographic texture.

Overall, emphasis has been placed on engineering pipeline steels having {1 1 1} planes parallel to their surfaces as a way of increasing their cracking resistance. However, there is no established consensus on how to engineer pipeline steels to achieve {1 1 1} planes. Interestingly, Omale et al reported that warm rolling with a finish rolling temperature of 700 °C favored the development of the γ-fiber texture, due to complete recrystallization [210]. According to the authors, the γ-fiber texture is better formed at the mid-thickness compared to the surface. This was also in line with Jack et al. report, that the shear-type deformation at the surface layer due to the sticking effect of the roller and the steel surface can lead to the formation of shear textures, which often exhibit {1 1 0} orientations parallel to the normal direction, ⟨1 1 0⟩||ND [211]. The inner layers (mid-thickness) are mainly deformed by plane strain deformation, which gives rise to the formation of conventional textures (γ-fiber and α-fiber) [212].

Masoumi et al. were able to establish that the development of dominant {0 1 1} grains parallel to the normal direction, and a small number of ⟨0 0 1⟩||ND grains obtained by isothermal rolling at 850 °C, increased the hydrogen-induced crack resistance; while the hot rolled sample with sharp ⟨0 0 1⟩||ND textures was highly susceptible to cracking [90]. They revealed that the preferential HIC propagation occurs along regions dominated by small grains within the X70 pipeline steel microstructure, where the said regions were confirmed to contain more dislocations and grain boundaries, which are known as hydrogen trap sites and zones for HIC initiation and propagation in the steel structure as shown in Fig. 15 a-c. The authors established the reason to be the high stored energy associated with small grains which is known for crack promotion around such regions. However, we recalled a controversial inference in the study, where the authors suggested the possibility of cracks propagating along boundaries of ⟨111⟩||ND and ⟨011⟩||ND oriented grains contrary to the belief that these orientations are HIC resistant [11,87,187,207,213]. Nevertheless, it is also understood that the grain boundaries of crack-resistant grains can be susceptible to cracking depending on their elastic energies. A perfect example is shown in Fig. 15d where HIC cracks were induced at ⟨001⟩ || ND oriented grain (red grain) but propagated through the boundaries of other grains with ⟨111⟩ || ND and ⟨011⟩ || ND orientation. The result was due to the grain boundaries through which the crack propagated, as

they were mainly HAGB. Despite the crack-resistant orientation of the so-called {1 1 1} grains, the crack continued its propagation because of the high stored energy stored in grain boundaries of small grains.

This is why some researchers have the opinion that texture has little or no effect on the HIC resistance of pipelines. Perhaps, since its effect is dependent on other microstructural features, it can be mitigated. However, it remains an interesting area of research and has attracted significant interest. Also, due to texture inhomogeneities, texture measurements will vary significantly depending on the processing history of the pipeline. Nevertheless, many studies have made use of the EBSD technique in correlating HIC and crystallographic texture even when a small sample area is used to account for the entire pipeline specimen [11,81,90,182]. We can draw inferences from different X70 pipeline steel samples with microstructures ranging from equiaxed ferrite-pearlite (Fig. 15g), banded ferrite-pearlite (Fig. 15e),ferritic-granular bainite (Fig. 15f), and bainitic-ferrite (Fig. 15h). It was established that *trans*-granular cracks propagated in all steels except the one with bainitic-ferrite microstructure. However, the most severe cracking occurred in the pipeline steel with banded ferritic-pearlite microstructure. While cracking resistance was noticed at CSL and LAGB, there was no dominance of a particular crystallographic orientation on the crack path. It was just composed of cracks that were preferentially propagating through the best-aligned slip planes, which correspond to {1 1 0}{1 2 3}, {1 1 2} planes, as well as {1 0 0} cleavage planes. Consequently, it was concluded that cracking was controlled by a dominantly slip-based mechanism and less cleavage. This is not the first study revealing no crystallographic texture dominance in steel lattices. Venegas et al. have already established the absence of any dominant orientation along the HIC propagation path on X46 pipeline steel [183]. While their study was performed on specimens obtained from an already-formed pipeline, it is quite interesting to note that the cracks aligned towards the radial direction of the pipeline in a somewhat 'S' shape, indicating a crack connection along slip planes. Also, pipelines experience hoop stresses along their radial direction during service, which means that strain fields near cracks could potentially cause the convergence of smaller cracks into larger ones. One of the recent areas of research regarding the corrosion behavior of pipeline steels is the role of grain size and crystallographic texture on corrosion [209]. This has set up an array of interest regarding the role of grain size in HIC and corrosion.

5.7. Grain size

Grain size is a microstructural parameter that hasn't been of great interest to researchers. Yet, few studies have shown its importance and roles in pipeline steel corrosion. Generally, ferrite grain size is an important factor for a pipeline's mechanical strength. That's why pipeline steel of properly refined grain sizes will show high mechanical strength [214–217]. However, due to higher energy and chemical activity on grain boundaries, as the density of these boundaries increases, there would be many electron activities and atom diffusion, subsequently resulting in failure [218,219]. While there is no established consensus regarding the role of grain sizes on hydrogen embrittlement, corrosion, and other problems encountered by pipeline steels, it is imperative to discuss a few studies regarding this subject matter. Another important idea is how grain sizes influence grain boundaries since bigger grain sizes will have a lower percentage of grain boundaries per area. Interestingly, grain boundaries have unique properties relative to the bulk material in terms of atomic coordination, reactivity, and diffusion rates [218]. On a plain view, it is expected that pipeline surfaces with relatively high grain boundary densities will show different electrochemical behavior in terms of corrosion than coarser-grained surfaces with lower grain boundary densities. While it has been established that yield strength is inversely proportional to grain size [215,220], there is no consensus on the relationship between grain size and corrosion rate, let alone, hydrogen-induced cracking (HIC). From a few studies, it is generally believed that the corrosion rate increases as grain sizes increase [221–224]. That is, the corrosion resistance of a material is directly proportional to its grain size.

Maryam et al. investigated the role of grain sizes on pipeline steel corrosion. The authors were able to study the corrosion resistance of different grain-sized pipeline steel samples. They concluded that two distinct stages for the dependency of corrosion current density (i_{corr}) on grain size exist. The authors revealed that above a limiting average grain size of~22 μm, i_{corr} decreased slowly with increasing grain size. Below this limiting value, i_{corr} increased rapidly, which was related to the increased density of grain boundaries as interpreted by theoretical calculation of the number of grains per unit area. While the issue of limiting average grain size remains controversial, the authors were not able to reveal a reason for such a shift. Perhaps, since there were no strain analyses in the author's experiments, it will be very difficult to know the reasons behind their conclusions since internal strains can affect the corrosion resistance of pipeline steels. Also, since it is known that NaCl corrosion medium has low passivation affinity, unlike other mediums with hydrogen evolution potential, it might be the reason for their conclusions [209]. On the other hand, since different microstructural features affect corrosion, it will be very challenging to ascertain the effect of only grain size on corrosion.

Y Li et al. also investigated the role of grain size on the corrosion of surface nano-crystallized low-carbon steel. They revealed that the corrosion rate of the SNC low-carbon steel increased with the decreasing grain size [225]. The authors attributed the decrease in corrosion resistance to the increased number of active sites in SNC low-carbon steel. However, the corrosion rate is different in different corrosion media. Wang et al. were able to report the corrosion properties of fine and coarse-grained steel samples [209]. According to their study, grain refinement decreased corrosion resistance in the NaCl solution but improved corrosion resistance in the $NaHCO_3$ solution. According to the authors, the reason is that coarse-grained steel is known to have anodic passivation, while grain-refined steel can induce self-passivation.

Interestingly, this was also in line with Jack and Szpunar's report on corrosion on similar steels that had ununiform grain sizes [186]. According to the authors, there was enough passivation in the region with greater density of grain boundaries, while little passivation in the region with bigger grain sizes (less grain boundaries). While the authors had the same conclusion as Wang et al., their reasons for their conclusion were quite different. They revealed that there is no hydrogen evolution during the corrosion process in the NaCl corrosion medium, unlike the $NaHCO_3$ solution, therefore less passivation and more corrosion affinity were reported. As such, hydrogen emission in a corrosion process creates room for more passivation, and thus, better corrosion resistance. Another interesting

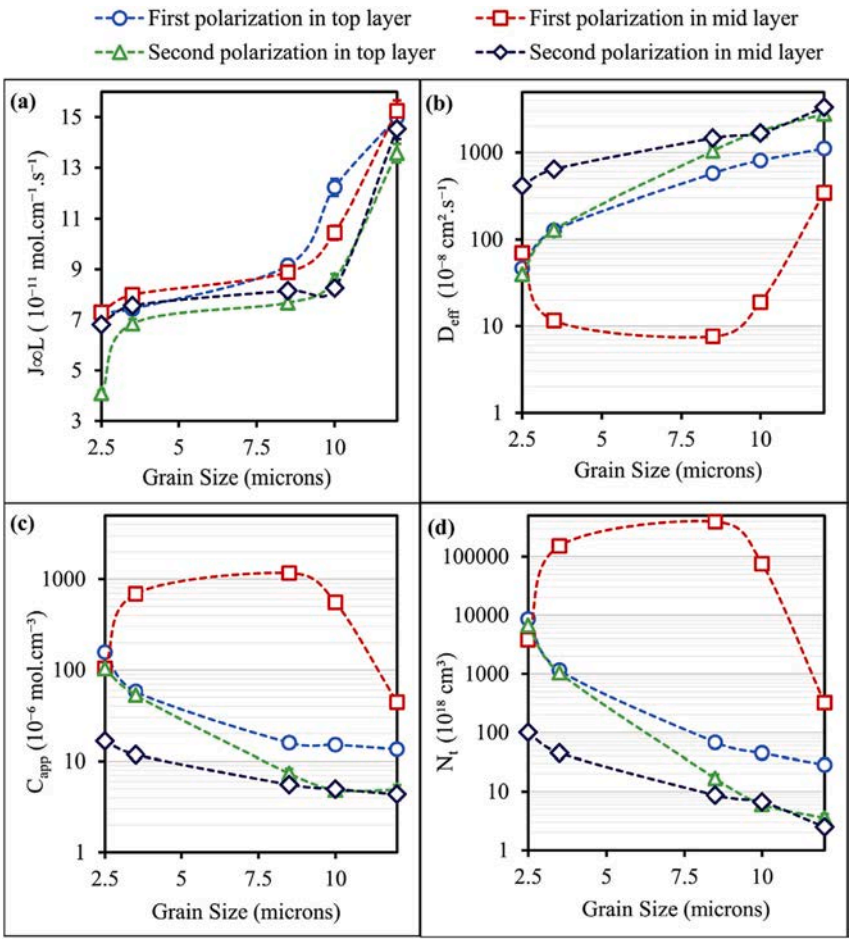

Fig. 16. Effect of grain growth on diffusion after dual-polarization (a) permeability (b) effective diffusion coefficient (c) apparent solubility and (d) trapping sites [226].

angle is how the diffusion of hydrogen in specimens of different grain sizes affects susceptibility to cracking. Thomas and Szpunar investigated the hydrogen diffusion and trapping in X70 pipeline steel. They concluded that the hydrogen diffusivity decreases with increasing grain size, and the density of trapping sites is reduced with decreasing grain size. Fig. 16 (a-d) shows the permeation parameters obtained for the annealed steel in the first and second polarization of the permeation experiments.

While this conclusion stresses the fact that finer grains have more trapping sites and experiences lesser hydrogen diffusion due to higher number of grain boundaries, it will be imperative to understand how grain size affects the mechanical properties of pipelines in relationship to diffusion and trapping density. While there is scanty literature on this, it remains worthwhile to carry more detailed investigation.

6. Effect of hydrogen on pipeline welds

The tailoring of the microstructure of pipeline steels in achieving desired microstructural parameters for better cracking and corrosion resistance is paramount, however, in an ideal situation, pipeline steels are welded together to transport oil and gas substances over longer distances. These microstructural variations across weld joints have been reported to cause cracking because of the formation of intermetallic compounds and high welding heat input [227]. With the presence of inclusions and retained atomic hydrogen, these cracks are easily initiated and propagated in pipeline welds [228]. The science behind the hydrogen effect in welds is that when hydrogen is introduced into the liquid weld pool, it becomes difficult for it to escape when the weld cools down, and this often initiates HIC in the heat-affected zone (HAZ) and the weld-metal (WM) due to stress build-up. When the applied heat is high, hydrogen solubility is increased, which in turn increases hydrogen retention potential after cooling down. Also, rapid cooling saturates the weld with hydrogen and enhances the tendency for the trapped hydrogen to migrate to other trap sites. This could potentially lead to cracking of the weldment, even at ambient temperature conditions. On the other hand, cooling welds at a slower rate causes low retention time for hydrogen in the weldment as it can escape before solidification. Welding often gives rise to three distinct zones such as unaffected base metal (BM), the heat affected zone (HAZ), and the weld metal (WM) or fusion zone (FZ). Out of these zones, the most

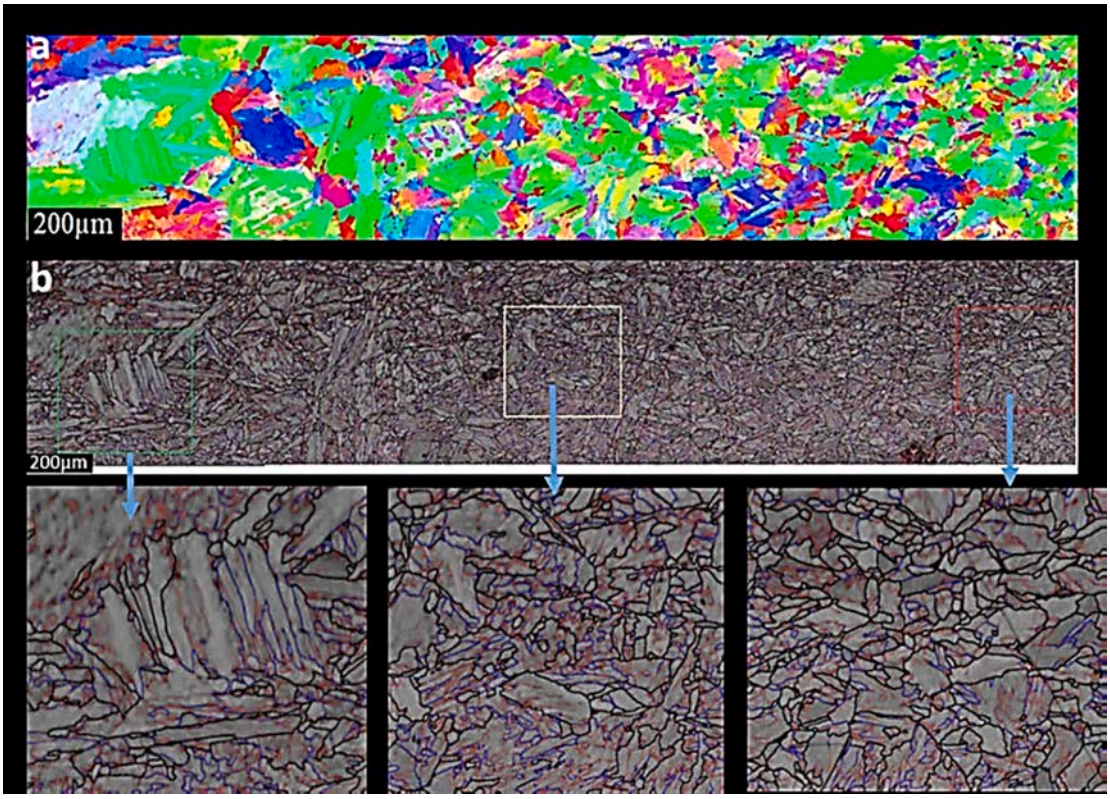

Fig. 17. (a) EBSD map of HAZ (b) image quality with imposed grain boundaries showing the subzones of HAZ (from CGHAZ to FGHAZ).

HIC-prone is the HAZ because of its higher hardenability in comparison to the base metal [229]. The HAZ, the zone between the BM and FZ, experiences peak temperature below the solidus temperature but is high enough to cause a change in the microstructure and mechanical properties of the area compared to the BM. The HAZ experiences different temperatures, moving from the FZ to the BM, this is what results in microstructural variation. This microstructural variation in the HAZ can be influenced by the heat input, the highest temperature reached, the holding time at the elevated temperature, and the cooling rate [230]. For instance, Zhu et al. investigated the effect of heat input on the interfacial characterization of the butter joint of hot-rolling CP-Ti/Q235 bimetallic sheets by Laser + CMT. They noticed that reducing the welding heat reduced the formation of intermetallic compounds, which improved the tensile strength of the weld when compared to higher welding heat [227]. Yuhua et al. also investigated the effect of welding crack in micro laser welded NiTiNb shape memory alloy and Ti6Al4V alloy dissimilar metals joints. The authors noticed a significant increase in weldment cracks after a higher laser power was used. The authors also revealed that a brittle Ti2Ni phase with more contents was present in the weld due to final solidification, which was the main cause of crack formation along with large stress concentration [231].

Due to temperature variations, four zones of the HAZ are known such as coarse-grained (CGHAZ), fine-grained (FGHAZ), inter-critical (ICHAZ), and tempered zones. It is worthwhile to know that the change in temperature leads to changes in grain sizes which in the end affects mechanical properties. For instance, Hashemi and Mohammadyani observed that the hardness of the welded joint in X65 pipeline steel varied as testing moved across the CGHAZ, FGHAZ, ICHAZ, and tempered zones [232]. Fig. 17 (a-b) shows the EBSD map and microstructure of the HAZ. From 17a, it can be deduced that there exists a variation of the grain boundary structures with distance from the CGHAZ to the FGHAZ.

In another study, Shaiful et al. investigated the impact of heat input on the hardness and toughness of austenitic 202-grade stainless steel weldments [233]. They found out that the joints made by using low heat input exhibited higher hardness and impact toughness values than those welded with medium and high heat input. It can be deduced that high heat input can lead to an increase in grain size, which has a knock-on effect on hardness and toughness value. The findings of Choubey et al. were also in line as they found that the tensile strength decreases with an increase in welding heat input [234].

There are many studies revolving around the influence of hydrogen on the integrity of pipeline welds. For instance, Yue investigated the HAZ hydrogen-induced cracking of high-strength naval steels using the Granjon implant test [229]. They found out that CGHAZ is the most HIC-prone HAZ because the CCT diagrams revealed both bainite and martensite form in the CGHAZ of HY-100 and HSLA-100 depending on the cooling rate, as shown in Fig. 18. While for BA-160, martensite was found to be the predominant phase in the CGHAZ. In addition, they advised pre-heating the pipeline before welding as a form of increasing HIC resistance of the HAZ, as pre-heat helps to reduce diffusible hydrogen during welding by slowing down the cooling rate. This was also in line with the study of [235] Wang et al. They also noticed brittle fractures in the CGHAZ for both the as-welded and PWHT X80 pipeline samples. Their reason for

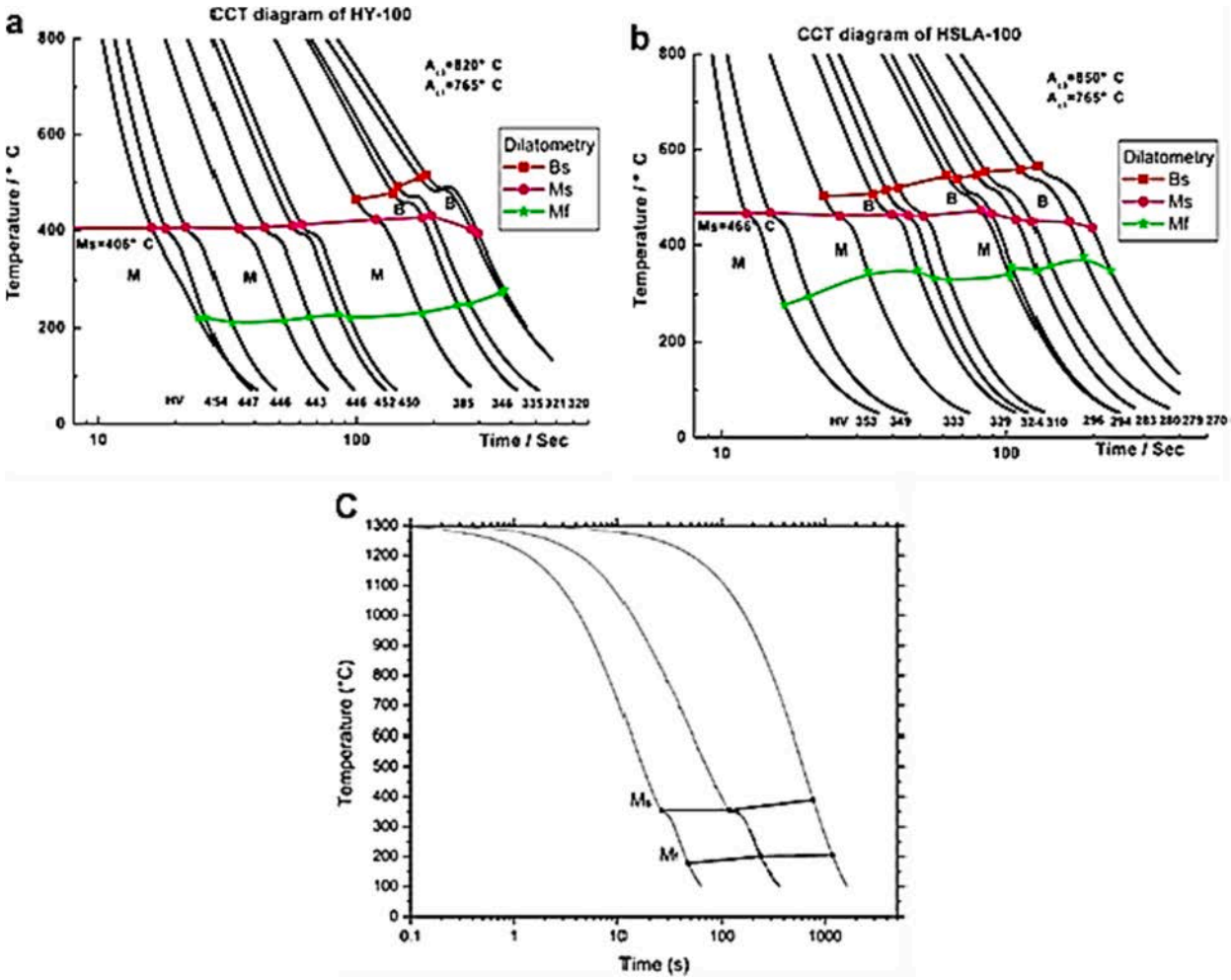

Fig. 18. Continuous cooling transformation diagrams for the CGHAZ of the three steels. a HY-100; b HSLA-100; c BA-160 [241].

the brittle fracture was because of the coarsening of the grain size on the fusion line, and the non-uniform distributions of Martensite/Austenite constituents. Fu et al. also investigated the HE behavior of SUS301L-MT stainless steel laser-arc hybrid welded joint localized zones. Utilizing an in situ electrochemical hydrogen charging during slow strain rate tensile (SSRT) tests, they noticed that the BM and HAZ zones exhibited higher plasticity loss than that of WM, but almost the same strength loss [236]. Luo et al. investigated the SCC behavior of X90 pipeline steel and its weld joint at different applied potentials in near-neutral solutions [236]. The authors noticed three mechanisms in the SCC behaviors of base metal and weld joint samples; anodic dissolution mechanism when the applied potential is open circuit potential (EOCP), anodic dissolution and hydrogen embrittlement mechanism when the applied potential is − 850 mV, and hydrogen embrittlement mechanism when the applied potential is − 1000 mV and − 1200 mV. Eliminating joint and residual stresses is another way of minimizing HIC in pipeline weldments [237]. This is because joint stresses in combination with the stress created from the presence of hydrogen, can lead to embrittlement. Interestingly, Zhu et al. studied the use of ameliorated longitudinal critically refracted—attenuation velocity method for welding residual stress measurement. The LCR-AV technique is based on the linear relationship between velocity, attenuation, and grain size, which is a valuable quantitative technology to estimate the residual stress of welded joints [238]. Also, the use of low hydrogen or baked electrodes, coupled with pre-heating and post-welding heat treatments is widely recommended [239,240].

7. Gaseous hydrogen and pipeline steels

Hydrogen transport using existing pipeline steels has recently stimulated a lot of research.

The awareness of the effect of greenhouse gases is setting hydrogen as the future energy vector [242]. While there is scanty literature on pipelines originally designed for hydrogen storage or transport, there is an increasing demand for the use of existing pipeline steels (not originally designed for hydrogen transport or storage) to transport hydrogen gas [243]. This has made this subject matter somewhat interesting to delve into. Hydrogen, which exists in 75 % of all matter [244] is colorless, odorless, and nontoxic. As a

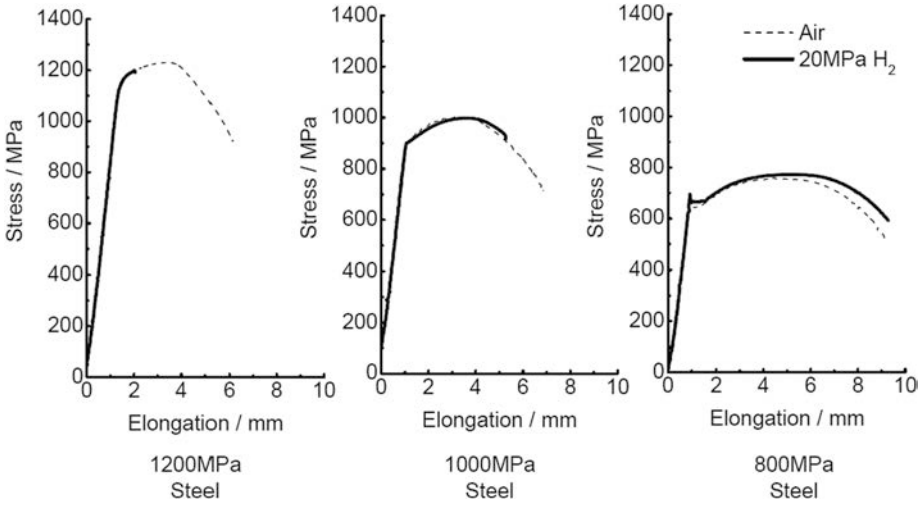

Fig. 19. Load-Displacement curve of pipeline steel sample [248].

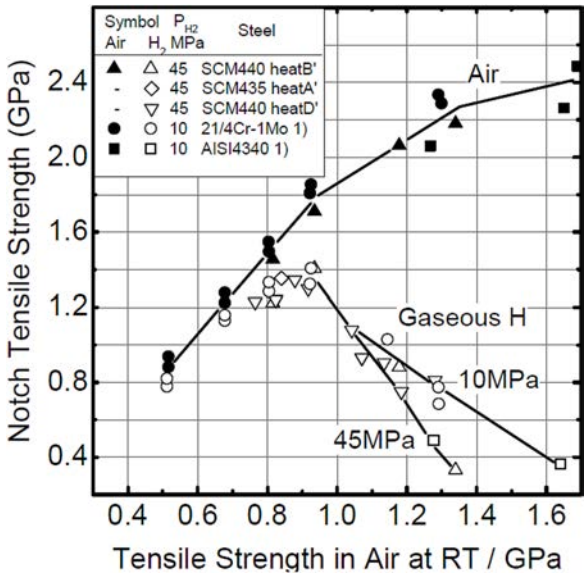

Fig. 20. Notch tensile strength as a function of the tensile strength of steel samples [248].

non-polluting substance, it can easily be released freely into the atmosphere [245]. However, it is very combustible and can be transported either as a liquid or as a gas [246]. While hydrogen can be produced in many ways, transportation and storage is more challenging than its production. Currently, hydrogen transportation and storage are operated under high-pressure (HP) conditions (i.e., 5–20 MPa for transportation, 35–100 MPa for storage) [247]. Just like other countries, Canada uses tube trailer trucks for transporting gaseous hydrogen, which is limited to the amount the truck can carry, causing high gas prices [242]. While Canada has developed a strategy for transporting hydrogen with trailer trucks, the envisioned sustainability during increased energy demand is not promising, increasing the need for using existing pipelines for transporting gaseous hydrogen. In the world today, only about 5,000 km of pipelines are used for hydrogen transport. However, increasing demand for energy has spiked the need for pipeline infrastructure expansion. This has led to the sorting of existing pipeline steels (not originally manufactured for hydrogen transportation.) for the transportation of hydrogen. To salvage the pressure on existing pipeline steels as a vessel for hydrogen gas transport, one needs to understand how hydrogen gas affects the mechanical properties of existing pipeline steels, by looking at the role of microstructure. Wada et al. were able to investigate the effect of hydrogen pressure on the mechanical properties of low alloy pipeline steels [248]. With a hydraulic servo-controlled testing machine, a tensile test was done on different steel samples under a gaseous hydrogen environment with a pressure of 20 MPa. From their mechanical testing, as the tensile strength of the pipeline increased, the elongation in gaseous hydrogen decreased. This means that a pipeline with high strength will fail faster in a gaseous hydrogen environment. It also shows that one of the main mechanical properties of pipeline steels vulnerable to hydrogen gas is ductility. These inferences are

Table 5
Tensile ductility data for 0.22 % carbon steel (normalized at 900 °C) in hydrogen gas with various pressures [250].

Pressure (psig)	Pressure(atm)	UTS (ksi)	Elongation (gage:30 mm) %	Reduction of Area %
Ambient (Air)	1(Air)	70.8	32	64
147 (H_2)	10 (H_2)		34.5	52
294 (H_2)	20 (H_2)		33	47
735 (H_2)	50 (H_2)		30	50
1470 (H_2)	100 (H_2)		30	36.5
2205 (H_2)	150 (H_2)		26	28
1470 (Argon)	100 (Argon)		36	62

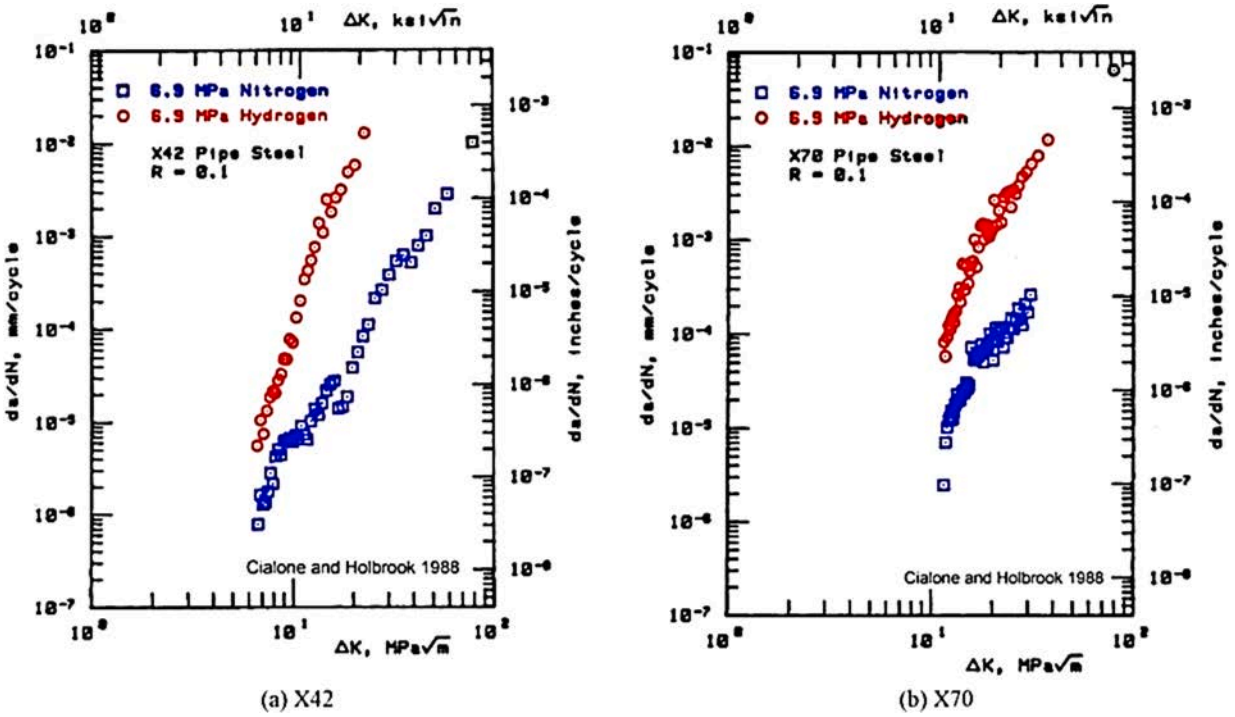

Fig. 21. Fatigue crack growth rates (da/dN) for (a) X42 and (b) X70 in 6.9 MPa (1000 psi) hydrogen and in 6.9 MPa (1000 psi) nitrogen at stress ratio R = 0.1.

evident as the steel sample with a tensile strength of 1200 MPa fractured under the hydrogen environment before reaching maximum tensile strength level, while the other sample with 1000 MPa strength fractured at the start of necking as shown in Fig. 19. The other sample of 800 MPa strength showed little or no hydrogen gas effect on tensile properties.

For the notched tensile test, the notch tensile strength(NTS) in gaseous hydrogen under the pressure of 10 MPa decreased above 930 MPa to 1000 MPa tensile level, while the NTS in gaseous hydrogen under pressure of 45 MPa had more significant decrease as shown in Fig. 20.

Hofmann and Rauls in 1961 carried out tensile test in hydrogen environment on 0.22 %carbon steel. These tensile tests obtained mechanical properties like yield stress, ultimate tensile strength, elongation, and reduction of area, of pipeline under hydrogen environment [249]. Table 5 shows the tensile ductility data for 0.22 % carbon steel (normalized at 900 °C) in hydrogen gas with various pressures.

Lam et al. also compiled a review showing the effect of hydrogen on the mechanical properties of pipeline steels, like tensile strength, fracture toughness, and fatigue strength [251]. Cialone and Holbrook investigated the tensile strength, subcritical crack growth, and fracture strength of API X42 and X70 pipeline steels under a hydrogen environment [252]. The fatigue test data of fatigue crack growth rate tests are shown in Fig. 21, where the fatigue crack growth rates in 6.9 MPa (1000 psig) hydrogen and 6.9 MPa (1000 psig) nitrogen are compared. A low-stress ratio (R = 0.1) was used in the fatigue testing. From Fig. 20, we can deduce that the da/dN appears to be higher in X42 steel than in X70 at the same ΔK level. In the case of X42, the fatigue crack growth rate can be 150 times greater than that in the nitrogen, under the same 6.9 MPa pressure. The tests were also carried out at higher stress ratios (R ranges from 0.1 to 0.8). These results for X42 are summarized in Fig. 22.

Zawierucha and Xu also investigated the fracture toughness of the as rolled and normalized API 5L Grade B pipeline steel [253]. Fig. 23 shows the corresponding fatigue crack growth rates with stress ratio R = 0.1 under 1.4 and 20.7 MPa hydrogen pressures. From

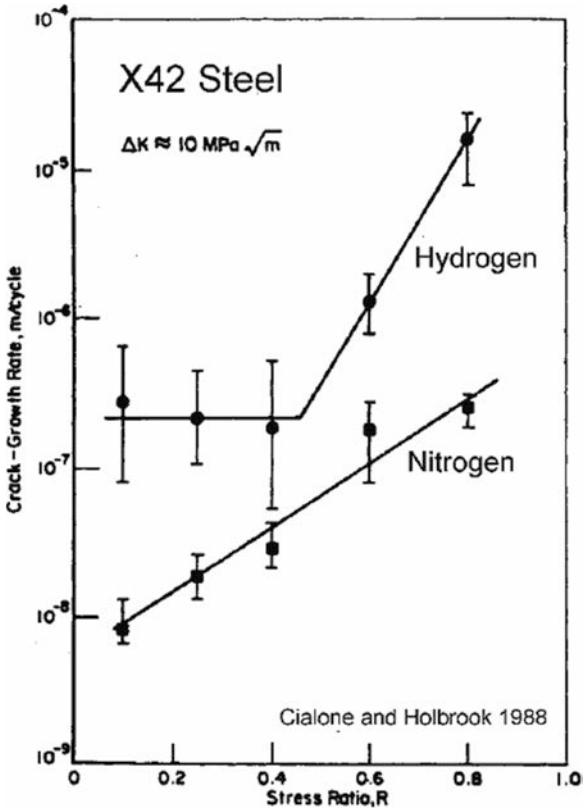

Fig. 22. Fatigue crack growth rates (da/dN) for X42 in hydrogen and in nitrogen at various stress ratios (R) [252].

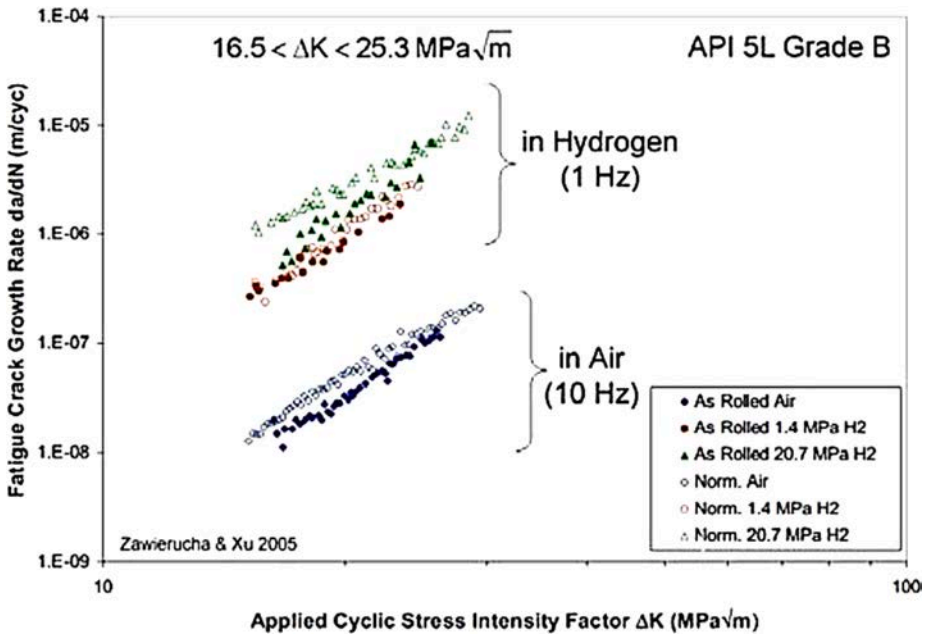

Fig. 23. Fatigue crack growth rates (da/dN) for as rolled and normalized API 5L Grade B steels in various pressures of hydrogen (1 Hz) and in air (10 Hz) [253].

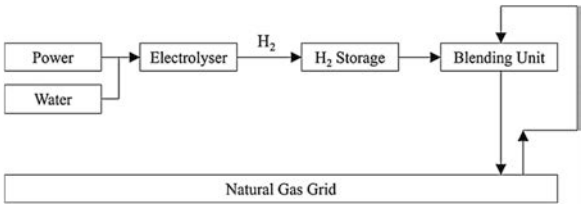

Fig. 24. Schematic showing a Typical System for Blending Hydrogen into Natural Gas Grids [256].

Table 6
Examples of Hydrogen Blending Systems [257].

Project	Country	Network	Electrolyser capacity	Hydrogen Blend (%)	Others
HyP SA	Australia	Distribution	1.2 MW	5 %	Uses green hydrogen
ATCO-CEIH	Australia	Distribution	O.15 MW	5–25 %	GC and PID control
HyDeploy	UK	Distribution	0.5 MW	20 %	Measures Wobbe index
Jupiter 1000	France	Transmission	1.0 MW	6 %	Injects hydrogen into transmission lines

Fig. 23, it can be deduced that the presence of hydrogen significantly increased the fatigue crack growth rate of the pipeline specimen by about 30 times that of the specimen in the air. In addition, over the tested ΔK range (i.e., $16.5 < \Delta K < 25.3$ MPa $\sqrt{m}$), the fatigue crack growth rate seemed insensitive to the pressure of hydrogen (i.e., da/dN only increased about 1.5 times when the hydrogen pressure changed from 1.4 MPa to 20.7 MPa). Additional hydrogen pressures were applied in the fatigue crack growth tests. Fig. 23 shows the dependence of fatigue crack growth rate on the hydrogen pressure when $\Delta K = 22$mMPa.

The lack of dedicated pipeline steels for hydrogen transport or storage has encouraged the blending of hydrogen and natural gas together for transportation. To use existing pipelines for transporting hydrogen, blending hydrogen with natural gas becomes the best method in achieving that. However, hydrogen's molecule size and its different properties with natural gases can create a unique feature when blended [254,255]. This becomes a threat to pipelines, especially pipelines originally designed for just natural gas transmission. Transporting this blended mixture with optimum transmission conditions requires increasing the flow rate, unlike the rate used in transmitting only natural gas [256]. However, this may lead to an increase in pressure and a shift from the design specifications of the existing pipelines, exposing them to imminent failures. So, it is imperative to consider the design changes and trade-offs in transporting blended hydrogen and natural gas. For instance, homogeneity of the blended substances is necessary for uniform behavior along the inner linings of the pipeline [257]. Energy consumption is also an issue to investigate. It is usually necessary because of the different densities of the blended substances due to stratification [256]. To prevent stratification, blended gas is transported under turbulent flow conditions, according to an investigation by the HyDeploy project [258].

Fig. 24. shows the components of a typical system for blending hydrogen into natural gas grids. Currently, there are several blending systems in operation, but the safety process is to ensure a homogenous mixing of hydrogen (in specific percentages) and natural gas. Table 6 shows some hydrogen blending systems in operations, obtained from [258–262].

Blending hydrogen with natural gasses doesn't fully eliminate the hydrogen embrittlement effect from pipelines, especially when a high percentage of hydrogen is being blended. However, according to ASME B31.12, carbon steels, including ASTM A 106 Grade B, ASTM A53 Grade B, and API 5L Grades X42 and X52, are judged to be fit for the transportation of hydrogen with pressures up to 14 MPa [263]. Nevertheless, the rising need for hydrogen in the future will necessitate higher pressure requirements and raise the demands for existing pipeline steels for hydrogen transportation, which requires more research and work, regardless of the limited literature about the subject matter.

8. Processing of pipeline steels designated for cold regions

Another important aspect to look at is the processing of pipeline steels designated for cold regions. Arctic regions are known for their low-temperature setting, and the fluctuations of their temperature, ranging from + 30^0c to -70^0c [264]. With the predicted decrease in petroleum from existing wells, the Arctic regions seem to be attracting interest from the oil and gas industries for petroleum exploration. While the data on petroleum in the unchartered parts of the world is still unclear, it is estimated that the undiscovered arctic petroleum accounts for 22 % of the unexplored fraction across the globe. That is, arctic petroleum represents 15 % of oil and 30 % of gas which is undiscovered worldwide [265]. While the Arctic region feels promising because of the abundance of petroleum resources, their low temperatures and climate fluctuations hinder exploration, because of the use of existing high-strength pipelines for resource transportation.

In summary, the microstructure of these existing pipeline steels needs to be tailored, as the mechanical properties of these existing pipelines need to be controlled to survive in Arctic environments. For existing pipeline steels, a swift temperature drop can ultimately alter the mechanical properties of the pipeline, due to a transition from a ductile to a brittle nature, called the ductile to brittle transition temperature (DBTT) [266–268]. As such the low-temperature toughness of pipelines becomes of interest, especially for pipelines designated for permafrost and arctic areas. For a pipeline to withstand low-temperature induced brittleness, it must have a

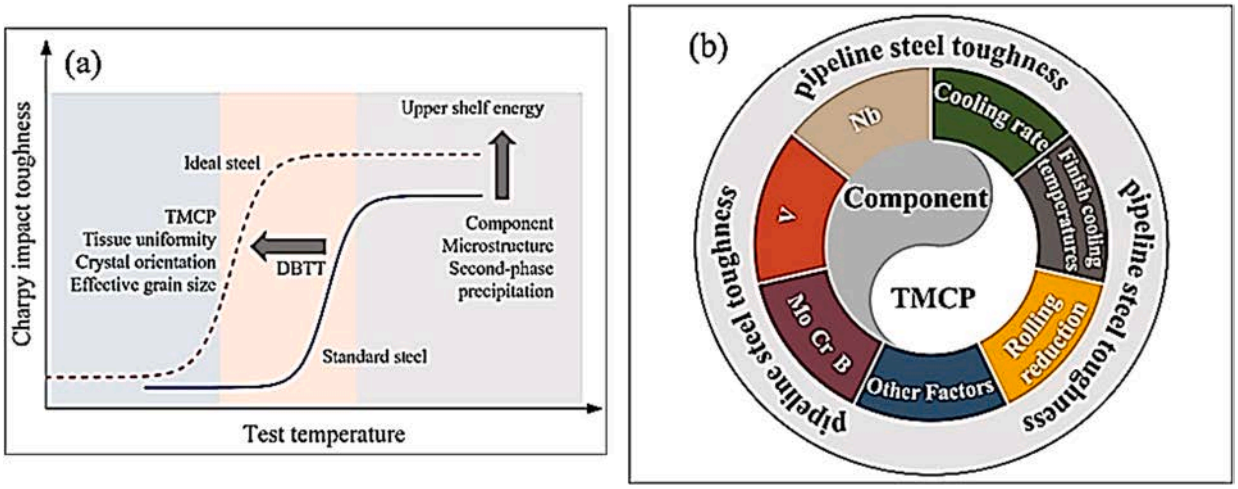

Fig. 25. Schematic diagram of low-temperature toughness optimization of pipeline steel. (a) Strategies for optimizing the low-temperature toughness properties of high-grade pipeline steel; (b) the typical factors affecting the low-temperature toughness properties of pipeline steel, including composition (Nb, V, Mo, Cr, B) and process parameters (finish cooling temperature, cooling rate, rolling reduction) [123].

low DBTT, responsible for maintaining its absorbed energy [123,269,270]. This DBTT depends on the chemical composition of the pipeline, microstructure, heat treatment, and so on [271]. Interestingly, grain size, amongst many other factors, greatly influences the DBTT of materials. Therefore, with adequate processing and microalloying, the low-temperature toughness of pipelines can be significantly improved. Fortunately, the method of making pipeline steels designated for cold environments is TMCP [84]. This involves the control of the processing of steels, right from the initial processing step to achieve better mechanical properties for the designated environment. From Fig. 25 a, the lower DBTT and higher upper shelf energy (USE) are desirable for the application of any specific pipeline steel.

Mechanical properties like toughness or ductility, at low temperatures, can be optimized by processing, which allows for the control of grain size, dislocation density (especially for pearlitic steels), phase composition, texture, and other microstructural characteristics, as shown in Fig. 22b [272]. Amidst the transportation and infrastructural difficulties in the Arctic regions, balancing pipeline strength and ductility remains a major concern. To balance strength and ductility, the processing of the pipeline needs to be controlled to enable:

1. Full dissolution of precipitates (carbonitrides and carbides).
2. Uniform refined ferrite grains through controlled dynamic recrystallization, precipitate hardening, and dissolution of carbides and carbonitrides [273].
3. Reduction in bainite lathes by controlling the finishing cooling temperature.
4. High presence of ferrite grains by creating more ferrite nucleation sites through controlled rolling reductions[274].
5. Optimum low-temperature toughness.

The following are the processing stages for producing pipelines designated for the arctic environment, with several recommendations from the literature.

8.1. Slap reheating temperature

This is the first important stage in the processing of steels for Arctic applications. It is important as it determines the austenite grain size (which gives an idea of the size of ferrite grains and their uniformity) and the quantity/quality of solid solution microalloying elements [275]. From Fig. 26a, it can be deduced that for the preferred precipitates to go into solution, a slab reheat temperature between 1130^0c and 1180^0c is recommended. From Fig. 26b, there is an insignificant increase in average austenite grain size between 1,130 and $1,180^0$c. Subsequently, a tangible austenite grain enlargement continues above $1,200^0$c. With this, it can be deduced that a slab reheating temperature between $1,140^0$c and $1,180^0$c is the recommended temperature for reheating X70 pipeline steel. It is, however, imperative to note that there is no optimum slab reheating temperature as it all depends on the composition of the steel pipe.

However, this is not in line with the findings of Ebrahimi et al. on Nb micro-alloyed steels. The authors revealed that the increase in the reheating temperature from 1180 to 1240^0c minimized pearlite content and promoted acicular ferrite in the rolled steel. According to the authors, the increased ferrite presence in combination with carbonitride precipitates improved strength and toughness in the steels [276].

Di Schino and Rufini also investigated the effect of slab reheating temperature on the mechanical properties of steels [277]. They increased the slab reheating temperature from 1075^0c to 1175^0c and observed an increase in the steel's hardenability. The authors,

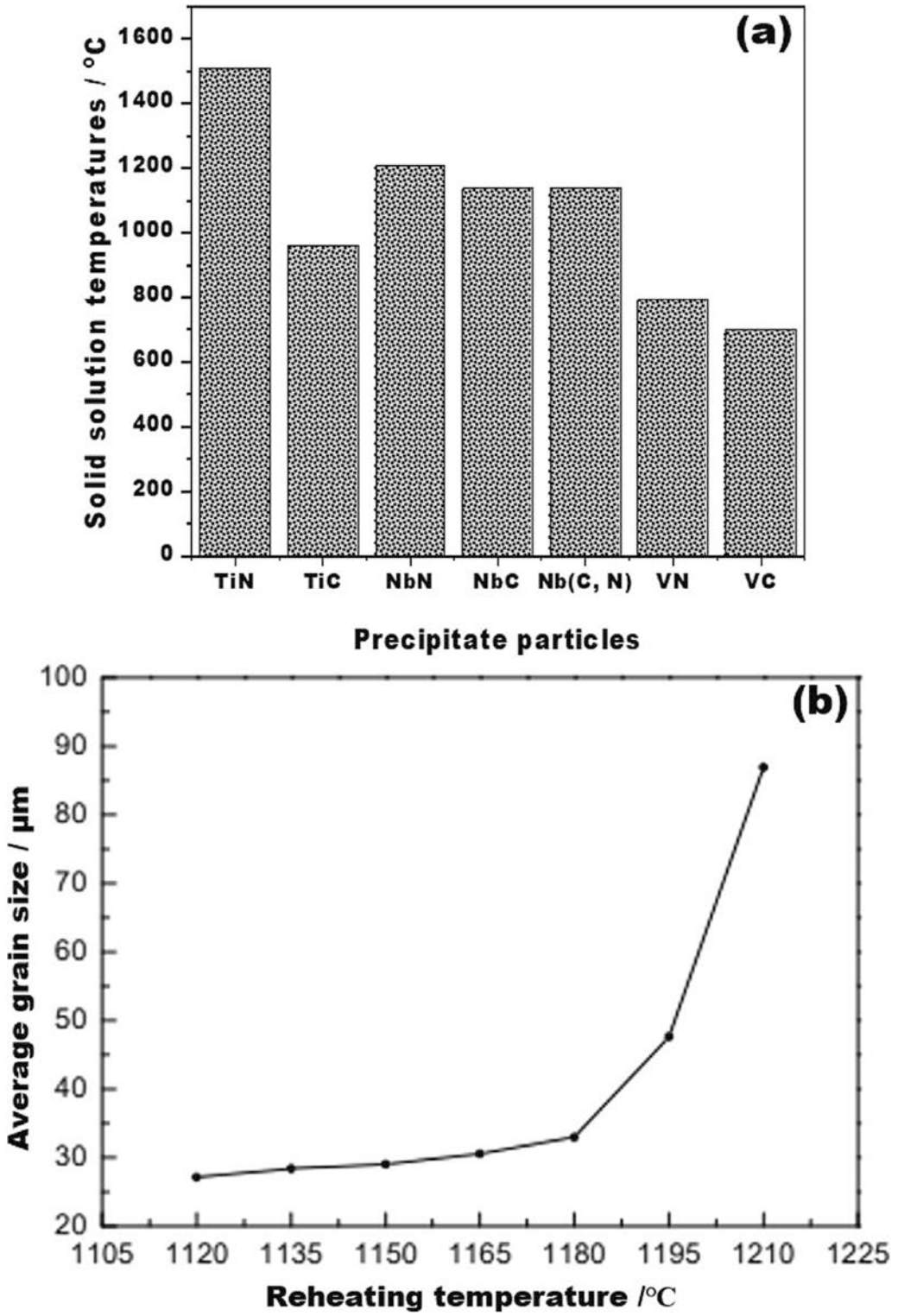

Fig. 26. (a) solid solution temperatures of typical carbonitride precipitate particles obtained from Nb, Ti, and V (b) influence of reheating temperature on average austenite grain size [275]).

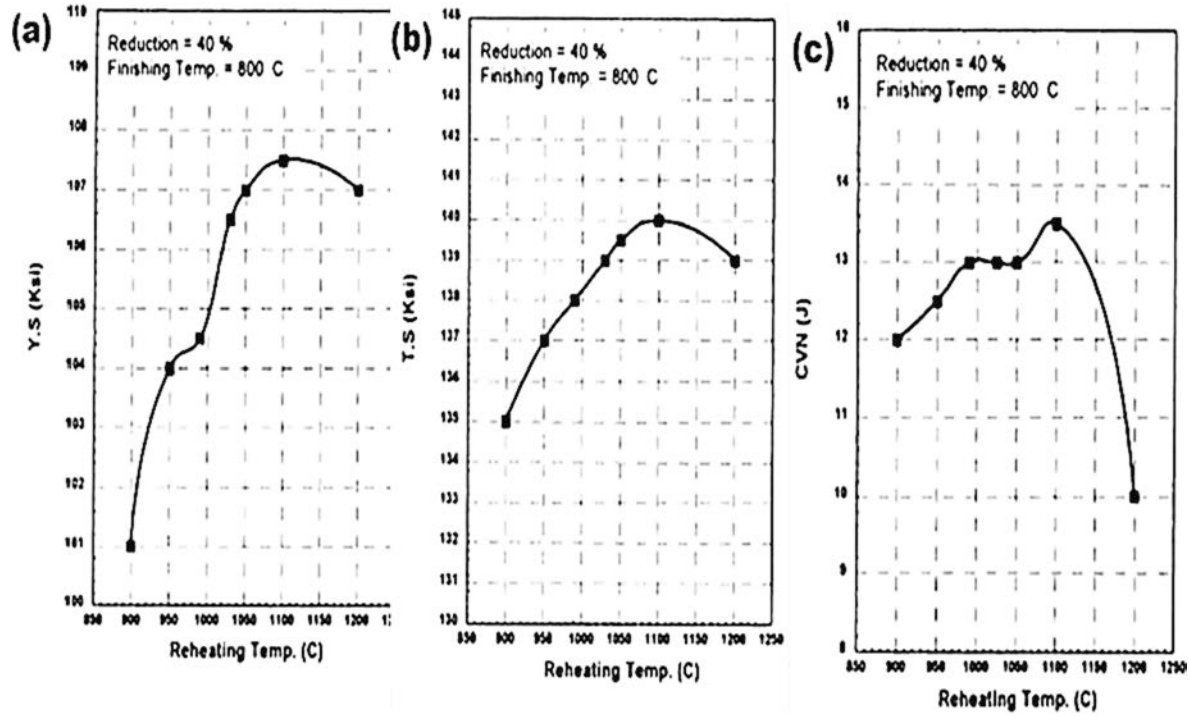

Fig. 27. Effect of reheating temperature on mechanical properties of AISI 4130 steel (a) yield strength vs. reheating temperature (b) tensile strength vs. reheating temperature (c) impact energy vs. reheating temperature [278].

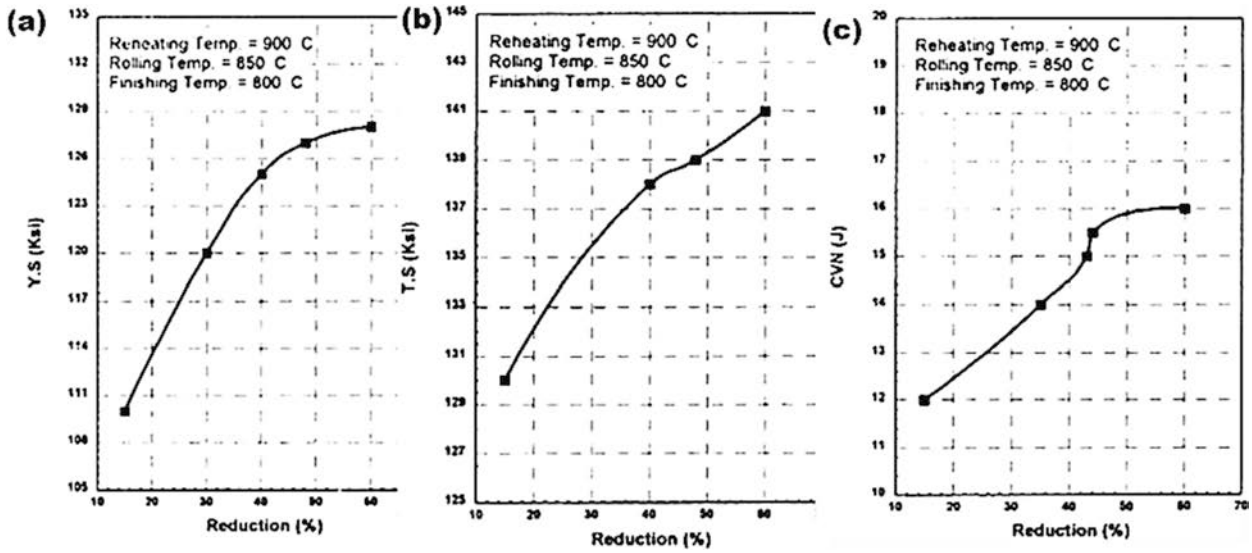

Fig. 28. Schematic representation of TMCP with the resulting EBSD micro- graphs obtained after applying different rolling reductions above and below Tnr [281].

however, attributed the increase to the size of austenite grains at relatively high reheating temperatures, which affects the extent of grain refinement in the final microstructure, which is also in line with the findings of Zhao et al. [275], as shown in Fig. 26b. The increased grain size contributed to the reduced toughness. Another interesting result was obtained by Jahazi and Egbali. They investigated how reheating temperature affects the mechanical properties of pipeline steels. In Fig. 27 (a-c), there is an illustration of the relationship between reheating temperature and the mechanical properties of pipeline steels. From the chart, it is visible that an increase in the reheating temperature results in an increase in strength and the absorbed energy, up to 1,100 ^{0}C. After that mark, at 1200 °C, there seems to be a decline in yield strength, impact energy, and tensile strength [278].

Table 7
Effect of micro-alloys on the toughness of pipeline steels.

S/N	ALLOYING ELEMENT	EFFECTS
1.	Niobium (Nb)	• Delays austenite recrystallization. • Lowers the phase transformation temperature [285–287]. • Enhances nucleation sites for phase transformation [288,289]. • Refines austenite and deformed austenite grains. • Refines the final microstructure and enhances toughness and strength, as seen in Fig. 29.
2.	Vanadium (V)	• Compensates for insufficient Niobium content [268]. • Better strengthening than Niobium but has poor grain refinement proficiency. • Retards the growth of austenite grains during heating to a lesser extent than Nb and Ti because of its high solubility.
3.	Molybdenum (M)	• Influences the precipitation activity of other microalloying elements like V, Nb, and Ti [290]. • Impedes the static recrystallization of high-temperature austenite. • Increases the activation energy for carbon diffusion within austenite, thereby reducing the dispersion coefficient in carbon and inhibiting the formation of pro-eutectic ferrite. • Causes direct transformation of supercooled austenite to bainite without the concomitant formation of polygonal ferrite [291,292].
4.	Chromium (Cr)	• Acts as a ferrite stabilizer. • Improves strength through chromium carbides [268].
5.	Titanium (Ti)	• Microstructure refinement due to grain size control. More effective retarding action than Nb and V on the growth of the austenite grains with the temperature of heating for rolling [293]. • Grain boundary strengthening. • Increased resistance to brittle fracture, and better toughness. • Less efficiency than Nb and V in precipitation strengthening, as titanium nitride TiN cannot be completely dissolved in the austenite in the heating for rolling at conventional temperatures [293,294].

9. Hot rolling

The hot rolling process is necessary for dynamic recrystallization which brings refined or coarse grains. Controlling this process allows the creation of nucleation sites for refined ferrite grains. Sych et al. proposed a 950^0c hot rolling temperature with a reduction of 70 percent to obtain fine-grained austenite [274]. The inability to rightfully control rolling deformation will lead to anisotropic microstructure in pipeline steel, making it unfit for arctic applications [264]. Some researchers have proposed reducing rolling temperature as a method of increasing toughness in pipeline steels. This was attributed to the minimization of recrystallization and austenite grain size enlargement [279,280]. Jahazi and Egbali also made an interesting conclusion related to the influence of rolling reductions on yield strength, tensile strength, and absorbed energy [278]. They found out that if the rolling reduction increased from 15 % to 60 %, strength also increased, however, the reduction recorded within 40 percent did not increase the absorbed energy. So, from Fig. 28 (a-c), it can be deduced that there is a balance in the rolling reduction between 45 and 50 % for pipeline steels designated for arctic regions, as from this range of reductions, we might see (a) pancaked austenite, (b) an increased dislocation density, and (c) an increase in nucleation sites for ferrite grains.

Apart from controlling these processing parameters to improve toughness of pipeline steels, the composition of micro-alloying elements also affects the temperature toughness of pipeline steels.

9.1. Effects of microalloying elements on the impact toughness of pipeline steels

The importance of microalloying elements goes beyond low DBTT to also affect the microstructure of pipeline steels. With a careful addition of micro-alloy elements with appropriate thermomechanical processing, a desired microstructure, such as AF [123,282] or fine polygonal ferrite [283,284] can be obtained. Table 7 shows the effects of some micro-alloying elements on the toughness of pipeline steels designated for low-temperature environments.

From Table 7, concerning V, Nb, and Ti, the retarding action on the growth of the austenite grains in hot rolling temperature is in this ascending order: V – Nb – Ti. But in the aspect of grain refinement: V – Ti – Nb.

10. Conclusion

Based on the above reviewed research articles on the effects of different microstructural parameters on the corrosion and cracking resistance of pipeline steels, the following conclusions can be made:

- Corrosion precedes HIC and remains the predominant environmental failure mechanism besetting pipelines under sour environments. The corrosion resistance of pipeline steels is mainly improved through cathodic protection, coating, and the use of corrosion inhibitors.
- Nb and Ti in micro-alloyed steels contribute significantly to retarding the austenite grain growth, thereby facilitating grain refinement, and improving mechanical properties. However, balancing toughness and strength property requirements largely depends on the judicious tailoring of several microstructural parameters through steel processing.

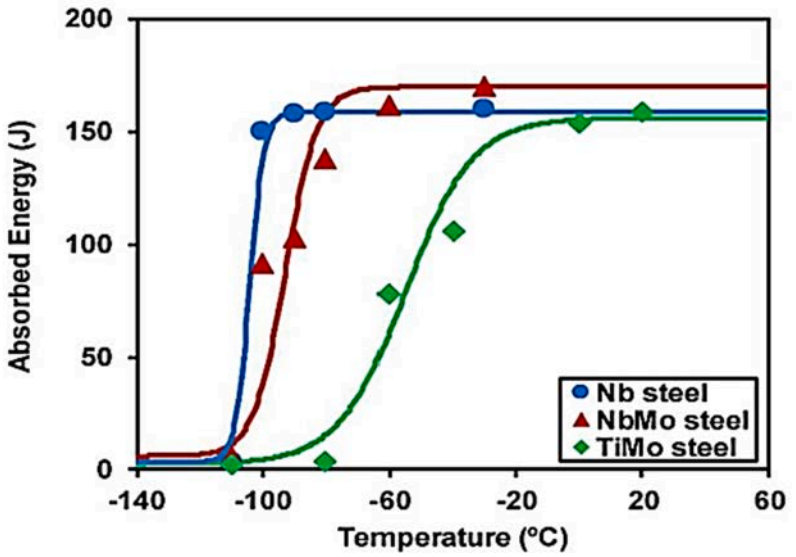

Fig 29. Different micro-alloyed steels (Nb, NbMo, TiMo) and their impact energy after coiling at 700^0c [123].

- Dislocation density, amongst other microstructural parameters, has a more profound effect on the HIC resistance of pipeline steels. There is currently no established hierarchy revealing how different microstructural parameters influence the corrosion and cracking resistance of pipeline steels, however, dislocation density plays a prominent role in determining the susceptibility of these steels to failure. An in-depth understanding of the hierarchy of effects of different microstructural parameters will greatly help steel manufacturers modulate the mechanical properties of pipeline steels to harmonize them with the distinct demands imposed by diverse service environments.
- Grain size, amongst other microstructural parameters, has a more profound effect on the mechanical properties of pipelines designated for cold applications, while the relationship between grain size and corrosion susceptibility remains a multifaceted subject, having several influence factors.
- Crystallographic texture and grain boundary characteristics have roles to play in improving the SCC resistance of pipeline steels. However, the degree to which crystallographic texture, amidst other microstructural parameters, affects cracking is not yet established. For instance, the direct influence of crystallographic texture in the arrest of propagating cracks is still unclear and debated, while low-angle grain boundaries and CSL boundaries have been seen to arrest cracks in steels.
- Welding heat reduction, removal of joint and residual stresses, as well as pre-heating before welding, can greatly help reduce cracking in pipeline welds. Elimination of these residual stresses also has positive impacts on the SSCC resistance of steel.
- Mobile hydrogen is a major threat to the cracking resistance of pipeline steels.
- The lack of dedicated pipeline steels for hydrogen transport or storage has encouraged the blending of hydrogen and natural gas together for transportation.

10.1. Future recommendations

- In a contemporary context, the employment of machine learning techniques avails a promising avenue for optimizing steel microstructure as revealed in this review. The combination of empirical data encompassing historical and contemporary insights on hydrogen embrittlement, in conjunction with detailed knowledge of pipeline steel processing and thermodynamic modeling, forms the bedrock of this approach. Combining these facets with the insights provided by thermodynamic models could give rise to a simulated optimum microstructure. A pivotal aspect of this context involves the creation of simulated environments that mirror the distinctive operational environments of the pipeline steels. Through calibrated adjustments to the pipeline steel's composition, these simulated models can be subjected to simulated testing protocols to assess the impact of these environments on the mechanical properties of the pipeline steel. Such an approach represents an innovative and rigorous means to iteratively tailor pipeline steel microstructure, rendering it amenable to the multifaceted demands of real service conditions.

CRediT authorship contribution statement

Meekness Nnoka: Writing – review & editing, Writing – original draft, Visualization, Methodology, Conceptualization. **Tonye Alaso Jack:** Writing – review & editing. **Jerzy Szpunar:** Writing – review & editing, Supervision.

Declaration of competing interest

The authors declare that they have no known competing financial interests or personal relationships that could have appeared to influence the work reported in this paper.

Data availability

No data was used for the research described in the article.

Acknowledgment

This work was supported by the NSERC Discovery (RGPIN-2021- 02774) and NSERC Alliance (ALLRP 549712-19) research grant. The authors are grateful for their support.

References

[1] M.-C. Zhao, K. Yang, Y. Shan, The effects of thermo-mechanical control process on microstructures and mechanical properties of a commercial pipeline steel, Mater. Sci. Eng. A 335 (2002) 14–20, https://doi.org/10.1016/S0921-5093(01)01904-9.
[2] X. Shi, W. Yan, W. Wang, L. Zhao, Y. Shan, K. Yang, HIC and SSC behavior of high-strength pipeline steels, Acta Metall.. Sinica (Engl. Lett.) 28 (2015), https://doi.org/10.1007/s40195-015-0257-1.
[3] M. Wang, E. Akiyama, K. Tsuzaki, Effect of hydrogen on the fracture behavior of high strength steel during slow strain rate test, Corros. Sci.. 49 (2007) 4081–4097, https://doi.org/10.1016/j.corsci.2007.03.038.
[4] V.K. Judge, J.G. Speer, K.D. Clarke, K.O. Findley, A.J. Clarke, Rapid thermal processing to enhance steel toughness, Sci. Rep. 8 (2018) 445, https://doi.org/10.1038/s41598-017-18917-3.
[5] C. Zhang, P. Li, S. Wei, L. You, X. Wang, F. Mao, D. Jin, C. Chen, K. Pan, C. Luo, J. Li, Effect of tempering temperature on impact wear behavior of 30Cr3Mo2WNi Hot-working die steel, Front. Mater. 6 (2019) 149, https://doi.org/10.3389/fmats.2019.00149.
[6] Y. Li, Z. Jiang, P. Wang, D. Li, Y. Li, Effect of a modified quenching on impact toughness of 52100 bearing steels, J. Mater. Sci. Technol. 160 (2023) 96–108, https://doi.org/10.1016/j.jmst.2023.02.057.
[7] P. Mazuro, J. Pieńkowska, E. Rostek, Influence of various heat treatments on hardness and impact strength of uddeholm balder: Cr-Mo-V-Ni Novel steel used for engine construction, Materials 14 (2021), https://doi.org/10.3390/ma14174943.
[8] O. Zvirko, H. Nykyforchyn, O. Tsyrulnyk, Evaluation of impact toughness of gas pipeline steels under operation using electrochemical method, Procedia Struct. Integrity 22 (2019) 299–304, https://doi.org/10.1016/j.prostr.2020.01.038.
[9] E. Ohaeri, U. Eduok, J. Szpunar, Hydrogen related degradation in pipeline steel: a review, Int. J. Hydrogen Energy 43 (2018) 14584–14617, https://doi.org/10.1016/j.ijhydene.2018.06.064.
[10] O. Lavigne, E. Gamboa, V. Luzin, M. Law, M. Giuliani, W. Costin, The effect of the crystallographic texture on intergranular stress corrosion crack paths, Mater. Sci. Eng. A 618 (2014) 305–309, https://doi.org/10.1016/j.msea.2014.09.038.
[11] M.A. Arafin, J.A. Szpunar, A new understanding of intergranular stress corrosion cracking resistance of pipeline steel through grain boundary character and crystallographic texture studies, Corros. Sci. 51 (2009) 119–128, https://doi.org/10.1016/j.corsci.2008.10.006.
[12] E. Villalba, A. Atrens, SCC of commercial steels exposed to high hydrogen fugacity, Eng. Fail. Anal. 15 (2008) 617–641, https://doi.org/10.1016/j.engfailanal.2007.10.004.
[13] G.M. Pressouyre, I.M. Bernstein, A quantitative analysis of hydrogen trapping, Metall. Trans. A 9 (1978) 1571–1580, https://doi.org/10.1007/BF02661939.
[14] J.-Y. Lee, S.M. Lee, Hydrogen trapping phenomena in metals with B.C.C. and F.C.C. crystals structures by the desorption thermal analysis technique, Surf. Coat. Technol. 28 (1986) 301–314, https://doi.org/10.1016/0257-8972(86)90087-3.
[15] W.C. Luu, J.K. Wu, Effects of sulfide inclusion on hydrogen transport in steels, Mater. Lett. 24 (1995) 175–179, https://doi.org/10.1016/0167-577X(95)00068-2.
[16] M. Elboujdaini, W. Revie, Effect of Non-Metallic Inclusions on Hydrogen Induced Cracking, in: T. Boukharouba, M. Elboujdaini, G. Pluvinage (Eds.), Damage and Fracture Mechanics: Failure Analysis of Engineering Materials and Structures, Springer Netherlands, Dordrecht, 2009: pp. 11–18. https://doi.org/10.1007/978-90-481-2669-9_2.
[17] H.S. Kim, C.-H. Chang, H.-G. Lee, Evolution of inclusions and resultant microstructural change with Mg addition in Mn/Si/Ti deoxidized steels, Scr. Mater. 53 (2005) 1253–1258.
[18] E. Sidorova, Non-metallic inclusions in pipeline steels and their effect on the corrosion resistance, n.d.
[19] F. Wang, H. Guo, W. Liu, S. Yang, S. Zhang, J. li, Control of MnS Inclusions in High- and Low-Sulfur Steel by Tellurium Treatment, Materials 12 (2019) 1034. https://doi.org/10.3390/ma12071034.
[20] E. Miyoshi, T. Tanaka, F. Terasaki, A. Ikeda, Hydrogen-induced cracking of steels under wet hydrogen sulfide environment, J. Eng. Ind. 98 (1976) 1221–1230, https://doi.org/10.1115/1.3439090.
[21] H. Wang, F. Wang, D. Qian, F. Chen, Z. Dong, L. Hua, Investigation of damage mechanisms related to microstructural features of ferrite-cementite steels via experiments and multiscale simulations, Int. J. Plast 170 (2023) 103745, https://doi.org/10.1016/j.ijplas.2023.103745.
[22] K.P. Kolhe, C.K. Datta, Prediction of microstructure and mechanical properties of multipass SAW, J. Mater. Process. Technol. 197 (2008) 241–249, https://doi.org/10.1016/j.jmatprotec.2007.06.066.
[23] J.A. Ávila, C.O.F.T. Ruchert, P.R. Mei, R.R. Marinho, M.T.P. Paes, A.J. Ramirez, Fracture toughness assessment at different temperatures and regions within a friction stirred API 5L X80 steel welded plates, Eng. Fract. Mech. 147 (2015) 176–186, https://doi.org/10.1016/j.engfracmech.2015.08.006.
[24] F. Chen, H. Zhang, Z. Li, Y. Luo, X. Xiao, Y. Liu, Residual stresses effects on fatigue crack growth behavior of rib-to-deck double-sided welded joints in orthotropic steel decks, Adv. Struct. Eng. 27 (2023) 35–50, https://doi.org/10.1177/13694332231213462.
[25] Z. Zhang, Y. Han, X. Lu, T. Zhang, Y. Bai, Q. Ma, Effects of N2 content in shielding gas on microstructure and toughness of cold metal transfer and pulse hybrid welded joint for duplex stainless steel, Mater. Sci. Eng. A 872 (2023) 144936, https://doi.org/10.1016/j.msea.2023.144936.
[26] A. Charles, Corrosion Mechanisms in Theory and Practice, 2nd Edition, Hardback, Electrochim Acta 48 (2003) 1081.
[27] M.A. Mohtadi-Bonab, Effects of different parameters on initiation and propagation of stress corrosion cracks in pipeline steels: A review, Metals (basel) 9 (2019), https://doi.org/10.3390/met9050590.
[28] M. Alfalah, M. Albdiry, A Critical Review on Corrosion and its Prevention in the Oilfield Equipment, 7 (2017) 162–189. https://doi.org/10.52716/jprs.v7i2.195.
[29] F. Luo, Q. Liu, J. Huang, H. Xiao, Z. Gao, W. Ge, F. Gao, Y. Wang, W. Chenxu, Effects of lattice strain on hydrogen diffusion, trapping and escape in bcc iron from ab-initio calculations, Int. J. Hydrogen Energy (2022), https://doi.org/10.1016/j.ijhydene.2022.11.206.
[30] L. Briottet, I. Moro, P. Lemoine, Quantifying the hydrogen embrittlement of pipeline steels for safety considerations, Int. J. Hydrogen Energy 37 (2012) 17616–17623, https://doi.org/10.1016/j.ijhydene.2012.05.143.

[31] B.D.B. Tiu, R.C. Advincula, Polymeric corrosion inhibitors for the oil and gas industry: Design principles and mechanism, React. Funct. Polym. 95 (2015) 25–45, https://doi.org/10.1016/j.reactfunctpolym.2015.08.006.
[32] V. Pandarinathan, K. Lepková, S.I. Bailey, R. Gubner, Impact of mineral deposits on CO2 corrosion of carbon steel, in: NACE CORROSION, NACE, 2013: p. NACE-2013.
[33] Z.B. Wang, L. Pang, Y.G. Zheng, A review on under-deposit corrosion of pipelines in oil and gas fields: Testing methods, corrosion mechanisms and mitigation strategies, Corros. Commun. 7 (2022) 70–81, https://doi.org/10.1016/j.corcom.2022.03.007.
[34] P. Zhang, A.T. Kan, M.B. Tomson, Chapter 24 - Oil Field Mineral Scale Control, in: Z. Amjad, K.D. Demadis (Eds.), Mineral Scales and Deposits, Elsevier, Amsterdam, 2015: pp. 603–617. https://doi.org/https://doi.org/10.1016/B978-0-444-63228-9.00024-3.
[35] F.M. AlAbbas, C. Williamson, S.M. Bhola, J.R. Spear, D.L. Olson, B. Mishra, A.E. Kakpovbia, Influence of sulfate reducing bacterial biofilm on corrosion behavior of low-alloy, high-strength steel API-5L X80, Int. Biodeter. Biodegr. 78 (2013) 34–42, https://doi.org/10.1016/j.ibiod.2012.10.014.
[36] H. Castaneda, X.D. Benetton, SRB-biofilm influence in active corrosion sites formed at the steel-electrolyte interface when exposed to artificial seawater conditions, Corros. Sci. 50 (2008) 1169–1183, https://doi.org/10.1016/j.corsci.2007.11.032.
[37] J.W. Costerton, P.S. Stewart, E.P. Greenberg, Bacterial Biofilms: A Common Cause of Persistent Infections, Science 284 (1999) (1979) 1318–1322, https://doi.org/10.1126/science.284.5418.1318.
[38] A. Junid, Cathodic Protection: A Brief Primer (2009).
[39] I. Thompson, J. Saithala, Review of pipeline coating systems from an operator's perspective, Corros. Eng. Sci. Technol. 51 (2015), https://doi.org/10.1179/1743278215Y.0000000038.
[40] I.B. Obot, N.K. Ankah, A.A. Sorour, Z.M. Gasem, K. Haruna, 8-Hydroxyquinoline as an alternative green and sustainable acidizing oilfield corrosion inhibitor, Sustainable, Mater. Technol. 14 (2017) 1–10, https://doi.org/10.1016/j.susmat.2017.09.001.
[41] S.A. Umoren, A. Madhankumar, Effect of addition of CeO2 nanoparticles to pectin as inhibitor of X60 steel corrosion in HCl medium, J. Mol. Liq. 224 (2016) 72–82, https://doi.org/10.1016/j.molliq.2016.09.082.
[42] H. He, S. E, L. Ai, X. Wang, J. Yao, C. He, B. Cheng, Exploiting machine learning for controlled synthesis of carbon dots-based corrosion inhibitors, J Clean Prod 419 (2023) 138210. https://doi.org/https://doi.org/10.1016/j.jclepro.2023.138210.
[43] C.F. Dong, X.G. Li, Z.Y. Liu, Y.R. Zhang, Hydrogen-induced cracking and healing behaviour of X70 steel, J. Alloy. Compd. 484 (2009) 966–972, https://doi.org/10.1016/j.jallcom.2009.05.085.
[44] G.T. Park, S.U. Koh, H.G. Jung, K.Y. Kim, Effect of microstructure on the hydrogen trapping efficiency and hydrogen induced cracking of linepipe steel, Corros. Sci. 50 (2008) 1865–1871, https://doi.org/10.1016/j.corsci.2008.03.007.
[45] D.B. Rosado, W. De Waele, D. Vanderschueren, S. Hertelé, Latest developments in mechanical properties and metallurgical features of high strength line pipe steels, in: 2013.
[46] M. Zhu, C. Du, X. li, Z. Liu, S. Wang, T. Zhao, J. Jia, Effect of Strength and Microstructure on Stress Corrosion Cracking Behavior and Mechanism of X80 Pipeline Steel in High pH Carbonate/Bicarbonate Solution, J Mater Eng Perform 87 (2014). https://doi.org/10.1007/s11665-014-0880-4.
[47] A. Torres-Islas, J.G. Gonzalez-Rodriguez, J. Uruchurtu, S. Serna, Stress corrosion cracking study of microalloyed pipeline steels in dilute NaHCO3 solutions, Corros. Sci. 50 (2008) 2831–2839, https://doi.org/10.1016/j.corsci.2008.07.007.
[48] M.G. Fontana, Stress Corrosion CORROSION, Ind. Eng. Chem. 46 (1954) 99A–102A.
[49] J.R. Davis, Forms of corrosion: Recognition and prevention, in: Corrosion—Understanding the Basics, ASM International Ohio, 2000: pp. 99–192.
[50] V.S. Sastri, Introduction and forms of Corrosion, Challenges in Corrosion: Costs, Causes, Consequences, and Control; John Wiley & Sons Inc.: Hoboken, NJ, USA (2015) 1–95.
[51] S.A. Abubakar, S. Mori, J. Sumner, A Review of Factors Affecting SCC Initiation and Propagation in Pipeline Carbon Steels, Metals (basel) 12 (2022), https://doi.org/10.3390/met12081397.
[52] R. Bodlos, Detailed microstructure characterization of a grade X70 steel modified with TiO2 using friction stir processing, 2018.
[53] C. Natividad, R. García, V.H. López, L.A. Falcón, M. Salazar, Mechanical and metallurgical properties of grade X70 steel linepipe produced by non-conventional heat treatment, Characterization of Metals and Alloys (2017) 3–11.
[54] B. Hwang, Y.M. Kim, S. Lee, N.J. Kim, S.S. Ahn, Correlation of microstructure and fracture properties of API X70 pipeline steels, Metall. Mater. Trans. A 36 (2005) 725–739, https://doi.org/10.1007/s11661-005-1004-4.
[55] J.K. Thomson, S.J. Pawel, A Qualitative Comparison of the C-Ring Test and the Jones Test as Standard Practice Test Methods for Studying Stress Corrosion Cracking in Ferritic Steels, Oak Ridge National Lab.(ORNL), Oak Ridge, TN (United States), 2015.
[56] Z.Y. Liu, X.G. Li, C.W. Du, G.L. Zhai, Y.F. Cheng, Stress corrosion cracking behavior of X70 pipe steel in an acidic soil environment, Corros. Sci. 50 (2008) 2251–2257, https://doi.org/10.1016/j.corsci.2008.05.011.
[57] Y. Cheng, P. Liu, M. Yang, Effects of Temperature and Applied Potential on the Stress Corrosion Cracking of X80 Steel in a Xinzhou Simulated Soil Solution, Materials 15 (2022), https://doi.org/10.3390/ma15072560.
[58] T.A. Nenasheva, A. Marshakov, V.E. Ignatenko, The effect of alternating current on stress corrosion cracking of X70 pipeline steel, Corrosion: Materials, Protection (2019) 10–19. https://doi.org/10.31044/1813-7016-2019-0-4-10-19.
[59] S. Longfei, L. Zhiyong, L. Xiaogang, G. Xingpeng, Z. Yinxiao, W. Wu, Influence of microstructure on stress corrosion cracking of X100 pipeline steel in carbonate/bicarbonate solution, J. Mater. Res. Technol. 17 (2022) 150–165, https://doi.org/10.1016/j.jmrt.2021.12.137.
[60] L. Wang, J. Xin, L. Cheng, K. Zhao, B. Sun, J. Li, X. Wang, Z. Cui, Influence of inclusions on initiation of pitting corrosion and stress corrosion cracking of X70 steel in near-neutral pH environment, Corros. Sci. 147 (2019) 108–127, https://doi.org/10.1016/j.corsci.2018.11.007.
[61] J.T. Bulger, B.T. Lu, J.L. Luo, Microstructural effect on near-neutral pH stress corrosion cracking resistance of pipeline steels, J. Mater. Sci. 41 (2006) 5001–5005, https://doi.org/10.1007/s10853-006-0131-7.
[62] E.V. Chatzidouros, A. Traidia, R.S. Devarapalli, D.I. Pantelis, T.A. Steriotis, M. Jouiad, Fracture toughness properties of HIC susceptible carbon steels in sour service conditions, Int. J. Hydrogen Energy 44 (2019) 22050–22063, https://doi.org/10.1016/j.ijhydene.2019.06.209.
[63] G. Rosenberg, I. Sinaiova, Evaluation of hydrogen induced damage of steels by different test methods, Mater. Sci. Eng. A 682 (2017) 410–422, https://doi.org/10.1016/j.msea.2016.11.067.
[64] G. Ghosh, P. Rostron, R. Garg, A. Panday, Hydrogen induced cracking of pipeline and pressure vessel steels: A review, Eng. Fract. Mech. 199 (2018) 609–618, https://doi.org/10.1016/j.engfracmech.2018.06.018.
[65] Q. Cui, J. Wu, D. Xie, X. Wu, Y. Huang, X. Li, Effect of nanosized NbC precipitates on hydrogen diffusion in X80 pipeline steel, Materials 10 (2017), https://doi.org/10.3390/ma10070721.
[66] A. Traidia, M. Alfano, G. Lubineau, S. Duval, A. Sherik, An effective finite element model for the prediction of hydrogen induced cracking in steel pipelines, Int. J. Hydrogen Energy 37 (2012) 16214–16230, https://doi.org/10.1016/j.ijhydene.2012.08.046.
[67] E. Entezari, J.L. González-Velázquez, D.R. López, M.A.B. Zúñiga, J.A. Szpunar, Review of current developments on high strength pipeline steels for HIC inducing service, Frattura Ed Integrita Strutturale 16 (2022) 20–45, https://doi.org/10.3221/IGF-ESIS.61.02.
[68] D.L. Johnson, G. Krauss, J.K. Wu, K.P. Tang, Correlation of microstructural Parameters and Hydrogen Permeation in Carbon Steel, Metall. Mater. Trans. A 18 (1987) 717–721, https://doi.org/10.1007/BF02649489.
[69] M. Cabrini, T. Pastore, Hydrogen Diffusion and EAC of Pipeline Steels Under Cathodic Protection, in: E.E. Gdoutos (Ed.), Fracture of Nano and Engineering Materials and Structures, Springer, Netherlands, Dordrecht, 2006, pp. 1005–1006.
[70] N. Shohoji, Comparative study of solubilities of hydrogen, nitrogen and carbon in α-iron, J. Mater. Sci. 21 (1986) 2147–2152, https://doi.org/10.1007/BF00547962.
[71] M. Smialowski, Softening vs. hardening effects produced in iron by charging with high fucacity hydrogen, Scr. Metall. 13 (1979) 393–395, https://doi.org/10.1016/0036-9748(79)90232-1.

[72] H. Matsui, H. Kimura, S. Moriya, The effect of hydrogen on the mechanical properties of high purity iron I Softening and Hardening of High Purity Iron by Hydrogen Charging during Tensile Deformation, Mater. Sci. Eng. 40 (1979) 207–216, https://doi.org/10.1016/0025-5416(79)90191-5.
[73] Y.-S. Chen, D. Haley, S.S.A. Gerstl, A.J. London, F. Sweeney, R.A. Wepf, W.M. Rainforth, P.A.J. Bagot, M.P. Moody, Direct observation of individual hydrogen atoms at trapping sites in a ferritic steel, Science 355 (2017) 1196–1199, https://doi.org/10.1126/science.aal2418.
[74] H.D.G.S. et al. Chen YS, Direct observation of individual hydrogen atoms at trapping sites in a ferritic steel, (n.d.).
[75] M. Javidi, S. Bahalaou Horeh, Investigating the mechanism of stress corrosion cracking in near-neutral and high pH environments for API 5L X52 steel, Corros. Sci. 80 (2014) 213–220, https://doi.org/10.1016/j.corsci.2013.11.031.
[76] J. Beavers, B. Harle, Mechanisms of High-pH and Near-Neutral-pH SCC of Underground Pipelines, J. Offshore Mech. Arctic Eng. Trans. ASME 123 (2001), https://doi.org/10.1115/1.1376716.
[77] X. Chen, X.G. Li, C.W. Du, Y.F. Cheng, Effect of cathodic protection on corrosion of pipeline steel under disbonded coating, Corros. Sci. 51 (2009) 2242–2245, https://doi.org/10.1016/j.corsci.2009.05.027.
[78] B.Y. Fang, A. Atrens, J.Q. Wang, E.H. Han, Z.Y. Zhu, W. Ke, Review of stress corrosion cracking of pipeline steels in “low” and “high” pH solutions, J. Mater. Sci. 38 (2003) 127–132, https://doi.org/10.1023/A:1021126202539.
[79] D. Kuang, Y.F. Cheng, Study of cathodic protection shielding under coating disbondment on pipelines, Corros. Sci. 99 (2015) 249–257, https://doi.org/10.1016/j.corsci.2015.07.012.
[80] V. Skalskyi, Z. Nazarchuk, O. Stankevych, B. Klym, Influence of occluded hydrogen on magnetoacoustic emission of low-carbon steels, Int. J. Hydrogen Energy 48 (2023) 6146–6156, https://doi.org/10.1016/j.ijhydene.2022.11.139.
[81] M.A. Arafin, J.A. Szpunar, Effect of bainitic microstructure on the susceptibility of pipeline steels to hydrogen induced cracking, Mater. Sci. Eng. A 528 (2011) 4927–4940, https://doi.org/10.1016/j.msea.2011.03.036.
[82] D. Hardie, E.A. Charles, A.H. Lopez, Hydrogen embrittlement of high strength pipeline steels, Corros. Sci. 48 (2006) 4378–4385, https://doi.org/10.1016/j.corsci.2006.02.011.
[83] X. Shi, W. Yan, W. Wang, L. Zhao, Y. Shan, K. Yang, Effect of Microstructure on Hydrogen Induced Cracking Behavior of a High Deformability Pipeline Steel, J. Iron Steel Res. Int. 22 (2015) 937–942, https://doi.org/10.1016/S1006-706X(15)30093-5.
[84] E. Ohaeri, J. Omale, A. Tiamiyu, K.M.M. Rahman, J. Szpunar, Influence of Thermomechanically Controlled Processing on Microstructure and Hydrogen Induced Cracking Susceptibility of API 5L X70 Pipeline Steel, J. Mater. Eng. Perform. 27 (2018) 4533–4547, https://doi.org/10.1007/s11665-018-3556-7.
[85] H. Li, R. Niu, W. Li, H. Lu, J. Cairney, Y.-S. Chen, Hydrogen in pipeline steels: Recent advances in characterization and embrittlement mitigation, J. Nat. Gas Sci. Eng. 105 (2022) 104709, https://doi.org/10.1016/j.jngse.2022.104709.
[86] J.I. Verdeja, J. Asensio, J.A. Pero-Sanz, Texture, formability, lamellar tearing and HIC susceptibility of ferritic and low-carbon HSLA steels, Mater Charact 50 (2003) 81–86, https://doi.org/10.1016/S1044-5803(03)00106-2.
[87] M.A. Mohtadi-Bonab, J.A. Szpunar, S.S. Razavi-Tousi, Hydrogen induced cracking susceptibility in different layers of a hot rolled X70 pipeline steel, Int. J. Hydrogen Energy 38 (2013) 13831–13841, https://doi.org/10.1016/j.ijhydene.2013.08.046.
[88] M.A. Mohtadi-Bonab, J.A. Szpunar, R. Basu, M. Eskandari, The mechanism of failure by hydrogen induced cracking in an acidic environment for API 5L X70 pipeline steel, Int. J. Hydrogen Energy 40 (2015) 1096–1107, https://doi.org/10.1016/j.ijhydene.2014.11.057.
[89] V. Venegas, F. Caleyo, T. Baudin, J.H. Espina-Hernández, J.M. Hallen, On the role of crystallographic texture in mitigating hydrogen-induced cracking in pipeline steels, Corros. Sci. 53 (2011) 4204–4212, https://doi.org/10.1016/j.corsci.2011.08.031.
[90] M. Masoumi, C.C. Silva, M. Béreš, D.H. Ladino, H.F.G. de Abreu, Role of crystallographic texture on the improvement of hydrogen-induced crack resistance in API 5L X70 pipeline steel, Int. J. Hydrogen Energy 42 (2017) 1318–1326, https://doi.org/10.1016/j.ijhydene.2016.10.124.
[91] M.A. Mohtadi-Bonab, J.A. Szpunar, S.S. Razavi-Tousi, A comparative study of hydrogen induced cracking behavior in API 5L X60 and X70 pipeline steels, Eng. Fail. Anal. 33 (2013) 163–175, https://doi.org/10.1016/j.engfailanal.2013.04.028.
[92] J.Q. Wang, A. Atrens, D.R. Cousens, N. Kinaev, Microstructure of X52 and X65 pipeline steels, J. Mater. Sci. 34 (1999) 1721–1728, https://doi.org/10.1023/A:1004538604409.
[93] J. Bauer, P. Flüss, E. Amoris, V. Schwinn, Microstructure and properties of thermomechanical controlled processing steels for linepipe applications, Ironmaking & Steelmaking 32 (2005) 325–330. https://doi.org/10.1179/174328105X48025.
[94] M. Liu, C.H. Wang, Y.C. Dai, X. Li, G.H. Cao, A.M. Russell, Y.H. Liu, X.M. Dong, Z.H. Zhang, Effect of quenching and tempering process on sulfide stress cracking susceptibility in API-5CT-C110 casing steel, Mater. Sci. Eng. A 688 (2017) 378–387, https://doi.org/10.1016/j.msea.2017.01.067.
[95] W. Kim, H. Jung, G. Park, S. Koh, K. Kim, Relationship between hydrogen-induced cracking and type I sulfide stress cracking of high-strength linepipe steel, Scripta Materialia - SCRIPTA MATER 62 (2010) 195–198, https://doi.org/10.1016/j.scriptamat.2009.10.028.
[96] J.P. Hirth, Effects of hydrogen on the properties of iron and steel, Metall. Trans. A 11 (1980) 861–890, https://doi.org/10.1007/BF02654700.
[97] R.A. Cottis, 2.10 - Hydrogen Embrittlement, in: B. Cottis, M. Graham, R. Lindsay, S. Lyon, T. Richardson, D. Scantlebury, H. Stott (Eds.), Shreir’s Corrosion, Elsevier, Oxford, 2010, pp. 902–922, https://doi.org/https://doi.org/10.1016/B978-044452787-5.00200-6.
[98] R.J. Pargeter, Susceptibility to SOHIC for Linepipe and Pressure Vessel Steels - Review of Current Knowledge., CORROSION 2007 (n.d.).
[99] M.S., K.R.D., and R.J.Horvath. Cayard, SOHIC Resistance of C-Mn Plate Steels Used in Refinery Service, CORROSION 2022 (n.d.).
[100] L. Jemblie, V. Olden, P. Mainçon, O.M. Akselsen, Cohesive zone modelling of hydrogen induced cracking on the interface of clad steel pipes, Int. J. Hydrogen Energy 42 (2017) 28622–28634, https://doi.org/10.1016/j.ijhydene.2017.09.051.
[101] S.P. Lynch, Progress Towards Understanding Mechanisms Of Hydrogen Embrittlement And Stress Corrosion Cracking, NACE - International Corrosion Conference Series (2007).
[102] A. Campari, M. Darabi, A. Alvaro, F. Ustolin, N. Paltrinieri, A machine learning approach to predict the materials’ susceptibility to hydrogen embrittlement, Chem. Eng. Trans. 99 (2023) 193–198, https://doi.org/10.3303/CET2399033.
[103] L.E. Faucon, T. Boot, T. Riemslag, S.P. Scott, P. Liu, V. Popovich, Hydrogen-Accelerated Fatigue of API X60 Pipeline Steel and Its Weld, Metals (basel) 13 (2023), https://doi.org/10.3390/met13030563.
[104] W. Gerberich, P.G. Marsh, J.W. Hoehn, Hydrogen Induced Cracking Mechanisms - Are There Critical Experiments?, in: Hydrogen Effects in Materials, 2013: pp. 539–554. https://doi.org/10.1002/9781118803363.ch47.
[105] R.A. Oriani, P.H. Josephic, Equilibrium and kinetic studies of the hydrogen-assisted cracking of steel, Acta Metall. 25 (1977) 979–988, https://doi.org/10.1016/0001-6160(77)90126-2.
[106] R. Oriani, A Mechanistic Theory of Hydrogen Embrittlement of Steels, Berichte Der Bunsengesellschaft Für Physikalische, Chemie 76 (2010) 848–857, https://doi.org/10.1002/bbpc.19720760864.
[107] A.R. Troiano, The Role of Hydrogen and Other Interstitials in the Mechanical Behavior of Metals, Metallogr. Microstruct. Anal. 5 (2016) 557–569, https://doi.org/10.1007/s13632-016-0319-4.
[108] I. Katzarov, A. Paxton, Hydrogen embrittlement II. Hydrogen-enhanced decohesion across (111) planes in alpha -Fe, Phys Rev Mater 1 (2017). https://doi.org/10.1103/PhysRevMaterials.1.033603.
[109] C.D. Beachem, A new model for hydrogen-assisted cracking (hydrogen “embrittlement”), Metallurgical, Transactions 3 (1972) 441–455, https://doi.org/10.1007/BF02642048.
[110] H.K. Birnbaum, P. Sofronis, Hydrogen-enhanced localized plasticity—a mechanism for hydrogen-related fracture, Mater. Sci. Eng. A 176 (1994) 191–202, https://doi.org/10.1016/0921-5093(94)90975-X.
[111] I.M. Robertson, H.K. Birnbaum, P. Sofronis, Chapter 91 Hydrogen Effects on Plasticity, in: J.P. Hirth, L. Kubin (Eds.), Dislocations in Solids, Elsevier, 2009, pp. 249–293.
[112] s Lynch, Mechanisms of hydrogen assisted cracking - A review, 2003.
[113] H.K. Birnbaum, Hydrogen effects on deformation — Relation between dislocation behavior and the macroscopic stress-strain behavior, Scr. Metall. Mater. 31 (1994) 149–153.

[114] I.M. Robertson, H.K. Birnbaum, An HVEM study of hydrogen effects on the deformation and fracture of nickel, Acta Metall. 34 (1986) 353–366, https://doi.org/10.1016/0001-6160(86)90071-4.
[115] J. Song, W.A. Curtin, Mechanisms of hydrogen-enhanced localized plasticity: An atomistic study using α-Fe as a model system, Acta Mater. 68 (2014) 61–69, https://doi.org/10.1016/j.actamat.2014.01.008.
[116] X. Shao, Research on the Steel for Oil and Gas Pipelines in Sour Environment, in: MATEC Web of Conferences, EDP Sciences, 2018. https://doi.org/10.1051/matecconf/201823804010.
[117] Y. Baik, Y. Choi, The effects of crystallographic texture and hydrogen on sulfide stress corrosion cracking behavior of a steel using slow strain rate test method, Phys. Met. Metallogr. 115 (2014) 1318+. https://link.gale.com/apps/doc/A408647453/AONE?u=googlescholar&sid=googleScholar&xid=603a3839.
[118] M.-C. Zhao, K. Yang, Strengthening and improvement of sulfide stress cracking resistance in acicular ferrite pipeline steels by nano-sized carbonitrides, Scr. Mater. 52 (2005) 881–886, https://doi.org/10.1016/j.scriptamat.2005.01.009.
[119] Y. Han, S. Zhong, L. Tian, J. Fei, Y. Sun, L. Zhao, L. Xu, Welding heat input for synergistic improvement in toughness and stress corrosion resistance of X65 pipeline steel with pre-strain, Corros. Sci. 206 (2022) 110478, https://doi.org/10.1016/j.corsci.2022.110478.
[120] E.G. Ohaeri, T. Jack, S. Yadav, J. Szpunar, J. Zhang, J. Qu, EBSD Microstructural studies on quenched-tempered API 5L X65 pipeline steel, Phil. Mag. 101 (2021) 1895–1912, https://doi.org/10.1080/14786435.2021.1946189.
[121] T. Oruch, K. Beckman, C. Duprè, G. Grewal, K. Christensen, LANL Engineering Standards Manual PD342 ASME B31.3 Process Piping Guide Revision 2 RECORDS OF REVISION, n.d.
[122] M. Ketkar, K. Patil, Review of Subsea Pipeline for Minimizing Thermal and Pressure Expansion, International Journal of Petroleum, Eng. Technol. 4 (2014) 1–13.
[123] S.Y. Han, S.Y. Shin, C.-H. Seo, H. Lee, J.-H. Bae, K. Kim, S. Lee, N.J. Kim, Effects of Mo, Cr, and V Additions on Tensile and Charpy Impact Properties of API X80 Pipeline Steels, Metall. Mater. Trans. A 40 (2009) 1851–1862, https://doi.org/10.1007/s11661-009-9884-3.
[124] A. Contreras, A. López, E.J. Gutiérrez, B. Fernández, A. Salinas, R. Deaquino, A. Bedolla, R. Saldaña, I. Reyes, J. Aguilar, R. Cruz, An approach for the design of multiphase advanced high-strength steels based on the behavior of CCT diagrams simulated from the intercritical temperature range, Mater. Sci. Eng. A 772 (2020) 138708, https://doi.org/10.1016/j.msea.2019.138708.
[125] H.F. Lan, L.X. Du, Q. Li, C.L. Qiu, J.P. Li, R.D.K. Misra, Improvement of strength-toughness combination in austempered low carbon bainitic steel: The key role of refining prior austenite grain size, J. Alloy. Compd. 710 (2017) 702–710, https://doi.org/10.1016/j.jallcom.2017.03.024.
[126] Q. Wu, M.A. Zikry, Dynamic fracture predictions of microstructural mechanisms and characteristics in martensitic steels, Eng. Fract. Mech. 145 (2015) 54–66, https://doi.org/10.1016/j.engfracmech.2015.06.002.
[127] E. Entezari, B. Avishan, H. Mousalou, S. Yazdani, Effect of Electro Slag Remelting (ESR) on the microstructure and mechanical properties of low carbon bainitic steel, Kov. Mater. Met. Mater. 56 (2018) 253–263, https://doi.org/10.4149/km_2018_4_253.
[128] S. Kim, J. Kwon, Y. Kim, W. Jang, S. Lee, J. Choi, Factors influencing fatigue crack propagation behavior of austenitic steels, Met. Mater. Int. 19 (2013) 683–690, https://doi.org/10.1007/s12540-013-4007-5.
[129] Z. Sami, S. Tahar, H. Mohamed, Microstructure and Charpy impact properties of ferrite–martensite dual phase API X70 linepipe steel, Mater. Sci. Eng. A 598 (2014) 338–342, https://doi.org/10.1016/j.msea.2014.01.052.
[130] T. Simm, L. Sun, S. Mcadam, P. Hill, M. Rawson, K. Perkins, The Influence of Lath, Block and Prior Austenite Grain (PAG) Size on the Tensile, Creep and Fatigue Properties of Novel Maraging Steel, Materials 2017 (2017) 730. https://doi.org/10.3390/ma10070730.
[131] X.Y. Qi, L.X. Du, J. Hu, R.D.K. Misra, High-cycle fatigue behavior of low-C medium-Mn high strength steel with austenite-martensite submicron-sized lath-like structure, Mater. Sci. Eng. A 718 (2018) 477–482, https://doi.org/10.1016/j.msea.2018.01.110.
[132] N. Amirjani, M. Ketabchi, M. Eskandari, M. Hizombor, Effect of Cooling Rate and Finish Rolling Temperature on Structure and Strength of API 5LX70 Linepipe Steel Plate, J. Mater. Eng. Perform. 29 (2020) 4275–4285, https://doi.org/10.1007/s11665-020-04961-0.
[133] R.A. Carneiro, R.C. Ratnapuli, V. de Freitas Cunha Lins, The influence of chemical composition and microstructure of API linepipe steels on hydrogen induced cracking and sulfide stress corrosion cracking, Materials Science and Engineering: A 357 (2003) 104–110. https://doi.org/https://doi.org/10.1016/S0921-5093(03)00217-X.
[134] B. Beidokhti, A. Dolati, A.H. Koukabi, Effects of alloying elements and microstructure on the susceptibility of the welded HSLA steel to hydrogen-induced cracking and sulfide stress cracking, Mater. Sci. Eng. A 507 (2009) 167–173, https://doi.org/10.1016/j.msea.2008.11.064.
[135] M. Jiang, L.-N. Chen, J. He, G.-Y. Chen, C.-H. Li, X.-G. Lu, Effect of controlled rolling/controlled cooling parameters on microstructure and mechanical properties of the novel pipeline steel, Adv. Manuf. 2 (2014) 265–274, https://doi.org/10.1007/s40436-014-0084-z.
[136] X. Wang, G. Yuan, J. Zhao, G. Wang, Microstructure and Strengthening/Toughening Mechanisms of Heavy Gauge Pipeline Steel Processed by Ultrafast Cooling, Metals (basel) 10 (2020), https://doi.org/10.3390/met10101323.
[137] HKDH Bhadeshia.(n.d.), Materials Algorithms Project, Https://Www.Phase-Trans.Msm.Cam.Ac.Uk/Map/Steel/Programs/Mucg83.Html. (n.d.).
[138] Sente Software Ltd. Sente Software Ltd.(n.d.)., JMatPro®, Available at: Http://Www.Jmatpro.Com (n.d.).
[139] Chen Y, Zhou X, Huang J, Chemical Component Optimization Based on Thermodynamic Calculation of Fe-1.93Mn-0.07Ni-1.96Cr-0.35Mo Ultra-High Strength Steel, 2018 Dec 25;12(1):65. Doi: 10.3390/Ma12010065. PMID: 30585230; PMCID: PMC6337213. (n.d.).
[140] L. Li, Y. He, B.C. De Cooman, P. Wollants, S.G. Huang, J. Vleugels, Computer-aided designing and manufacturing of advanced steels, Rare Met. 25 (2006) 407–411, https://doi.org/10.1016/S1001-0521(06)60076-4.
[141] T. Yamashita, K. Okuda, T. Obara, Application of thermo-calc to the developments of high-performance steels, J. Phase Equilib. 20 (1999) 231–237, https://doi.org/10.1361/105497199770335767.
[142] T. Jack, R. Pourazizi, E. Ohaeri, J. Szpunar, J. Zhang, J. Qu, Investigation of the hydrogen induced cracking behaviour of API 5L X65 pipeline steel, Int. J. Hydrogen Energy 45 (2020) 17671–17684, https://doi.org/10.1016/j.ijhydene.2020.04.211.
[143] P. Rivera, V. Ramunni, P. Bruzzoni, Hydrogen trapping in an API 5L X60 steel, Corros. Sci. 54 (2012) 106–118, https://doi.org/10.1016/j.corsci.2011.09.008.
[144] Y.-S. Chen, H. Lu, J. Liang, A. Rosenthal, H. Liu, G. Sneddon, I. McCarroll, Z. Zhao, W. Li, A. Guo, J.M. Cairney, Observation of hydrogen trapping at dislocations, grain boundaries, and precipitates, Science 367 (2020) (1979) 171–175, https://doi.org/10.1126/science.aaz0122.
[145] S.P. Lynch, 2 - Hydrogen embrittlement (HE) phenomena and mechanisms, in: V.S. Raja, T. Shoji (Eds.), Stress Corrosion Cracking, Woodhead Publishing, 2011, pp. 90–130.
[146] D. Li, R.P. Gangloff, J.R. Scully, Hydrogen trap states in ultrahigh-strength AERMET 100 steel, Metall. Mater. Trans. A 35 (2004) 849–864, https://doi.org/10.1007/s11661-004-0011-1.
[147] Chan Yao, Hongliang Ming, Jianqiu Wang, En-Hou Han, Effect of Cold Deformation on the Hydrogen Permeation Behavior of X65 Pipeline Steel, National Center for Materials Service Safety, University of Science and Technology Beijing, Beijing 100083, China (n.d.).
[148] L.B. Peral, Z. Amghouz, C. Colombo, I. Fernández-Pariente, Evaluation of hydrogen trapping and diffusion in two cold worked CrMo(V) steel grades by means of the electrochemical hydrogen permeation technique, Theor. Appl. Fract. Mech. 110 (2020) 102771, https://doi.org/10.1016/j.tafmec.2020.102771.
[149] W.Y. Choo, J.Y. Lee, Effect of cold working on the hydrogen trapping phenomena in pure iron, Metall. Trans. A 14 (1983) 1299–1305, https://doi.org/10.1007/BF02664812.
[150] A. Thomas, J.A. Szpunar, Effect of Cold-Rolling on Hydrogen Diffusion and Trapping in X70 Pipeline Steel, J. Eng. Mater. Technol. 143 (2021), https://doi.org/10.1115/1.4049320.
[151] M. Koyama, M. Rohwerder, C. Tasan, A. Bashir, E. Akiyama, K. Takai, D. Raabe, K. Tsuzaki, Recent progress in microstructural hydrogen mapping in steels: quantification, kinetic analysis, and multi-scale characterisation, Mater. Sci. Technol. 33 (2017), https://doi.org/10.1080/02670836.2017.1299276.
[152] W.Y. Choo, J.Y. Lee, Thermal analysis of trapped hydrogen in pure iron, Metall. Trans. A 13 (1982) 135–140, https://doi.org/10.1007/BF02642424.
[153] J.-G. Roquefere, J. Lang, A. Yonkeu, J. Dufour, J. Huot, Effect of iron on the hydriding properties of the Mg6Pd hydrogen storage system, Int. J. Hydrogen Energy 36 (2011) 2165–2169, https://doi.org/10.1016/j.ijhydene.2010.11.075.

[154] H. Wu, A.V. Skripov, T.J. Udovic, J.J. Rush, S. Derakhshan, H. Kleinke, Hydrogen in Ti3Sb and Ti2Sb: Neutron vibrational spectroscopy and neutron diffraction studies, J. Alloy. Compd. 496 (2010) 1–6, https://doi.org/10.1016/j.jallcom.2009.12.187.
[155] A. Griesche, E. Dabah, T. Kannengiesser, A. Hilger, N. Kardjilov, I. Manke, B. Schillinger, Measuring Hydrogen Distributions in Iron and Steel Using Neutrons, in: 10th World Conference on Neutron Radiography 69, 2015, https://doi.org/10.1016/j.phpro.2015.07.062.
[156] A. Griesche, E. Dabah, T. Kannengiesser, Neutron imaging of hydrogen in iron and steel, Can. Metall. Q. 54 (2015) 38–42, https://doi.org/10.1179/1879139514Y.0000000162.
[157] J. Takahashi, K. Kawakami, T. Tarui, Direct observation of hydrogen-trapping sites in vanadium carbide precipitation steel by atom probe tomography, Scr. Mater. 67 (2012) 213–216, https://doi.org/10.1016/j.scriptamat.2012.04.022.
[158] J. Takahashi, K. Kawakami, Y. Kobayashi, T. Tarui, The first direct observation of hydrogen trapping sites in TiC precipitation-hardening steel through atom probe tomography, Scr. Mater. 63 (2010) 261–264, https://doi.org/10.1016/j.scriptamat.2010.03.012.
[159] J. Takahashi, K. Kawakami, Y. Kobayashi, Origin of hydrogen trapping site in vanadium carbide precipitation strengthening steel, Acta Mater. 153 (2018) 193–204, https://doi.org/10.1016/j.actamat.2018.05.003.
[160] Y.-S. Chen, D. Haley, S.S.A. Gerstl, A.J. London, F. Sweeney, R.A. Wepf, W.M. Rainforth, P.A.J. Bagot, M.P. Moody, Direct observation of individual hydrogen atoms at trapping sites in a ferritic steel, Science 355 (2017) (1979) 1196–1199, https://doi.org/10.1126/science.aal2418.
[161] J. Wilde, A. Cerezo, G. Smith, Three-dimensional atomic-scale mapping of a Cottrell atmosphere around a dislocation in iron, Scripta Materialia - SCRIPTA MATER 43 (2000) 39–48, https://doi.org/10.1016/S1359-6462(00)00361-4.
[162] M.K. Miller, Atom probe tomography characterization of solute segregation to dislocations and interfaces, J. Mater. Sci. 41 (2006) 7808–7813, https://doi.org/10.1007/s10853-006-0518-5.
[163] M. Kuzmina, M. Herbig, D. Ponge, S. Sandlöbes, D. Raabe, Linear complexions: Confined chemical and structural states at dislocations, Science 349 (2015) (1979) 1080–1083, https://doi.org/10.1126/science.aab2633.
[164] G.P. Tiwari, A. Bose, J.K. Chakravartty, S.L. Wadekar, M.K. Totlani, R.N. Arya, R.K. Fotedar, A study of internal hydrogen embrittlement of steels, Mater. Sci. Eng. A 286 (2000) 269–281, https://doi.org/10.1016/S0921-5093(00)00793-0.
[165] V.P. Ramunni, T.D.P. Coelho, P.E.V. de Miranda, Interaction of hydrogen with the microstructure of low-carbon steel, Mater. Sci. Eng. A 435–436 (2006) 504–514, https://doi.org/10.1016/j.msea.2006.07.089.
[166] Bhadeshia HKDH., Prevention of hydrogen embrittlement in steels., (n.d.).
[167] H. Ha, J.-H. Ai, J. Scully, Effects of Prior Cold Work on Hydrogen Trapping and Diffusion in API X-70 Line Pipe Steel During Electrochemical Charging, Corrosion 70 (2014) 166–184, https://doi.org/10.5006/0990.
[168] O. Barrera, D. Bombac, Y. Chen, T.D. Daff, E. Galindo-Nava, P. Gong, D. Haley, R. Horton, I. Katzarov, J.R. Kermode, C. Liverani, M. Stopher, F. Sweeney, Understanding and mitigating hydrogen embrittlement of steels: a review of experimental, modelling and design progress from atomistic to continuum, J. Mater. Sci. 53 (2018) 6251–6290, https://doi.org/10.1007/s10853-017-1978-5.
[169] K. Findley, M. O'Brien, H. Nako, Critical assessment: mechanisms of hydrogen induced cracking in pipeline steels, Mater. Sci. Technol. 31 (2015), https://doi.org/10.1179/1743284715Y.0000000131.
[170] D. Diniz, E. Silva, J. Carrasco, J. Barbosa, A. Silva, Effect of Reversible Hydrogen Trapping on Crack Propagation in the API 5CT P110 Steel - A Numerical Simulation, Int. J. Multiphys. 8 (2014) 313–323, https://doi.org/10.1260/1750-9548.8.3.313.
[171] M. Dadfarnia, P. Sofronis, T. Neeraj, Hydrogen interaction with multiple traps: Can it be used to mitigate embrittlement? Int. J. Hydrogen Energy 36 (2011) 10141–10148, https://doi.org/10.1016/j.ijhydene.2011.05.027.
[172] H. Grabke, F. Gehrmann, E. Riecke, Hydrogen in microalloyed steels, Steel Research, v.72, 225-235 (2001) 72 (2001). https://doi.org/10.1002/srin.200100110.
[173] A. McNabb, P.K. Foster, A new analysis of diffusion of hydrogen in iron and ferritic steels, Trans. Metall. Soc. AIME 227 (1963) 618.
[174] R.L.S. Thomas, J.R. Scully, R.P. Gangloff, Internal Hydrogen Embrittlement of Ultrahigh-Strength AERMET 100 Steel, n.d.
[175] G.M. Pressouyre, I.M. Bernstein, An Example of the Effect of Hydrogen Trapping on Hydrogen Embrittlement, n.d.
[176] Y. Momotani, A. Shibata, T. Yonemura, Y. Bai, N. Tsuji, Effect of initial dislocation density on hydrogen accumulation behavior in martensitic steel, Scr. Mater. 178 (2020) 318–323, https://doi.org/10.1016/j.scriptamat.2019.11.051.
[177] M. Connolly, M. Martin, P. Bradley, D. Lauria, A. Slifka, R. Amaro, C. Looney, J.-S. Park, in situ high energy X-ray diffraction measurement of strain and dislocation density ahead of crack tips grown in hydrogen, Acta Mater. 180 (2019), https://doi.org/10.1016/j.actamat.2019.09.020.
[178] P. Tsong-Pyng, C.J. Altstetter, Effects of deformation on hydrogen permeation in austenitic stainless steels, Acta Metall. 34 (1986) 1771–1781, https://doi.org/10.1016/0001-6160(86)90123-9.
[179] M.R. Louthan, R.G. Derrick, Hydrogen transport in austenitic stainless steel, Corros. Sci. 15 (1975) 565–577, https://doi.org/10.1016/0010-938X(75)90022-0.
[180] A. Telang, A.S. Gill, K. Zweiacker, C. Liu, J.M.K. Wiezorek, V.K. Vasudevan, Effect of thermo-mechanical processing on sensitization and corrosion in alloy 600 studied by SEM- and TEM-Based diffraction and orientation imaging techniques, J. Nucl. Mater. 505 (2018) 276–288, https://doi.org/10.1016/j.jnucmat.2017.07.053.
[181] M. Eskandari, M.R. Yadegari-Dehnavi, A. Zarei-Hanzaki, M.A. Mohtadi-Bonab, R. Basu, J.A. Szpunar, In-situ strain localization analysis in low density transformation-twinning induced plasticity steel using digital image correlation, Opt. Lasers Eng. 67 (2015) 1–16, https://doi.org/10.1016/j.optlaseng.2014.10.005.
[182] A.A. Saleh, D. Hejazi, A.A. Gazder, D.P. Dunne, E.V. Pereloma, Investigation of the effect of electrolytic hydrogen charging of X70 steel: II Microstructural and Crystallographic Analyses of the Formation of Hydrogen Induced Cracks and Blisters, Int J Hydrogen Energy 41 (2016) 12424–12435, https://doi.org/10.1016/j.ijhydene.2016.05.235.
[183] V. Venegas, F. Caleyo, J.L. González, T. Baudin, J.M. Hallen, R. Penelle, EBSD study of hydrogen-induced cracking in API-5L-X46 pipeline steel, Scr. Mater. 52 (2005) 147–152, https://doi.org/10.1016/j.scriptamat.2004.09.015.
[184] V. Venegas, F. Caleyo, J.M. Hallen, T. Baudin, R. Penelle, Role of Crystallographic Texture in Hydrogen-Induced Cracking of Low Carbon Steels for Sour Service Piping, Metall. Mater. Trans. A 38 (2007) 1022–1031, https://doi.org/10.1007/s11661-007-9130-9.
[185] J.F. Humphreys, A. Rollett, G.S. Rohrer, Recrystallization and related annealing phenomena, (2017).
[186] T. Jack, J. Szpunar, Effect of Nb-induced microstructure on pipeline steel corrosion and stress corrosion cracking performance in acidic environment, Corros. Sci. 218 (2023) 111196, https://doi.org/10.1016/j.corsci.2023.111196.
[187] S.I. Wright, D.P. Field, Recent studies of local texture and its influence on failure, Mater. Sci. Eng. A 257 (1998) 165–170, https://doi.org/10.1016/S0921-5093(98)00835-1.
[188] M. Koyama, E. Akiyama, K. Tsuzaki, D. Raabe, Hydrogen-assisted failure in a twinning-induced plasticity steel studied under in situ hydrogen charging by electron channeling contrast imaging, Acta Mater. 61 (2013) 4607, https://doi.org/10.1016/j.actamat.2013.04.030.
[189] M. Zhou, H. Yu, Effects of precipitates and inclusions on the fracture toughness of hot rolling X70 pipeline steel plates, Int. J. Miner. Metall. Mater. 19 (2012), https://doi.org/10.1007/s12613-012-0632-0.
[190] T. Depover, O. Monbaliu, E. Wallaert, K. Verbeken, Effect of Ti, Mo and Cr based precipitates on the hydrogen trapping and embrittlement of Fe–C–X Q&T alloys, Int. J. Hydrogen Energy 40 (2015) 16977–16984, https://doi.org/10.1016/j.ijhydene.2015.06.157.
[191] W. Qin, J.A. Szpunar, A general model for hydrogen trapping at the inclusion-matrix interface and its relation to crack initiation, Phil. Mag. 97 (2017) 3296–3316, https://doi.org/10.1080/14786435.2017.1378451.
[192] K.O. Findley, M.K. O'Brien, H. Nako, Critical Assessment 17: Mechanisms of hydrogen induced cracking in pipeline steels, Mater. Sci. Technol. 31 (2015) 1673–1680, https://doi.org/10.1080/02670836.2015.1121017.
[193] F.G. Wei, K. Tsuzaki, Quantitative analysis on hydrogen trapping of TiC particles in steel, Metall. Mater. Trans. A 37 (2006) 331–353, https://doi.org/10.1007/s11661-006-0004-3.

[194] T.Y. Jin, Z.Y. Liu, Y.F. Cheng, Effect of non-metallic inclusions on hydrogen-induced cracking of API5L X100 steel, Int. J. Hydrogen Energy 35 (2010) 8014–8021, https://doi.org/10.1016/j.ijhydene.2010.05.089.
[195] M.A. Mohtadi-Bonab, M. Eskandari, A focus on different factors affecting hydrogen induced cracking in oil and natural gas pipeline steel, Eng. Fail. Anal. 79 (2017) 351–360, https://doi.org/10.1016/j.engfailanal.2017.05.022.
[196] S.P. Ringer, W.B. Li, K.E. Easterling, On the interaction and pinning of grain boundaries by cubic shaped precipitate particles, Acta Metall. 37 (1989) 831–841, https://doi.org/10.1016/0001-6160(89)90010-2.
[197] K. Oikawa, K. Ishida, T. Nishizawa, Effect of titanium addition on the formation and distribution of MnS inclusions in steel during solidification, ISIJ Int. 37 (1997) 332–338.
[198] Y.I. Ito, S. Nara, Y. Kato, M. Suda, Shape control of alumina inclusions by double calcium addition treatment, Tetsu-To-Hagane/Journal of the Iron and Steel Institute of Japan 93 (2007) 355–361.
[199] J. Moon, S.-J. Kim, C. Lee, Role of Ca treatment in hydrogen induced cracking of hot rolled API pipeline steel in acid sour media, Met. Mater. Int. 19 (2013) 45–48.
[200] H. reza Hajibagheri, A. Heidari, R. Amini, An experimental investigation of the nature of longitudinal cracks in oil and gas transmission pipelines, J Alloys Compd 741 (2018) 1121–1129. https://doi.org/https://doi.org/10.1016/j.jallcom.2017.12.311.
[201] Q. Wu, M. Zikry, Prediction of diffusion assisted hydrogen embrittlement failure in high strength martensitic steels, J. Mech. Phys. Solids 85 (2015) 143–159, https://doi.org/10.1016/j.jmps.2015.08.010.
[202] Z. Peng, J. Liu, F. Huang, Q. Hu, C. Cao, S. Hou, Comparative study of non-metallic inclusions on the critical size for HIC initiation and its influence on hydrogen trapping, Int. J. Hydrogen Energy 45 (2020) 12616–12628, https://doi.org/10.1016/j.ijhydene.2020.02.131.
[203] W.K. Kim, S.U. Koh, B.Y. Yang, K.Y. Kim, Effect of environmental and metallurgical factors on hydrogen induced cracking of HSLA steels, Corros. Sci. 50 (2008) 3336–3342, https://doi.org/10.1016/j.corsci.2008.09.030.
[204] H.B. Xue, Y.F. Cheng, Characterization of inclusions of X80 pipeline steel and its correlation with hydrogen-induced cracking, Corros. Sci. 53 (2011) 1201–1208, https://doi.org/10.1016/j.corsci.2010.12.011.
[205] X. Jiang, G. Li, H. Tang, J. Liu, S. Cai, J. Zhang, Modification of Inclusions by Rare Earth Elements in a High-Strength Oil Casing Steel for Improved Sulfur Resistance, Materials 16 (2023), https://doi.org/10.3390/ma16020675.
[206] O. Lavigne, E. Gamboa, J. Griggs, V. Luzin, M. Law, A. Roccisano, High-pH inclined stress corrosion cracking in Australian and Canadian gas pipeline X65 steels, Mater. Sci. Technol. 32 (2016), https://doi.org/10.1080/02670836.2015.1132030.
[207] M.A. Mohtadi-Bonab, M. Eskandari, J.A. Szpunar, Texture, local misorientation, grain boundary and recrystallization fraction in pipeline steels related to hydrogen induced cracking, Mater. Sci. Eng. A 620 (2015) 97–106, https://doi.org/10.1016/j.msea.2014.10.009.
[208] M. Masoumi, C. Silva, M. Béreš, D. Hincapie, H. Abreu, Role of crystallographic texture on the improvement of hydrogen-induced crack resistance in API 5L X70 pipeline steel, Int. J. Hydrogen Energy 42 (2016), https://doi.org/10.1016/j.ijhydene.2016.10.124.
[209] P. Wang, L. Ma, X. Cheng, X. Li, Effect of grain size and crystallographic orientation on the corrosion behaviors of low alloy steel, J. Alloy. Compd. 857 (2021), https://doi.org/10.1016/j.jallcom.2020.158258.
[210] J. Omale, E. Ohaeri, J. Szpunar, M. Arafin, F. Fateh, Microstructure and texture evolution in warm rolled API 5L X70 pipeline steel for sour service application, Mater Charact 147 (2018), https://doi.org/10.1016/j.matchar.2018.12.003.
[211] T.A. Jack, J. Szpunar, J. Zhang, J. Qu, Sensitivity of mechanical properties of pipeline steels to microalloying additions and structural characteristics, Mater. Sci. Eng. A 826 (2021) 141984, https://doi.org/10.1016/j.msea.2021.141984.
[212] D. Raabe, Overview on basic types of hot rolling textures of Steels, Steel Res. Int. 74 (2003) 327–337, https://doi.org/10.1002/srin.200300194.
[213] D.G. Rodrigues, C.M. de Alcântara, T.R. de Oliveira, B.M. Gonzalez, The effect of grain size and initial texture on microstructure, texture, and formability of Nb stabilized ferritic stainless steel manufactured by two-step cold rolling, J. Mater. Res. Technol. 8 (2019) 4151–4162, https://doi.org/10.1016/j.jmrt.2019.07.024.
[214] M. Nouroozi, H. Mirzadeh, M. Zamani, Effect of microstructural refinement and intercritical annealing time on mechanical properties of high-formability dual phase steel, Mater. Sci. Eng. A 736 (2018) 22–26.
[215] E.O. Hall, The Deformation and Ageing of Mild Steel: III Discussion of Results, Proc. Phys. Soc. London, Sect. B 64 (1951) 747, https://doi.org/10.1088/0370-1301/64/9/303.
[216] R.W. Armstrong, 60 Years of Hall-Petch: Past to Present Nano-Scale Connections, Mater. Trans. 55 (2014) 2–12, https://doi.org/10.2320/matertrans.MA201302.
[217] M.Y. Liu, B. Shi, C. Wang, S.K. Ji, X. Cai, H.W. Song, Normal Hall-Petch behavior of mild steel with submicron grains, Mater. Lett. 57 (2003) 2798–2802, https://doi.org/10.1016/S0167-577X(02)01377-0.
[218] K.D. Ralston, N. Birbilis, C.H.J. Davies, Revealing the relationship between grain size and corrosion rate of metals, Scr. Mater. 63 (2010) 1201–1204, https://doi.org/10.1016/j.scriptamat.2010.08.035.
[219] K.D. Ralston, N. Birbilis, Effect of Grain Size on Corrosion: A Review, Corrosion 66 (2010), https://doi.org/10.5006/1.3462912.
[220] S.N. Naik, S.M. Walley, The Hall-Petch and inverse Hall-Petch relations and the hardness of nanocrystalline metals, J. Mater. Sci. 55 (2020) 2661–2681, https://doi.org/10.1007/s10853-019-04160-w.
[221] T.C. Tsai, T.H. Chuang, Role of grain size on the stress corrosion cracking of 7475 aluminum alloys, Mater. Sci. Eng. A 225 (1997) 135–144.
[222] E. Sikora, X.J. Wei, B.A. Shaw, Corrosion Behavior of Nanocrystalline Bulk Al-Mg-Based Alloys, Corrosion 60 (2004) 387–398, https://doi.org/10.5006/1.3287748.
[223] P. Wang, L. Ma, X. Cheng, X. Li, Influence of grain refinement on the corrosion behavior of metallic materials: A review, Int. J. Miner. Metall. Mater. 28 (2021) 1112–1126, https://doi.org/10.1007/s12613-021-2308-0.
[224] W. Zhang, F. Liu, L. Liu, Q. Li, L. Liu, F. Liu, C. Huang, Effect of grain size and distribution on the corrosion behavior of Y2O3 dispersion-strengthened 304 stainless steel, Mater. Today Commun. 31 (2022) 103723, https://doi.org/10.1016/j.mtcomm.2022.103723.
[225] Y. Li, F. Wang, G. Liu, Grain Size Effect on the Electrochemical Corrosion Behavior of Surface Nanocrystallized Low-Carbon Steel, Corrosion 60 (2004) 891–896, https://doi.org/10.5006/1.3287822.
[226] A. Thomas, J.A. Szpunar, Hydrogen diffusion and trapping in X70 pipeline steel, Int. J. Hydrogen Energy 45 (2020) 2390–2404, https://doi.org/10.1016/j.ijhydene.2019.11.096.
[227] Z.Y. Zhu, Y.L. Liu, G.Q. Gou, W. Gao, J. Chen, Effect of heat input on interfacial characterization of the butter joint of hot-rolling CP-Ti/Q235 bimetallic sheets by Laser + CMT, Sci. Rep. 11 (2021) 10020, https://doi.org/10.1038/s41598-021-89343-9.
[228] E.G. Ohaeri, W. Qin, J. Szpunar, A critical perspective on pipeline processing and failure risks in hydrogen service conditions, J. Alloy. Compd. 857 (2021), https://doi.org/10.1016/j.jallcom.2020.158240.
[229] X. Yue, Investigation on heat-affected zone hydrogen-induced cracking of high-strength naval steels using the Granjon implant test, Welding in the World 59 (2015) 77–89, https://doi.org/10.1007/s40194-014-0181-4.
[230] S. By Omale Idokoh Joseph, MICROSTRUCTURE AND MECHANICAL PROPERTIES OF WELDS IN PIPELINE STEEL, n.d.
[231] C. Yuhua, M. Yuqing, L. Weiwei, H. Peng, Investigation of welding crack in micro laser welded NiTiNb shape memory alloy and Ti6Al4V alloy dissimilar metals joints, Opt. Laser Technol. 91 (2017) 197–202, https://doi.org/10.1016/j.optlastec.2016.12.028.
[232] S.H. Hashemi, D. Mohammadyani, Characterisation of weldment hardness, impact energy and microstructure in API X65 steel, Int. J. Press. Vessel. Pip. 98 (2012) 8–15, https://doi.org/10.1016/j.ijpvp.2012.05.011.
[233] W. Shaiful, H. Muda, N. Syahida, M. Nasir, S. Mamat, S. Jamian, Effect of welding heat input on microstructure and mechanical properties at coarse grain heat affected zone of ABS grade a steel, 2015.
[234] A. Choubey, V.S. Jatti, Influence of Heat Input on Mechanical Properties and Microstructure of Austenitic 202 grade Stainless Steel Weldments, n.d. http://www.sitpune.edu.inhttp://www.sitpune.edu.in.

[235] X. Wang, D. Wang, L. Dai, C. Deng, C. Li, Y. Wang, K. Shen, Effect of Post-Weld Heat Treatment on Microstructure and Fracture Toughness of X80 Pipeline Steel Welded Joint, Materials 15 (2022), https://doi.org/10.3390/ma15196646.
[236] Z.H. Fu, B.J. Yang, M.L. Shan, T. Li, Z.Y. Zhu, C.P. Ma, X. Zhang, G.Q. Gou, Z.R. Wang, W. Gao, Hydrogen embrittlement behavior of SUS301L-MT stainless steel laser-arc hybrid welded joint localized zones, Corros. Sci. 164 (2020) 108337, https://doi.org/10.1016/j.corsci.2019.108337.
[237] Y. Javadi, N.E. Sweeney, E. Mohseni, C.N. MacLeod, D. Lines, M. Vasilev, Z. Qiu, C. Mineo, S.G. Pierce, A. Gachagan, Investigating the effect of residual stress on hydrogen cracking in multi-pass robotic welding through process compatible non-destructive testing, J. Manuf. Process. 63 (2021) 80–87.
[238] Q. Zhu, J. Chen, G. Gou, H. Chen, P. Li, Ameliorated longitudinal critically refracted—Attenuation velocity method for welding residual stress measurement, J. Mater. Process. Technol. 246 (2017) 267–275, https://doi.org/10.1016/j.jmatprotec.2017.03.022.
[239] X. Cao, B. Rivaux, M. Jahazi, J. Cuddy, A. Birur, Effect of pre- and post-weld heat treatment on metallurgical and tensile properties of Inconel 718 alloy butt joints welded using 4 kW Nd:YAG laser, J. Mater. Sci. 44 (2009) 4557–4571, https://doi.org/10.1007/s10853-009-3691-5.
[240] B. Malard, F. De Geuser, A. Deschamps, Microstructure distribution in an AA2050 T34 friction stir weld and its evolution during post-welding heat treatment, Acta Mater. 101 (2015) 90–100, https://doi.org/10.1016/j.actamat.2015.08.068.
[241] J.L. Caron, S.S. Babu, J.C. Lippold, Welding-Induced Microstructure Evolution of a Cu-Bearing High-Strength Blast-Resistant Steel, Metall. Mater. Trans. A 42 (2011) 4015–4031, https://doi.org/10.1007/s11661-011-0801-1.
[242] H. Strategy, Enabling A Low-Carbon Economy, Energy (2020).
[243] A. Laureys, R. Depraetere, M. Cauwels, T. Depover, S. Hertelé, K. Verbeken, Use of existing steel pipeline infrastructure for gaseous hydrogen storage and transport: A review of factors affecting hydrogen induced degradation, J. Nat. Gas Sci. Eng. 101 (2022), https://doi.org/10.1016/j.jngse.2022.104534.
[244] S.Z. Baykara, Hydrogen: A brief overview on its sources, production and environmental impact, Int. J. Hydrogen Energy 43 (2018) 10605–10614, https://doi.org/10.1016/j.ijhydene.2018.02.022.
[245] A. Godula-Jopek, Hydrogen production: by electrolysis, John Wiley & Sons, 2015.
[246] W. Cheng, Y.F. Cheng, A techno-economic study of the strategy for hydrogen transport by pipelines in Canada, Journal of Pipeline Science and Engineering 3 (2023), https://doi.org/10.1016/j.jpse.2023.100112.
[247] M. Li, H. Zhang, Y. Zeng, J. Liu, Adsorption and dissociation of high-pressure hydrogen on Fe (100) and Fe2O3 (001) surfaces: Combining DFT calculation and statistical thermodynamics, Acta Mater. 239 (2022), https://doi.org/10.1016/j.actamat.2022.118267.
[248] EFFECT OF HYDROGEN GAS PRESSURE ON THE MECHANICAL PROPERTIES OF LOW ALLOY STEEL FOR HYDROGEN PRESSURE VESSELS, n.d. http://asmedigitalcollection.asme.org/PVP/proceedings-pdf/PVP2007/42843/481/4580547/481_1.pdf.
[249] W. and R.W., 1961, A. für das E. p. 1. Hofmann, Hofmann, W. and Rauls, W., 1961, Archiv für das Eisenhüttenwesen, p. 1., (n.d.).
[250] 7 Author, R.P. Jewett, R.J. Walter, W.T. Chandler, R.P. Froh_Rg, 4. Title and Subtitle HYDROGEN ENVIRONMENT_{BRI_T OF METALS, n.d.
[251] P.S. Lam, R.L. Sindelar, T.M. Adams, LITERATURE SURVEY OF GASEOUS HYDROGEN EFFECTS ON THE MECHANICAL PROPERTIES OF CARBON AND LOW ALLOY STEELS, 2007. http://asmedigitalcollection.asme.org/PVP/proceedings-pdf/PVP2007/42843/501/4580259/501_1.pdf.
[252] H.J. Cialone, J.H. Holbrook, Sensitivity of Steels to Degradation in Gaseous Hydrogen, in: 1988. https://api.semanticscholar.org/CorpusID:136781893.
[253] R. Zawierucha, X. Kang, Hydrogen pipeline steels, Mater. Sci. Technol. 3 (2005) 79–90.
[254] D. Krieg, Konzept und Kosten eines Pipelinesystems zur Versorgung des deutschen Straßenverkehrs mit Wasserstoff, Forschungszentrum Jülich (2012).
[255] Y. Zhao, V. McDonell, S. Samuelsen, Influence of hydrogen addition to pipeline natural gas on the combustion performance of a cooktop burner, Int. J. Hydrogen Energy 44 (2019) 12239–12253, https://doi.org/10.1016/j.ijhydene.2019.03.100.
[256] J.B. Cristello, J.M. Yang, R. Hugo, Y. Lee, S.S. Park, Feasibility analysis of blending hydrogen into natural gas networks, Int. J. Hydrogen Energy 48 (2023) 17605–17629, https://doi.org/10.1016/j.ijhydene.2023.01.156.
[257] M. Kong, S. Feng, Q. Xia, C. Chen, Z. Pan, Z. Gao, Investigation of Mixing Behavior of Hydrogen Blended to Natural Gas in Gas Network, Sustainability 13 (2021), https://doi.org/10.3390/su13084255.
[258] T. Isaac, HyDeploy: The UK's First Hydrogen Blending Deployment Project, Clean, Energy 3 (2019) 114–125, https://doi.org/10.1093/ce/zkz006.
[259] MARCOGAZ. Odorisation of natural gas and hydrogen mixtures., Https://Www.Marcogaz.Org/Wp-Content/Uploads/ 2021/07/ODOR-Hydrogen-and-Odorisation.Pdf; 2021. (n.d.).
[260] GRTgaz, Immeuble Bora, 6, rue Raoul-Nordling, 92277 Bois- Colombes Cedex. Technical and economic conditions for injecting hydrogen into natural gas networksdFinal report June 2019. France, INIS-FRe20e0156 2019., Https://Www. Afgaz.Fr/Wp-Content/Uploads/Technical-Economicconditions- for-Injecting-Hydrogen-into-Natural-Gas-Ne.Pdf. (n.d.).
[261] ATCO Gas Australia. Clean energy Innovation Hub lessons. Arena Insights Forum 2019:2e8., Https://Arena.Gov.Au/ Assets/2019/12/Atco-Clean-Energy-Innovation-Hub-Lessions. Pdf. (n.d.).
[262] Australian Gas Infrastructure Group. R. enewable hydrogen, hydrogen Park SA. World Plumbing Conference. 2019., Https://Www.Worldplumbing.Org/Wp-Content/Uploa Ds/2020/ 06/VikramSingh_RenewableHydrogenHydrogenParkSA.Pdf. (n.d.).
[263] The American Society of Mechanical Engineers. ASME B31.12 Hydrogen Piping & Pipelines. New York, NY. 2019., The American Society of Mechanical Engineers. ASME B31.12 Hydrogen Piping & Pipelines. New York, NY. 2019. (n.d.).
[264] E.G. Ohaeri, J.A. Szpunar, An overview on pipeline steel development for cold climate applications, J. Pipeline Sci. Eng. 2 (2022) 1–17, https://doi.org/10.1016/j.jpse.2022.01.003.
[265] L. Lindholt, S. Glomsrød, The role of the Arctic in future global petroleum supply, Discussion Papers (2011).
[266] Y. Ren, X. Shi, Z. Yang, Y. Shan, W. Ye, G. Cai, K. Yang, Strength, strain capacity and toughness of five dual-phase pipeline steels, J. Iron Steel Res. Int. 28 (2021) 752–761, https://doi.org/10.1007/s42243-020-00522-w.
[267] B. Paermentier, S. Cooreman, S. Coppieters, R. Talemi, A novel methodology to characterise the ductile-to-brittle transition behaviour of pipeline steels using the dynamic tensile tear test, Int. J. Press. Vessel. Pip. 206 (2023) 105073, https://doi.org/10.1016/j.ijpvp.2023.105073.
[268] P. Bai, C. Shang, H.-H. Wu, G. Ma, S. Wang, G. Wu, J. Gao, Y. Chen, J. Zhang, J. Zhu, X. Mao, A review on the advance of low-temperature toughness in pipeline steels, J. Mater. Res. Technol. 25 (2023) 6949–6964, https://doi.org/10.1016/j.jmrt.2023.07.119.
[269] P. Fassina, F. Bolzoni, G. Fumagalli, L. Lazzari, L. Vergani, A. Sciuccati, Influence of Hydrogen and Low Temperature on Pipeline Steels Mechanical Behaviour, Procedia Eng. 10 (2011) 3226–3234, https://doi.org/10.1016/j.proeng.2011.04.533.
[270] I. Tamura, H. Sekine, T. Tanaka, C. Ouchi, Chapter 4 - Deformation of austenite in the nonrecrystallization region, in: I. Tamura, H. Sekine, T. Tanaka, C. Ouchi (Eds.), Thermomechanical Processing of High-Strength Low-Alloy Steels, Butterworth-Heinemann, 1988, pp. 80–100.
[271] M.F.G. Ramirez, J.W.C. Hernández, D.H. Ladino, M. Masoumi, H. Goldenstein, Effects of different cooling rates on the microstructure, crystallographic features, and hydrogen induced cracking of API X80 pipeline steel, J. Mater. Res. Technol. 14 (2021) 1848–1861, https://doi.org/10.1016/j.jmrt.2021.07.060.
[272] E., H.M., H.A.M. Ostby, Ostby, E. , Hauge, M. , Horn, A.M. , 2015. Development of materials requirement philoso- phies for design to avoid brittle behaviour in steel structures under Arctic conditions. In: Proceedings of the 25th International Ocean Polar Engineering Conference, Kona, Big Island, Hawaii, USA, pp. 309–315 ., Development of Materials Requirement Philoso- Phies for Design to Avoid Brittle Behaviour in Steel Structures under Arctic Conditions. (n.d.).
[273] G.R. Ebrahimi, M. Javdani, H. Arabshahi, Effect of thermo-mechanical parameters on microstructure and mechanical properties of microalloyed steels. Braz. J. Phys. 40, 454–458 ., Ebrahimi, G.R. , Javdani, M. , Arabshahi, H. , 2010. Effect of Thermo-Mechanical Parameters on Microstructure and Mechanical Properties of Microalloyed Steels. Braz. J. Phys. 40, 454–458 . (n.d.).
[274] O. V Sych, E.I. Khlusova, E.A. Yashin, Scientific and technological principles of development of new cold-resistant arc-steels (steels for arctic applications), in: IOP Conf Ser Mater Sci Eng, IOP Publishing, 2017: p. 012013.
[275] X. Zhao, L. Chen, Effect of Reheating Temperature on Austenite Grain Size and Solid Solution of Second Phase Particles of the Pipeline Steel Slab, in: IOP Conf Ser Mater Sci Eng, IOP Publishing, 2018: p. 022019.
[276] G.R. Ebrahimi, M. Javdani, H. Arabshahi, Effect of thermo-mechanical parameters on microstructure and mechanical properties of microalloyed steels. , Ebrahimi, G.R. , Javdani, M. , Arabshahi, H. , 2010. Effect of Thermo-Mechanical Parameters on Microstructure and Mechanical Properties of Microalloyed Steels. Braz. J. Phys. 40, 454–458 . (n.d.).

[277] A. Di Schino, R. Rufini, Thermo-mechanical process parameters effect on a 9% Cr-2% W steel, Thermo-Mechanical Process Parameters Effect on a 9% Cr-2% W Steel. Metalurgija 57, 272–274 . (n.d.).
[278] M. Jahazi, B. Egbali, The influence of hot rolling parameters on the microstructure and mechanical properties of an ultra-high strength steel, J. Mater. Process. Technol. 103 (2000) 276–279, https://doi.org/10.1016/S0924-0136(00)00474-X.
[279] G. de Caux, F. Golini, T.J. Rayner, The Design of Steel for High Strength Line Pipe Requiring Excellent Notch Toughness and Corrosion Properties for Arctic Applications, in: NACE CORROSION, NACE, 1998: p. NACE-98361.
[280] V. Carretero Olalla, V. Bliznuk, N. Sanchez, P. Thibaux, L.A.I. Kestens, R.H. Petrov, Analysis of the strengthening mechanisms in pipeline steels as a function of the hot rolling parameters, Mater. Sci. Eng. A 604 (2014) 46–56, https://doi.org/10.1016/j.msea.2014.02.066.
[281] Y. Tian, H.T. Wang, Q.B. Ye, Q.H. Wang, Z.D. Wang, G.D. Wang, Effect of rolling reduction below γ non-recrystallization temperature on pancaked γ, microstructure, texture and low-temperature toughness for hot rolled steel, Mater. Sci. Eng. A 794 (2020) 139640.
[282] X. Zuo, Z. Zhou, Study of pipeline steels with acicular ferrite microstructure and ferrite-bainite dual-phase microstructure, Mater. Res. 18 (2015) 36–41.
[283] L. Lan, C. Qiu, D. Zhao, X. Gao, Microstructural Evolution and Mechanical Properties of Nb-Ti Microalloyed Pipeline Steel, J. Iron Steel Res. Int. 18 (2011) 57–63, https://doi.org/10.1016/S1006-706X(11)60024-1.
[284] J. Hu, L.X. Du, M. Zang, S.J. Yin, Y.G. Wang, X.Y. Qi, X.H. Gao, R.D.K. Misra, On the determining role of acicular ferrite in V-N microalloyed steel in increasing strength-toughness combination, Mater Charact 118 (2016) 446–453, https://doi.org/10.1016/j.matchar.2016.06.027.
[285] Y.B. Xu, Y.M. Yu, B.L. Xiao, Z.Y. Liu, G.D. Wang, Modelling of microstructure evolution during hot rolling of a high-Nb HSLA steel, J. Mater. Sci. 45 (2010) 2580–2590, https://doi.org/10.1007/s10853-010-4229-6.
[286] S. Shanmugam, R.D.K. Misra, J. Hartmann, S.G. Jansto, Microstructure of high strength niobium-containing pipeline steel, Mater. Sci. Eng. A 441 (2006) 215–229, https://doi.org/10.1016/j.msea.2006.08.017.
[287] J. Zrník, T. Kvackaj, A. Pongpaybul, P. Sricharoenchai, J. Vilk, V. Vrchovinsky, Effect of thermomechanical processing on the microstructure and mechanical properties of Nb–Ti microalloyed steel, Materials Science and Engineering: A 319–321 (2001) 321–325. https://doi.org/https://doi.org/10.1016/S0921-5093(01)01033-4.
[288] M. Suehiro, An Analysis of the Solute Drag Effect of Nb on Recrystallization of Ultra Low Carbon Steel, ISIJ Int. 38 (1998) 547–552, https://doi.org/10.2355/isijinternational.38.547.
[289] B. Dutta, E.J. Palmiere, C.M. Sellars, Modelling the kinetics of strain induced precipitation in Nb microalloyed steels, Acta Mater. 49 (2001) 785–794, https://doi.org/10.1016/S1359-6454(00)00389-X.
[290] J. Zhang, W. Sun, H. Sun, Mechanical Properties and Microstructure of X120 Grade High Strength Pipeline Steel, J. Iron Steel Res. Int. 17 (2010) 63–67, https://doi.org/10.1016/S1006-706X(10)60185-9.
[291] G. Qiao, F. Xiao, X. Zhang, Y. Cao, B. Liao, Effects of contents of Nb and C on hot deformation behaviors of high Nb X80 pipeline steels, Trans. Nonferrous Met. Soc. Chin. 19 (2009) 1395–1399, https://doi.org/10.1016/S1003-6326(09)60039-X.
[292] J.H. Kong, L. Zheng, C.S. Xie, Development and production of X80 hot-rolled thick steel strips in WISCO, (2005).
[293] Y.I. Matrosov, Comparison of the Effect of Microadditions of Niobium, Titanium and Vanadium on Formation of Microstructure of Low-Carbon Low-Alloy Steels, Met. Sci. Heat Treat. 65 (2023) 152–158, https://doi.org/10.1007/s11041-023-00907-0.
[294] N.R. Fonstein ArcelorMittal Global, D. East Chicago, Effects of Nb, V and Ti on the Evolution of Structure of Medium Carbon Steels during Various Steps of Hot Forging, n.d.